Kinetics and Dynamics of Trapped Bose-condensed Gases.

ACADEMISCH PROEFSCHRIFT

ter verkrijging van de graad van doctor
aan de Universiteit van Amsterdam,
op gezag van de Rector Magnificus
prof. dr. J.J.M. Franse
ten overstaan van een door het college voor promoties
ingestelde commissie in het openbaar te verdedigen
in de Aula der Universiteit
op dinsdag 12 oktober 1999 te 11:00 uur

door

Peter O. Fedichev

geboren te Moscow

Contents

CHAPTER 1

Introduction

1.1. Background.

Bose-Einstein condensation (BEC) predicted already in 1924 [1, 2] has been observed recently (1995) in pioneering experiments with clouds of magnetically trapped alkali atoms at JILA [3], MIT [4] and RICE [5], and later in more than a dozen laboratories all over the world. The phenomenon was spotted by the mass media and called "a new form of matter". Since then the field of quantum gases has greatly expanded, attracting a wide attention of both scientific community and general public.

The idea of BEC originally came from quantummechanical analogy between matter waves in non-interacting gases and light waves. Indeed, as the temperature of a sample drops, the de Broglie wavelength of particles increases. Below a certain temperature (Bose condensation point), a characteristic particle wavelength exceeds the mean interparticle separation and the wave packets of particles start overlapping. Then the quantum statistics comes into play. Under this condition, for bosons (particles with an integer spin) it is favorable to fill a single quantum state. The latter state represents a macroscopic quantum object which is usually called Bose condensate and manifests itself as a phase transition accompanied by a sudden change of physical properties of the sample.

The phenomenon of BEC lies in the basis of our understanding of much of statistical and condensed matter physics. After the original Einstein analysis of Bose condensation in an ideal gas, the superfluidity in helium was considered by London (1938) as a possible manifestation of BEC in strongly interacting systems. The notion of Bose-condensation led to the first successful phenomenological model of superconductivity [6] and was further developed into the concept of spontaneous symmetry breaking [7]. Since then, the implications of BEC were found at every scale in the physical world. Bose condensation of hypothetical Higgs particles appears to be an important constituent of modern unified theory of electroweak interactions [7]. The remedies of the BEC phase transition right after the Big Bang should persist for a very long time and may be responsible for the recently discovered large-scale inhomogeneity of the mass distribution in the Universe [8]. Another kind of artifacts remaining from those times are so called "cosmic strings", hypothetical analogues of vortex rings in liquid helium [9]. BEC of pions, the particles mediating the strong interaction of nuclons inside atomic nuclei, is expected to occur in very massive atomic nuclei or inside the core of neutron stars (see [10] for a review). In particular, the non-periodic variations of gamma-radiation coming from rapidly spinning pulsars may be attributed to the dissipative dynamics of vortices inside the superfluid core of the stars [11]. All mentioned phenomena, though different in energy and spatial scales, have much in common and can be described within a single theoretical framework based on the idea of spontaneous symmetry breaking.

BEC experiments in ultra-cold gases provide a beautiful example of Bose-condensation in an interacting system. Contrary to a classical gas, for a Bose-condensed gas the interaction between atoms, though being very weak, plays an important role and dilute ultra-cold gases demonstrate the whole variety of physical phenomena characteristic for superfluid systems. From a theoretical point of view, these systems are close to an ideal gas. The presence of a small parameter related to the ratio of interparticle interaction radius to the mean interparticle separation (gaseous parameter) provides a deep understanding of underlying physical phenomena, from first principles. On the experimental side, the magnetically trapped gaseous samples are well isolated from the environment and can be

controlled by relatively simple optical techniques. This could be compared with research of liquid helium, which has been a major experimental source of information about interacting Bose condensed systems, where the evidence of BEC comes from an experiment as difficult as measurement of momentum distribution of helium particles by neutron scattering, and no closed theory is available because of the high density of the samples. This combination of experimental and theoretical "accessibility" of BEC in ultra-cold gases allows one to get a good insight in fundamental concepts of condensed matter physics and perform a precision test of existing theories.

The achievement and studies of BEC in ultra-cold gases require cooling of metastable atomic samples, which became possible due to recent progress in manipulation, trapping and cooling of cold atoms. In fact, the Bose-Einstein condensate in a trapped gas can be considered as a coherent standing matter wave in a trap, which is in many ways similar to a laser mode excited inside an optical cavity. Further exploiting this analogy makes it feasible to create an atom laser capable of generating coherent beams of cold atoms. Now this technology is being actively developed in view of possible applications ranging from precise atom interferometry and cold collision studies to atom lithography and quantum computing.

First attempts to reach quantum degeneracy in atomic gases began with atomic hydrogen more than 20 years ago. In the first set of experiments hydrogen atoms in the lower Zeeman state were trapped in a "magnetic bottle" (with walls covered by liquid helium) and cooled to sub-Kelvin temperatures [12–14]. This approach was promising, since due to a rather large density of the gas sample one expected a relatively high BEC transition temperature. But at realistic achievable temperatures the density required for BEC turned out to be so high that recombination losses and heating became crucial [12–16]. In the second set of experiments, performed at MIT and the University of Amsterdam, spin polarized atoms were magnetically trapped (wall-less confinement) and further cooled down by evaporation. The first observation of BEC in spin polarized hydrogen has been recently reported by the hydrogen group at MIT [17]. Another important experimental achievement came from the University of Turku (Finland), where the regime of quantum degeneracy was reached in a two-dimensional gas of hydrogen atoms adsorbed on the surface of liquid helium [18]. This opens an interesting direction of research, since the nature of BEC in low dimensional systems is drastically different from that in three dimensions.

Another constituent of successful BEC experiments came from the developments of laser-based techniques for manipulating cold neutral atoms, such as laser cooling and magneto-optical trapping (see [19–21] for review). Alkali atoms are much better suited for optical manipulations than atomic hydrogen, since their optical transitions can easily be excited with commercially available CW lasers. The temperature of such a sample can be further lowered by transferring atoms from the magneto-optical to a magnetostatic trap and evaporatively cooling them [22,23]. Such a combination of optical and evaporative cooling has led to the discovery of BEC in ultra-cold alkali atom gases. There is an increasing number of successful BEC experiments with $^{87}\mathrm{Rb}$ [3, 24–27], $^{23}\mathrm{Na}$ [4, 28–30], and interesting experiments with $^{7}\mathrm{Li}$ on BEC in gases with attractive interparticle interaction [5]. There are also ongoing experiments on vapors of cesium, potassium and metastable triplet helium.

From a theoretical point of view, the situation in dilute Bose-condensed trapped gases is unique compared with, for example, liquid helium. First, due to a very low density of the Bose condensates, many of the physical properties of the system can be understood within the so called "mean-field" approximation. A characteristic feature of the mean-field approach in dilute gases is the principal role of two-body interparticle interactions, whereas the effects of higher-order collisions lead to a relatively slow decay of the system due to recombination. In dilute ultra-cold gases the interparticle interaction is characterized by a single parameter a, the two-body s-wave scattering length. Secondly, finite size effects enhance the manifestation of interparticle interaction in physical properties of trapped condensates and make their behavior even qualitatively different from that in spatially homogeneous weakly interacting gases.

A principal question for BEC in atomic gases concerns the sign of the scattering length a. For $a > 0$ elastic interaction between atoms is repulsive and the Bose condensate is stable with respect to this interaction. If $a < 0$ elastic interaction is attractive and this is the origin of a collapse of the condensate in a homogeneous gas [31]. For trapped gases with $a < 0$ the situation is practically the same, provided the interaction between particles exceeds the level spacing in the trapping field [32, 33]. If this interaction is much smaller than the level spacing, due to the finite size effects there is a gap between the ground state and one-particle excitations and it is possible to form a metastable Bose-condensed state [33]. Among the alkalis there are atomic gases with both positive and negative a [34].

1.2. Outline of the Thesis.

This Thesis is devoted to theoretical investigation of dynamics and kinetics of dilute Bose - condensed trapped gases. The key aspect that links together the various parts of the Thesis is related to the role of interparticle interaction in the described macroscopic quantum phenomena. The results of the Thesis are of direct relevance for the ongoing experimental studies.

The Thesis is organized in the following way. After the Introduction (Chapter 1) in Chapter 2 we give a brief overview of BEC theory for ultra-cold gases. In Chapter 3, we discuss the issue of two and three body interactions in ultra-cold gases. The first section is devoted to three-body recombination, the process in which two atoms form a bound state and a third one carries away the binding energy. This process may be thought as an initial stage in the formation of clusters intermediate in size between individual atoms and bulk matter. Three-body recombination limits achievable densities in trapped ultra-cold gases and, hence, places limitations on the possibilities to observe Bose-Einstein condensation.

Then, in the second section we develop the idea of manipulating the value and the sign of the scattering length by using nearly resonant light. Since changing a directly affects the mean field interaction between the atoms, this offers a possibility to investigate macroscopic quantum phenomena associated with BEC by observing the evolution of a Bose condensed gas in response to light. As the light essentially couples the ground and excited atomic states and the interaction between atoms in the excited state is much stronger than in the ground state, already at moderate light intensities the scattering amplitude can be significantly changed.

The manipulation of the interparticle interaction opens the way of studying macroscopic quantum phenomena associated with the dynamics of the condensates. Together with other possibilities, such as instantaneous changing the trap frequencies [33] or changing the interparticle interaction by external magnetic field [35], the laser activation of a Bose-condensate should lead to the creation of macroscopically excited, but yet coherent condensate states. At the same time, the trapped Bose-Einstein condensates are well isolated from the environment, and thus the appearance of relaxation dynamics first observed at JILA at effectively zero temperature poses a question of how the gas sample, being initially a pure condensate, subsequently reaches a new equilibrium state. This is directly related to the fundamental problem of the appearance of irreversibility in a quantum system with a large number of particles. Also, the question of the formation of a thermal component, remains to be fully resolved. In Chapter 4 we analyze the dynamics of two trapped interacting Bose-Einstein condensates in the absence of thermal cloud and identify two regimes for the evolution: a regime of slow periodic oscillations and a regime of strong non-linear mixing leading to the damping of the relative motion of the condensates.

The description of the detailed behavior of evolving condensates at finite temperatures requires to develop a theory beyond the mean field. This relates, in particular, to the temperature-dependent damping rates and energy shifts of elementary excitations of a condensate. In Chapter 5 we develop a finite temperature perturbation theory capable of calculating the damping rates and energy shifts of the excitations in both spatially homogeneous and trapped Bose-Einstein condensates.

Of fundamental interest are macroscopically excited Bose-condensed states, such as vortices in non-rotating traps. The creation and observation of quantum vortices is a promising option for observing superfluidity in trapped gases, as quantization of circulation and the related phenomenon of persistent currents are the most striking properties of superfluids. These studies are especially interesting for the investigation of the relation between Bose-Einstein condensation and superfluidity. In Chapter 6 we develop a theory for the dissipative dynamics of a vortex state in a trapped Bose-condensed gas at finite temperature and draw a scenario of decay of this state in a static trap.

CHAPTER 2

Overview

Bose-Einstein condensation is a quantum statistics phenomenon which occurs in a system of bosons (particles with an integer spin) when the characteristic thermal de Broglie wavelength of the particles exceeds the mean interparticle separation. In this Chapter we give a brief introduction to the BEC physics, outlining important concepts and basic methods used for theoretical studies of trapped ultra-cold gases throughout the Thesis.

2.1. Thermodynamics of an ideal Bose-gas.

We start with thermodynamic description of an ideal gas of N bosons in a harmonic trapping potential. The gas sample is assumed to be in thermal equilibrium at temperature T, and we will calculate thermodynamic averages over the grand canonical ensemble, where the system is characterized by chemical potential μ and fluctuating number of particles. This approach is well justified in trapped Bose gases by the fact that the number of particles in current BEC experiment may be as high as 10^6 and in the thermodynamic limit ($N \to \infty$) the grand canonical description is equivalent to that in the canonical ensemble (fixed N and fluctuating μ).

The energy spectrum of an individual atom in a harmonic trap is characterized by a set of three non-negative integer quantum numbers $\{n\} = \{n_x, n_y, n_z\}$ and reads

$$\epsilon_{\{n\}} = \sum_{i=x,y,z} \hbar\omega_i (n_i + 1/2),$$

where ω_x, ω_y and ω_z are the trap frequencies along three Cartesian directions. Hereinafter we adopt the convention $k_B = 1$(k_B is the Boltzmann constant). The average number of particles in the state $\{n\}$ is given by the well known Bose-Einstein expression:

$$N_B(\epsilon_{\{n\}}) = (e^{(\epsilon_{\{n\}} - \mu)/T} - 1)^{-1}.$$

The value of the chemical potential is fixed by the condition

$$N(T, \mu) = \sum_{\lambda} N_B(\epsilon_\lambda) = N, \tag{2.1.1}$$

which expresses the total number of particles through the sum of the occupation numbers of all available states.

Since in the thermodynamic limit the Bose-condensation phenomenon occurs at temperatures greatly exceeding the ground state energy $\sim \hbar\omega$ of a particle in the trapping potential, for the calculation of thermodynamic functions at $T \gg \hbar\omega$ we can use a quasiclassical approximation. This can be accomplished in Eq.(2.1.1) by turning from summation over the discrete quantum states to integration over the classical phase space:

$$N(T, \mu) = \int \frac{d^3 r d^3 p}{(2\pi\hbar)^3} N_B(\epsilon(\mathbf{p}, \mathbf{r})), \tag{2.1.2}$$

where $\epsilon(\mathbf{p}, \mathbf{r}) = p^2/2m + \sum_i m\omega_i^2 r_i^2/2$ is the classical Hamiltonian depending on the particle coordinate $\mathbf{r}$ and momentum $\mathbf{p}$. The integral in Eq.(2.1.2) can be calculated by introducing the auxiliary

integral $\int d\epsilon\delta(\epsilon-\epsilon(\mathbf{p},\mathbf{r}))=1$ in the integrand and changing the order of the integrations. This leads to the equation

$$N(T,\mu)=\int d\epsilon N_B(\epsilon)\int\frac{d^3rd^3p}{(2\pi\hbar)^3}\delta(\epsilon-\epsilon(\mathbf{p},\mathbf{r})).$$

The second integral a function of the excitation energy and represents the quasiclassical density of states, which depends on the symmetry of the trapping potential. The calculation of the remaining integral over the energy leads to the following relation between the chemical potential and the number of particles:[1]

$$\frac{T^3}{\hbar^3\omega^3}\zeta_3(e^{\mu/T})=N, \tag{2.1.3}$$

where $\omega=(\omega_x\omega_y\omega_z)^{1/3}$. For high temperatures the argument $\alpha=\exp(\mu/T)$ of the ζ-function is small, $\zeta_3(\alpha)\approx\alpha$, and the chemical potential is large and negative:

$$\mu\approx -T\log N\left(\frac{T}{\hbar\omega}\right)^3.$$

With further decrease of temperature the argument of the logarithm decreases and the chemical potential approaches zero as α approaches 1. For $\alpha>1$ the ζ-function diverges and Eq.(2.1.3) does not have solutions, which means that at temperatures smaller than

$$T_c=\hbar\omega\left(\frac{N}{\zeta_3(1)}\right)^{1/3} \tag{2.1.4}$$

the quasiclassical approach breaks down. The temperature T_c is called the BEC temperature, or the critical temperature of the BEC phase transition. The appearance of Eq.(2.1.4) can be easily understood qualitatively. The characteristic de Broglie wavelength of a particle at a given temperature is $\lambda\sim\sqrt{\hbar^2/mT}$. At a given temperature the particles fill the spatial region characterized by the thermal size $l_T\sim\sqrt{T/m\omega^2}$. For the maximum density of the particles in the trap we have $n_{max}\sim N/l_T^3$ and for the mean interparticle separation $d\sim(l_T^3/N)^{1/3}$. For $d\sim\lambda$ the thermal wavepackets start overlapping and the atoms loose their identity and the gas sample enters the regime of quantum degeneracy, defined by the condition $T<T_c$, with T_c from Eq.(2.1.4). This estimate reproduces the transition temperature (2.1.4) up to a numerical coefficient of the order of unity. Since the number of particles in the BEC experiments is usually very large, typically $N\sim10^4-10^7$, the phase transition occurs at temperatures greatly exceeding the ground state energy. Hence, the number of populated states in the trap at temperatures $T\sim T_c$ remains very large. This justifies our classical treatment of excited states.

To resolve the apparent contradiction at $T<T_c$ one has to return to Eq.(2.1.1), where at very low temperatures the first term corresponding to the ground state turns out to be larger than the contribution of all other terms. Indeed, at very low temperatures the occupation number of the ground state, given by

$$N_0=(e^{(\epsilon_0-\mu)/T}-1)^{-1},$$

diverges. This means that the chemical potential counted from the ground state energy, $\mu=-T\log(1+1/N_0)$, is very close to zero and the occupation number of the ground state N_0 is macroscopically large. Moreover, since the ground state is never degenerate, the occupation number of the next higher state is smaller than N_0 for sufficiently low temperature (nice discussion of this issue can be found in [37]). In fact, for any temperature below T_c the sum in Eq.(2.1.1) can be transformed to integration only for excited states , whereas the occupation of the ground state has to be added explicitly.

[1] Here we introduce the generalized Riemann ζ-function: $\zeta_r(\alpha)=\sum_{n=1}^{\infty}\alpha^n/n^r$.

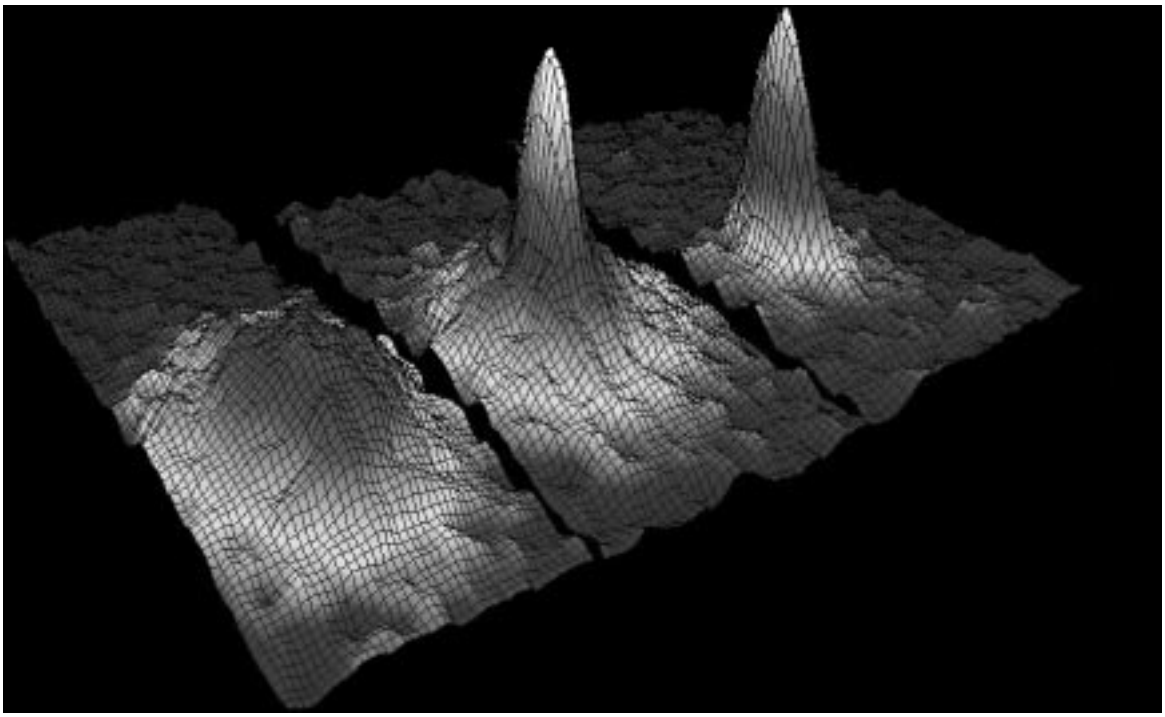

FIGURE 2.1.1. The time sequence from JILA [36] experiment. The slides from left to right correspond to lower temperatures.

This observation, together with the observation that the chemical potential is negligible at very low temperatures, leads to the following expression

$$N = N_0 + \int \frac{d^3r d^3p}{(2\pi\hbar)^3} N_B(\epsilon(\mathbf{p},\mathbf{r}))|_{\mu=0} \tag{2.1.5}$$

for the total number of particles in the sample at $T < T_c$. This equation determines the number of particles in the ground state of the system (Bose-Einstein condensate) as a function of temperature. The rest of the particles are called excitations, or above condensate particles. The number of excitations is given by the second term in Eq. (2.1.5) and can be readily calculated: $N'(T) = N - N_0 = N(T/T_c)^3$. From this we find the number of particles in the condensate

$$N_0 = N(1 - (T/T_c)^3). \tag{2.1.6}$$

This expression predicts accumulation of a macroscopic number of particles in the ground state at temperatures below T_c. If the total number of particles is sufficiently large, the effect can be dramatic. This is seen, for example, in the JILA experiment (Fig.2.1.1). The quantitative comparison of the prediction of Eq.(2.1.6) with experimental data is shown in Fig.2.1.2.

2.2. BEC in an interacting gas.

In order to describe an interacting system we turn to the Hamiltonian of a trapped Bose gas in second quantization

$$\hat{H} = \int d^3r \hat{\Psi}^\dagger(\mathbf{r}) \left(-\frac{\hbar^2\Delta}{2m} + V(\mathbf{r}) \right) \hat{\Psi}(\mathbf{r}) +$$

$$\frac{1}{2} \int d^3r d^3r' V_{12}(\mathbf{r}-\mathbf{r}') \hat{\Psi}^\dagger(\mathbf{r}) \hat{\Psi}^\dagger(\mathbf{r}') \hat{\Psi}(\mathbf{r}) \hat{\Psi}(\mathbf{r}'), \tag{2.2.1}$$

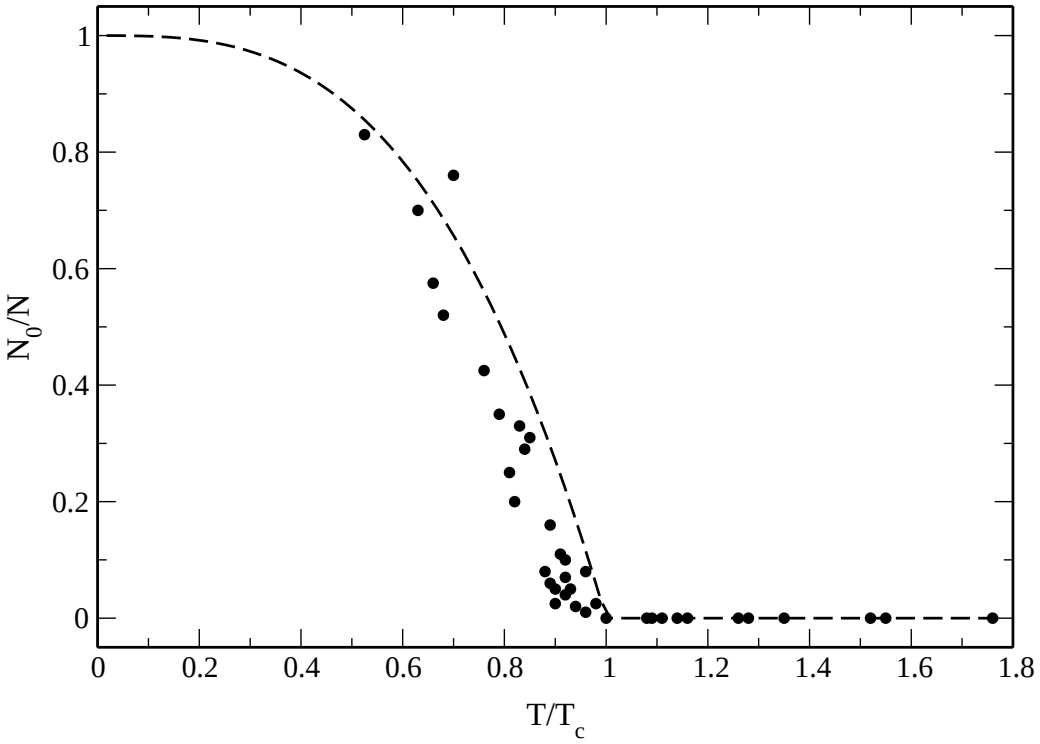

FIGURE 2.1.2. The fraction of condensate particles as a function of temperature. Here the dashed line shows the prediction of Eq.(2.1.6) and the dots stand for measured values (the distinguishable shift of the Bose-condensation temperature originates in interaction effects and thus can not be accounted by Eq.(2.1.6) derived for an ideal gas)

where $\hat{\Psi}(\mathbf{r})$ is the field operator of atoms, $V(\mathbf{r})$ is the external potential, and $V_{12}(\mathbf{r})$ is the potential of interaction between two atoms. In ultra-cold dilute Bose-gases the characteristic de Broglie wavelength of particles and the mean interparticle separation are usually much larger than the characteristic radius of interparticle interaction. This means that the interaction potential V_{12} in (2.2.1) can be approximated by a zero-range potential $\tilde{U}\delta(\mathbf{r})$, provided the coupling constant $\tilde{U}$ is chosen to give the same asymptotic behavior of the wavefunction at large interparticle separation as the solution of exact scattering problem corresponding to the potential V_{12}. This gives $\tilde{U} = 4\pi\hbar^2 a/m$.

The Hamiltonian (2.2.1) does not imply any statistics. The difference between Bose and Fermi particles comes from the commutation relations between the Ψ-operators. For Bose-statistics we have

$$[\hat{\Psi}^\dagger(\mathbf{r}), \hat{\Psi}(\mathbf{r}')] = \delta(\mathbf{r} - \mathbf{r}'). \tag{2.2.2}$$

Commuting the Ψ-operators with the Hamiltonian , we obtain the following equation of motion

$$i\hbar\frac{\partial\hat{\Psi}}{\partial t} = (-\frac{\hbar^2\Delta}{2m} + V(\mathbf{r}) + \tilde{U}\hat{\Psi}^\dagger\hat{\Psi})\hat{\Psi}. \tag{2.2.3}$$

From this equation we see that interparticle interaction in low-temperature gases leads to the appearance of an "effective" potential $V_{eff} = \tilde{U}\hat{\Psi}^\dagger\hat{\Psi}$ acting on a particle and proportional to the density operator at the point $\mathbf{r}$. Since the density is always positive, the sign of the potential energy is determined by the sign of the coupling constant $\tilde{U}$. In particular, if the scattering length is positive, then the potential energy of interparticle interaction increases with density, and thus we are dealing with effectively repulsive interaction. For $a < 0$ the interaction energy is negative and for a spatially homogeneous gas sample it is energetically favorably to shrink to as small volume as possible, i.e. to collapse. Therefore, a spatially homogeneous gas characterized by a negative scattering length is

thermodynamically unstable. The solution of the operator equation (2.2.3) allows one, in principle, to access any interesting property of an interacting Bose-gas. At the same time, the equation is too complicated and its full solution is generally not possible.[2]

The apparent difficulty is conveniently resolved for a weakly interacting Bose-condensed gas by using the concept of spontaneous symmetry breaking. As we have already seen, in a non-interacting system Bose-condensation manifests itself as a sudden appearance of macroscopic occupation of the ground state. This provides an abrupt change of such macroscopic properties as heat capacity at the transition point and therefore the BEC phase transition is of the second order. According to the general theory of second order phase transitions, the system below the critical temperature is characterized by a non vanishing order parameter, a quantity which disappears above the critical temperature. Since a distinctive feature of a Bose-condensed system is the appearance of macroscopically populated quantum state (condensate), the condensate wavefunction is the corresponding order parameter. Then, the idea is to replace the analysis of Eq.(2.2.3) by the solution of a classical equation for the order parameter, i.e. for the condensate wavefunction.

To give a quantitative meaning to these arguments, we split the Ψ-operator in two parts. The first one, is responsible for the creation/annihilation of particles in the Bose-condensed state. This state is macroscopically populated, and in the thermodynamic limit we can neglect the commutator for the condensate part of the Ψ-operator and consider this part as a classical quantity Ψ_0 satisfying the classical version of Eq.(2.2.3):

$$i\hbar\frac{\partial\Psi_0}{\partial t} = (-\frac{\hbar^2\Delta}{2m} + V(\mathbf{r}) + \tilde{U}|\Psi_0|^2)\Psi_0. \tag{2.2.4}$$

This equation is called the Gross-Pitaevskii (GP) [38–40] equation and constitutes the backbone of the mean-field description of Bose condensates at zero temperature. It represents the Schrödinger equation for a condensate particle moving in the external potential $V(\mathbf{r})$ and the mean field of all other condensate particles. The finite-temperature generalizations of Eq.(2.2.4) are discussed in Chapter 5. The remaining part of the Ψ-operator, denoted below as $\hat{\Psi}'$, describes excitations and preserves the commutation relations (2.2.2).

Eq.(2.2.4) has a discrete set of solutions characterized by a static density profile. Separating a trivial time-dependence by the substitution $\Psi_0 \rightarrow \Psi_0 \exp(-i\mu t)$, in equilibrium we obtain a static equation for the condensate wavefunction

$$\mu\Psi_0 = (-\frac{\hbar^2\Delta}{2m} + V(\mathbf{r}) + \tilde{U}|\Psi_0|^2)\Psi_0. \tag{2.2.5}$$

For a spatially homogeneous Bose-condensed gas, i.e. for a gas sample contained within a big box with $V(\mathbf{r}) = 0$ everywhere inside, we find the spatially independent solution in the form

$$\Psi_0 = \sqrt{n_0}\exp(i\Phi), \tag{2.2.6}$$

where the condensate density, n_0, and the global phase, Φ, are spatially independent everywhere except in the vicinity of the walls. The density of the condensate particles and the chemical potential are related to each other in a simple way: $\mu = \tilde{U}n_0$. The phase Φ can not be found from the equation and therefore is determined by the initial conditions leading to every different realization of a Bose-condensation experiment. This allows one to say that the global phase Φ appears spontaneously in the course of Bose-condensation. An interesting discussion of this subject is presented in [41]. The appearance of this ambiguity is in fact a consequence of the gauge symmetry of the initial Hamiltonian (2.2.1).

[2] Except in a number of exactly solvable cases, such as, the 1D case for the attractive interparticle interaction, time dependent dynamics of a condensate in a harmonic trap in 2D, and topological excitations (vortices and kinks).

Together with the normalization condition

$$N_0 = \int d^3r |\Psi_0|^2, \tag{2.2.7}$$

the ground-state solution of Eq.(2.2.5) gives a relation between μ and the number of particles in the trapped condensate, N_0. To analyze possible static solutions of Eq.(2.2.5) we first turn to the case of negligible interparticle interaction $\tilde{U} \to 0$. This means that the mean-field term is small and GP equation coincides with the Schrödinger equation for a particle moving in an external potential $V(\mathbf{r})$. For the special case of a harmonic trapping potential the solutions of Eq.(2.2.5) exist only for a discrete set of values of the chemical potential, coinciding with energy states of a quantum harmonic oscillator. This gives an infinite set of excited Bose-condensed states characterized by different values of the condensate energy per particle. For the ground Bose-condensed state we get the wavefunction corresponding to the chemical potential $\mu = \sum_i \hbar\omega_i/2$

$$\Psi_0(\mathbf{r}) = \sqrt{N_0} \prod_i \exp(-x_i^2/2l_{0i}^2)/(\pi l_{0i})^{1/2}, \tag{2.2.8}$$

where $l_i = (\hbar/m\omega_i)^{1/2}$ is the localization length of the ground state in a harmonic oscillator with frequency ω_i. To find out an error brought by neglecting the mean-field interaction term, one should compare its maximum value (reached at the center of the condensate) with the trap frequencies. Using Eq.(2.2.8) we see that the interaction effects are negligible under the condition

$$\eta = \max_i \left| \frac{\tilde{U}|\Psi_0(0)|^2}{\hbar\omega_i} \right| \ll 1. \tag{2.2.9}$$

This is the case for rather small condensates, where

$$N_0 \ll \min_j \frac{\prod_i l_{0i}}{a l_{0j}^2}.$$

This has an important consequence for a trapped Bose-condensate with attractive interaction between particles. As we have seen from thermodynamic considerations, in the spatially homogeneous case such a condensate is unstable. At the same time, under the condition (2.2.9) the collapse in a trapped gas is suppressed, since in a trapped gas there is a gap $\sim \hbar\omega$ between the condensate and elementary excitations. Therefore, for sufficiently small Bose-condensates, due to a discrete character of the energy spectrum in a finite system, a condensate with macroscopically large number of particles can exist even for attractive interparticle interaction [33].

In the opposite limiting case $a > 0$ the shape of the condensate is dominated by the interparticle interaction. Here the interaction smears out the discrete structure of the energy levels and a condensate with attractive interaction is clearly unstable. In this overview we limit ourselves to positive values of $\tilde{U}$. In this case the condensate wavefunction can be found by disregarding the kinetic energy term in Eq.(2.2.5). This corresponds to the so called "Thomas-Fermi" approximation and leads to the algebraic expression for the condensate wavefunction [42, 43]:

$$\Psi_0^{TF}(\mathbf{r}) = \sqrt{\frac{\mu - V(\mathbf{r})}{\tilde{U}}}, \tag{2.2.10}$$

if $\mu > V(\mathbf{r})$ and zero otherwise. For a harmonic trap the condensate has a parabolic shape with the size $l_{ci} = (2\mu/m\omega_i^2)^{1/2}$ in the i-th direction. Close to the condensate border the Thomas-Fermi approximation fails and the exact shape of Ψ_0 has to be found from Eq.(2.2.5) by treating all terms on the equal footing, or should be calculated numerically. Substituting the maximum density $n_{0max} = \mu/\tilde{U}$ to the criterion (2.2.9) we see that this criterion is equivalent to $\tilde{U} n_{0max} \ll \hbar\omega$. Using Eq.(2.2.7),

the chemical potential in the Thomas-Fermi regime is related to the number of condensate particles as

$$\mu = (\frac{15\tilde{U}m^{3/2}\overline{\omega}^3}{\pi 2^{9/2}})^{2/5} N_0^{2/5}.$$

Throughout the Thesis we are mainly interested in the properties of the Thomas-Fermi condensates, since it is just this case which is analogous to the bulk superfluid matter. For the same number of condensate particles there are also stationary solutions of Eq.(2.2.5), corresponding to higher values of the chemical potential. These are excited Bose-condensed states characterized by the condensate wavefunction having one or more nodes.

2.3. Dynamics of Bose-condensates

The solution (2.2.10) represents an approximation to the ground state condensate wavefunction and does not contain any time dependence. The time-dependent dynamics of trapped Bose-condensates in the mean-field approximation is studied within the framework of the time dependent GP equation (2.2.4). For arbitrary Thomas-Fermi parameters $\mu/\hbar\omega_i$ the solution can only be obtained numerically. At the same time, in harmonic traps the dynamics can be approached by using the presence of a scaling symmetry inherent to the Hamiltonian (2.2.1). This is the case for the evolution under variations of both the trap frequencies [44–46] and the interparticle interaction (scattering length a) in 3D Thomas-Fermi condensates [47]. Consider a condensate trapped in 3D harmonic trap characterized by trapping frequencies $\omega_i(t)$ in every spatial direction. Neglecting the spatial derivatives of the condensate density profile and turning to rescaled coordinate and time variables $\rho_i = r_i/b_i(t)$, $\tau = \int^t dt/\prod_i b_i(t)$, we introduce a function $\chi_0(\boldsymbol{\rho}, \tau)$ such that

$$\Psi_0(t, r) = \frac{1}{\prod_i b_i^{1/2}(t)} \chi_0(\rho_i, \tau) \exp\left(i \sum_i \frac{m r_i^2}{2\hbar} \frac{\dot{b}_i(t)}{b_i(t)} - i\mu\tau(t)\right). \tag{2.3.1}$$

Then, setting $\partial\chi_0/\partial t = 0$, the equation of motion

$$i\hbar \frac{\partial \Psi_0}{\partial t} = \left(-\frac{\hbar^2 \Delta}{2m} + \sum_i \frac{m\omega_i^2(t) r_i^2}{2} + \tilde{U}|\Psi_0|^2 \right) \Psi_0 \tag{2.3.2}$$

is reduced to the stationary GP equation in the ρ-variables for $\chi_0(\boldsymbol{\rho})$, with the initial (constant) frequencies and scattering length. Assume, that the variation of trap frequencies is switched on at the time $t = 0$. Then, the scaling parameters $b_i(t)$ satisfy the initial conditions: $b_i(0) = 1$, $\dot{b}(0) = 0$ and, in the simplest case of varying only the frequencies in a spherically symmetric trap, are determined by the equations

$$\ddot{b}(t) + \omega^2(t) b(t) = \omega_0^2 / b^4(t), \tag{2.3.3}$$

where $\omega_0 = \omega(0)$ is the initial value of trap frequency. This means that in the ρ variables $\chi_0(\boldsymbol{\rho})$ is just the initial static condensate wavefunction, and Eq.(2.3.1) gives a universal scaling solution for the wavefunction of the evolving condensate, $\Psi_0(\mathbf{r}, t)$, at any time t.

According to Eq.(2.3.1), the condensate evolves in time by changing its size but preserving the shape. The scaling approach has been successfully used to explain the data of the JILA [48] and MIT [49] experiments on free expansion of condensates after switching off the trap and the measurements of eigenfrequencies of the lowest oscillation modes of trapped condensates [50, 51].

To illustrate how the eigenfrequencies of small condensate oscillations can be found within the scaling approach, we consider the evolution of a spherically symmetric condensate after a small abrupt change of the frequency from ω_0 to ω_f. The condition $|\omega_f - \omega_0| \ll \omega_0$ guarantees that actually only

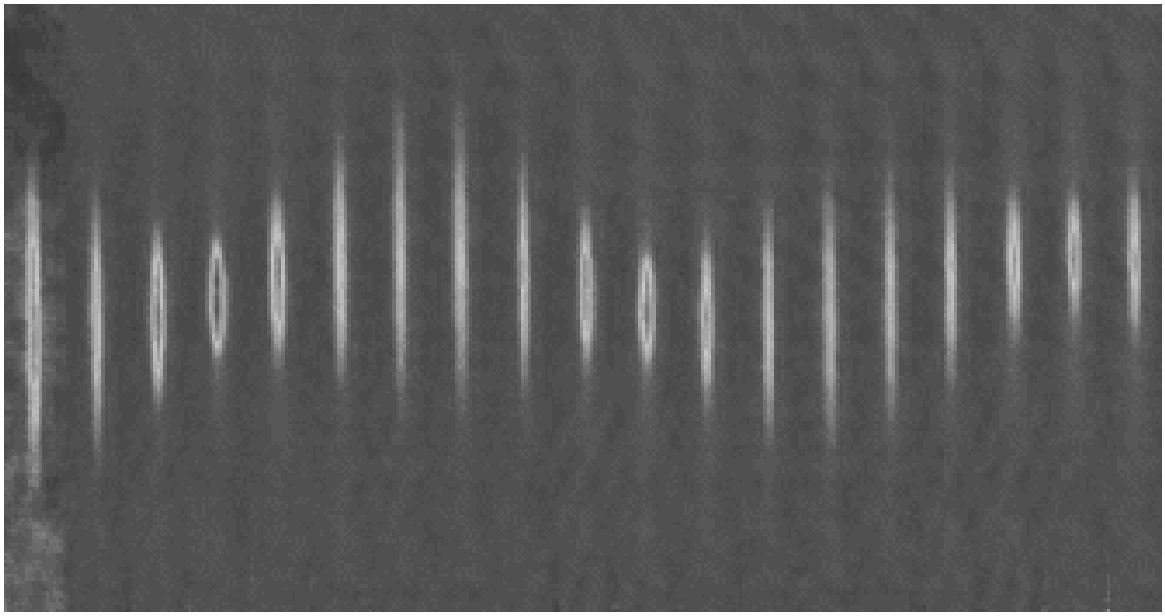

FIGURE 2.3.1. Time sequence of condensate oscillations in a magnetic trap measured by non-destructive imagining technique (MIT) [49]

one mode of the condensate oscillations is excited, and the solution for the scaling parameter, obtained from Eq.(2.3.3), is given by

$$b(t) = b_0 + (1 - b_0)\cos(\sqrt{5}\omega_0 t), \tag{2.3.4}$$

where $b_0 = (\omega_0/\omega_f)^{2/5}$ is the equilibrium value. This solution describes undamped spherically symmetric oscillations of the condensate occurring at frequency $\sqrt{5}\omega_0$ (analogues behavior in a cylindrical trap is shown in Figure 2.3.1). The requirement of small frequency change guarantees that b_0 is very close to 1 and the condensate wavefunction (2.3.1) is close to the equilibrium shape. As the difference between the final and the initial frequencies increases, the number of excited modes also grows and the behavior of the system becomes more and more complicated. In particular, one can expect the interaction between excited modes and stochastization of their motion [47], and the damping of condensate oscillations already at zero temperature [52].

In the linear regime, where the deviation of the condensate wavefunction from its equilibrium value is small, one can find a general solution of Eq.(2.2.4) for an arbitrary external potential $V(\mathbf{r})$. The solution is a superposition of the equilibrium Ψ_0 and elementary excitations of the condensate. The equations for the excitations are obtained by linearizing Eq.(2.2.4) with regard to small deviations of Ψ_0 from its equilibrium value, i.e. with regard to fluctuating (quantum) part Ψ' of the field.[3] For a spatially inhomogeneous Bose-condensed gas , after removing trivial phase factors by the substitution $(\Psi_0, \Psi') \to (\Psi_0, \Psi')\exp(-i\mu t)$, we obtain

$$\left\{ \begin{array}{rcl} i\hbar\partial\hat{\Psi}'/\partial t & = & (-\hbar^2\Delta/2m + V(\mathbf{r}) - \mu + 2\tilde{U}|\Psi_0|^2)\hat{\Psi}' + \tilde{U}\Psi_0^2\hat{\Psi}'^{\dagger}, \\ -i\hbar\partial\hat{\Psi}'^{\dagger}/\partial t & = & (-\hbar^2\Delta/2m + V(\mathbf{r}) - \mu + 2\tilde{U}|\Psi_0|^2)\hat{\Psi}'^{\dagger} + \tilde{U}\Psi_0^{*2}\hat{\Psi}'. \end{array} \right. \tag{2.3.5}$$

Eqs.(2.3.5) are linear, and therefore a general solution can be written in the form of the Bogolyubov transformation:

$$\hat{\Psi}' = \sum_{\nu}(u_\nu(\mathbf{r})b_\nu \exp(-i\epsilon_\nu t) - v_\nu(\mathbf{r})b_\nu^{\dagger}\exp(i\epsilon_\nu t)), \tag{2.3.6}$$

[3] The analysis of elementary excitations of a spatially homogeneous Bose-condensed gas was performed in a different form by Bogolyubov [53].

where the eigenfunctions u_ν, v_ν and eigenfrequencies ϵ_ν of elementary excitations follow from the system of linear equations:

$$\left\{ \begin{array}{rcl} \epsilon_\nu u_\nu & = & (-\hbar^2\Delta/2m + V(\mathbf{r}) - \mu + 2\tilde{U}|\Psi_0|^2)u_\nu - \tilde{U}\Psi_0^2 v_\nu, \\ -\epsilon_\nu v_\nu & = & (-\hbar^2\Delta/2m + V(\mathbf{r}) - \mu + 2\tilde{U}|\Psi_0|^2)v_\nu - \tilde{U}\Psi_0^{*2} u_\nu. \end{array} \right. \tag{2.3.7}$$

Similar equations have been found by De-Gennes [54] for inhomogeneous superconductors, and now Eqs.(2.3.5) are called Bogolyubov-De Gennes equations. The eigenfunctions are normalized by the condition

$$\int d^3r(|u_\nu|^2 - |v_\nu|^2) = 1. \tag{2.3.8}$$

Together with Eq.(2.3.6), this allows one to rewrite the Hamiltonian (2.2.1) in the form

$$\hat{H} = \hat{H}_0 + \sum_\nu \epsilon_\nu b_\nu^\dagger b_{\nu,} \tag{2.3.9}$$

where H_0 is the ground state (condensate) energy. This Hamiltonian may be interpreted as the sum of the ground state energy and the energies of excitations (Bogolyubov quasiparticles) characterized by the operators b_ν and $b_\nu^\dagger$. The commutation relations (2.3.8) ensure that the pair $b_\nu, b_\nu^\dagger$ is a pair of Boson annihilation/creation operators and thus the operator $b_\nu^\dagger b_\nu$ is an operator of the occupation number of the state ν. In thermal equilibrium we have $\langle b_\nu^\dagger b_\nu \rangle = N_B(\epsilon_\nu)$. Since the number of quasiparticles is not conserved, the chemical potential of the gas of excitation is zero [31].

For the spatially homogeneous case Eqs.(2.3.7) are solved for pairs $u_\mathbf{k}, v_\mathbf{k}$ in the form of plain waves characterized by the wavevector $\mathbf{k}$. The corresponding eigenfrequencies are given by the Bogolyubov dispersion law

$$\epsilon_k = \sqrt{\left(\frac{\hbar^2 k^2}{2m}\right)^2 + \mu\frac{\hbar^2 k^2}{m}}. \tag{2.3.10}$$

For large k, such that $\epsilon_k \gg \mu$, the dispersion relation (2.3.10) recovers the Hamiltonian of a classical particle moving in the mean field of the condensate

$$\epsilon_k = \frac{\hbar^2 k^2}{2m} + n_0\tilde{U}.$$

In the opposite limiting case, for small k, the dispersion relation is linear in k:

$$\epsilon_k = c_S k, \tag{2.3.11}$$

and the corresponding elementary excitations are sound waves (phonons) propagating with the velocity $c_S = \sqrt{\hbar^2\mu/m}$, which depends on the interparticle interaction.

The spectrum of elementary excitations of a trapped Bose-condensed gas, following from Eqs. (2.3.7), depends on the trapping potential $V(\mathbf{r})$. For the low-energy excitations ($\varepsilon_\nu \ll \mu$) of Thomas-Fermi condensates in harmonic traps the problem has been solved analytically [55–57]. For example, in a spherically symmetric trap elementary excitations are characterized by three quantum numbers: angular momentum l, its projection m, and the principle quantum number n counting the number of nodes for the radial part of the wavefunction. Due to a finite size of the condensate the energy spectrum is discrete. It is given by the relation [55]

$$\epsilon_{nl} = \hbar\omega(2n^2 + 2nl + 3n + l)^{1/2}, \tag{2.3.12}$$

(here the states belonging to the same value of l and different m are degenerate). For the lowest spherically symmetric excitation (breathing mode) we have $n = 1$, $l = 0$ and $\epsilon_{10} = \hbar\omega\sqrt{5}$, in

full agreement with the result of the scaling theory (2.3.4). Inside the condensate spatial region the normalized wavefunctions ($f_\nu^\pm = u_\nu \mp v_\nu$) are given by

$$f_{nl}^{\pm} = \left(\frac{(4n+2l+3)}{l_c^3}\right)^{1/2} \left(\frac{2\mu(1-r^2/l_c^2)}{\epsilon}\right)^{\pm 1/2} \left(\frac{r}{l_c}\right)^l P_n^{(l+1/2,0)}\left(1-2\frac{r^2}{l_c^2}\right),$$

where $P_n^{(a,b)}(r)$ are classical Jacobi polynomials. Outside the condensate spatial region the wavefunctions $f_{nl}^+ = f_{nl}^-$ and coincide with the wavefunction of a particle (with energy ϵ_{nl}) in the harmonic oscillator potential.

For the case of cylindrical symmetry the wavefunctions have a similar form [56, 57]

$$f_\nu^\pm = \left(\frac{2\mu(1-\tilde\rho^2-\tilde z^2)}{\varepsilon_\nu}\right)^{\pm 1/2} W(\tilde\rho,\tilde z),$$

where $\tilde\rho = \rho/l_\rho$, $\tilde z = z/l_z$ and $W(\tilde\rho,\tilde z) = \rho^{|m|}B_{nm}(\rho,z)\exp(im\phi)$, with m being the projection of the angular momentum on the symmetry axis, and $B_{nm}(\tilde\rho,\tilde z)$ polynomials of $\tilde\rho$ and $\tilde z$. These polynomials and the corresponding eigenenergies ε_ν can be found from the equations

$$\begin{aligned}[(1-\tilde\rho^2-\tilde z^2)(\frac{\partial^2}{\partial\tilde\rho^2}+\frac{(2|m|+1)}{\tilde\rho}\frac{\partial}{\partial\tilde\rho}+\beta^2\frac{\partial^2}{\partial\tilde z^2}) &- 2(\tilde\rho\frac{\partial}{\partial\tilde\rho}\\ +\beta^2\frac{\partial^2}{\partial\tilde z^2}) + 2(\frac{\epsilon_{nm}^2}{\hbar^2\omega_\rho^2}-m)]B_{nm}(\tilde\rho,\tilde z) &= 0,\end{aligned}$$

where $\beta = \omega_z/\omega_\rho$ is the ratio of the axial to radial frequency. Quadrupole oscillations with $m=2$ ($n=0$) are purely radial, and $\varepsilon_{02} = \sqrt{2}\hbar\omega_\rho$. For the quadrupole oscillations with $m=0$ ($n=2$) there are two coupled frequencies [45, 55, 58]:

$$\epsilon_{20}^{\pm} = \hbar\omega_\rho\left[2+\frac{3}{2}\beta^2 \pm \sqrt{(2-\frac{3}{2}\beta^2)^2+2\beta^2}\right]^{1/2}.$$

The frequencies ϵ_{02} and ϵ_{20}^- were studied experimentally in details by the JILA [48] and MIT [49] groups. The measured values of the frequencies for small temperatures agree well with the above outlined results of the mean field theory [45, 55, 58]. In later experiments at higher temperatures also temperature-dependent frequency shifts and damping of the elementary excitations have been observed [50, 51]. These effects originate from the interaction between quasiparticles and thus their description requires a development of beyond mean-field description of trapped Bose-condensed gases. Such a theory is presented in Chapter 5 and allows us to calculate higher order corrections (with respect to small gaseous parameter (n_0a^3)) to the eigenenergies of the excitations.

2.4. Superfluidity and vortices.

The form of the energy spectrum of low energy excitations is closely related to the phenomenon of superfluidity (in liquid helium observed as viscous-free flow) [31]. Consider a liquid flowing with a constant velocity v along a capillary. Due to the presence of viscosity, i.e. the friction of the liquid against the walls or the friction within the liquid itself, the kinetic energy of the liquid would be dissipated and the flow would gradually slow down. It is more convenient to discuss the flow in a reference frame moving with the liquid. In such a system the liquid is at rest and the walls of the capillary move with velocity $-v$. Once the viscosity is present, the liquid should start moving. This motion arises from the appearance of elementary excitations in the liquid. Suppose that an elementary excitation characterized by momentum p and energy ϵ_p appears in the liquid. Then, since the liquid is not moving, the energy of the liquid E_0 is equal to the energy of the excitation ϵ_p and the momentum of the liquid P_0 is equal to the momentum of the excitation, p. Returning to the reference frame, where

the capillary is at rest, we recalculate the momentum and energy by using the well-known Galilean transform:

$$E = E_0 + \mathbf{P}_0\mathbf{v} + Mv^2/2,$$

$$\mathbf{P} = \mathbf{P}_0 + M\mathbf{v},$$

where M is the mass of the liquid. Setting $\mathbf{P}_0 = \mathbf{p}$ and $E_0 = \varepsilon_p$, we have

$$E = \epsilon_p + \mathbf{pv} + Mv^2/2.$$

Since $Mv^2/2$ is the initial energy of the moving liquid, the energy change due to the appearance of the excitation is $\Delta\epsilon = \epsilon_p + \mathbf{pv}$, and in order to initiate the motion of the liquid this quantity should be negative.

The energy change $\Delta\epsilon$ is minimum when $\mathbf{p}$ and $\mathbf{v}$ are antiparallel, and the condition $\Delta\epsilon < 0$ is equivalent to

$$v > \epsilon_p/p. \tag{2.4.1}$$

This condition for the occurrence of excitations in a moving liquid should be fullfiled for at least some values of p. Hence, finding the condition of the existence of dissipativeless (superfluid) flow is equivalent to finding the minimum of ϵ_p/p. Geometrically, this ratio is a slope of the line (in the (p, ϵ_p)-plane) linking the origin and a given point on the ϵ_p curve. Its minimum value is given by the point at which the line coincides with the tangent of the curve. If this minimum is not zero, then for the liquid moving with velocity less than a certain value the dissipation ceases and the liquid exhibits the phenomenon of superfluidity. The application of this criterion to the dispersion relation (5.2.18) shows, that a spatially homogeneous dilute Bose-condensed gas can flow without friction with velocities less than the speed of sound c_S. The condition (2.4.1) is known as the Landau condition for the critical velocity.

The demonstration of superfluidity in a trapped Bose-condensed gas is not an easy task, since a trapped condensate is a comparatively small finite system. As the size of the condensate in the trap is $l_c = (2\mu/m\omega^2)^{1/2}$, the lowest possible wavevector $k \sim 1/l_c$. Then, according to Eq.(2.3.11), for the lowest phonon-like excitations we obtain $\epsilon \sim \hbar\omega$, which agrees with the result of Eq.(2.3.12). Clearly, the system can not be excited by an external perturbation with frequency below the trap frequency, and this property has nothing to do with Bose condensation. It is just a consequence of the finite size of the system.

The manifestation of superfluidity in trapped condensates can be found through the creation and observation of macroscopically excited Bose-condensed states, such as vortices carrying persistent currents. The existence quantized vortices follows from general properties of a superfluid flow and therefore is inherent to any superfluid system. Remarkably, much of the physical properties of the vortex states, as well as their dynamics, can be understood from general considerations, without even using the microscopic Hamiltonian (2.2.1).

Calculating the current density for the wavefunction (2.2.6) we obtain

$$\mathbf{j}_{cond} = \frac{i\hbar}{m}(\Psi_0^*\nabla\Psi_0 - \nabla\Psi_0^*\Psi_0) = \frac{\hbar}{m}n_0\nabla\Phi.$$

This quantity has a meaning of macroscopic current density associated with condensate particles. This motion may exist even in thermodynamic equilibrium. It is non-dissipative and therefore the velocity

$$\mathbf{v}_S = \frac{\hbar}{m}\boldsymbol{\nabla}\Phi \tag{2.4.2}$$

determines the velocity of superfluid flow.[4] As it is obvious from this equation, the superfluid motion is potential flow, i.e. $\mathrm{rot}\mathbf{v}_S = 0$ (the latter property is also known as irrotational nature of a superfluid flow).

This brings a very important difference in the rotational properties of normal and superfluid liquids. Consider a classical liquid in a vessel rotating with angular velocity $\mathbf{\Omega}$. Due to friction against the walls, the liquid as a whole would be gradually driven into rotation together with the vessel. In a superfluid, only the "normal" component, i.e. the gas of excitations, follows the rotation of the walls, while the superfluid component remains at rest. In fact, it can not rotate as a whole, since such a motion would imply $\mathbf{v}_S = \mathbf{\Omega} \times \mathbf{r}$ for the velocity $\mathbf{v}_S$ at a given point $\mathbf{r}$. Then $\mathrm{rot}\mathbf{v}_S = 2\mathbf{\Omega}$, which contradicts with the property of irrotational flow for a superfluid in motion.

At the same time, for sufficiently large $\mathbf{\Omega}$ the state with the superfluid at rest becomes thermodynamically unstable. In fact, the energy of the system in the rotating frame is given by

$$E' = E - (\mathbf{M}\mathbf{\Omega}),$$

where E and $\mathbf{M}$ are the energy and angular momentum of the superfluid in the lab frame. The condition of thermodynamic equilibrium is that this quantity is a minimum. For a sufficiently fast rotation the state with $M \neq 0$ has lower energy that the $M = 0$ state, i.e. the superfluid motion should eventually occur. The apparent contradiction of this statement with the irrotational nature of superfluid flow is solved by the assumption that the vorticity occurs only on certain lines inside the liquid, where the velocity is singular. The rest of the liquid executes the motion with $\mathrm{rot}\mathbf{v}_S = 0$. These lines are known as vortex lines or vortex filaments. In a finite system they either terminate on the surface of the liquid or exist in the form of closed loops (vortex rings).

The superfluid velocity $\mathbf{v}_S$ is singular at the vortex line and, hence, the circulation of $\mathbf{v}_S$ along the contour C embracing the vortex is not zero and has a finite value, say $2\pi\kappa$:

$$\oint_C \mathbf{v}_S d\mathbf{l} = 2\pi\kappa. \tag{2.4.3}$$

Using (2.4.2), we see that the same contour integral is equal to $\hbar\delta\Phi/m$, where $\delta\Phi$ is the phase change along the contour. The latter quantity has to be an integer multiplier of 2π, which immediately leads to the quantization of circulation [59]:

$$\kappa = \frac{\hbar}{m} Z,$$

where Z is an integer called the charge of the vortex.

Eq.(2.4.3) is sufficient for finding the velocity field surrounding the vortex. This equation is similar to the Stokes theorem in magnetostatics, with the magnetic field replaced by $\mathbf{v}_S$ and electric currents being analogous the vortex filaments. Therefore, the solution of Eq.(2.4.3) can be obtained by using the Biot-Savart law. For an infinitely long vortex line we have $\mathbf{v}_S(\mathbf{r}) = [\boldsymbol{\kappa} \times \hat{\mathbf{r}}]/r$, where $\mathbf{r}$ is the distance from the vortex filament, and $\boldsymbol{\kappa}$ is the vector along the vortex line, with the modulus equal to the vortex circulation. This shows the presence of a persistent current around the vortex line. Interaction of a vortex with the thermal background causes the appearance of mutual friction forces leading to the dissipative dynamics and eventual decay of vortex states in trapped Bose-condensed gases.

[4] Although the velocity of superfluid flow coincides with the velocity of condensate particles, the density of superfluid component differs from the condensate density. This follows already from the fact that at zero temperature the entire liquid is superfluid, whereas the number of particles in the condensate can be as low as 10%, according to the measurements in liquid He.

CHAPTER 3

Two and three body interactions in ultra-cold gases.

3.1. Three-body recombination of ultra-cold atoms to a weakly bound s level

We discuss three-body recombination of ultra-cold atoms to a weakly bound s level. In this case, characterized by large and positive scattering length a for pair interaction, we find a repulsive effective potential for three-body collisions, which strongly reduces the recombination probability and makes simple Jastrow-like approaches absolutely inadequate. In the zero temperature limit we obtain a universal relation, independent of the detailed shape of the interaction potential, for the (event) rate constant of three-body recombination: $\alpha_{rec} = 3.9\hbar a^4/m$, where m is the atom mass.

Three-body recombination, the process in which two atoms form a bound state and a third one carries away the binding energy, is an important issue in the physics of ultra-cold gases. This process represents the initial stage in the formation of clusters intermediate in size between individual atoms and bulk matter. Three-body recombination limits achievable densities in high-field-seeking spin-polarized atomic hydrogen [60–63] and in trapped alkali atom gases (see [64] and references therein) and, hence, places limitations on the possibilities to observe Bose-Einstein condensation in these systems.

Extensive theoretical studies of three-body recombination in ultra-cold hydrogen [60–63] and alkalis [64] showed that the rate constant of this process, $\alpha_{\rm rec}$, strongly depends on the shape of the potential of interaction between atoms and on the energies of bound states in this potential. In alkalis the recombination is caused by elastic interatomic interaction, and in the zero temperature limit $\alpha_{\rm rec}$ varies approximately as a^2 [64], where a is the scattering length for pair interaction.

All these studies, except one in spin-polarized hydrogen (see [61–63]), rely on Jastrow-like approximations for the initial-state wavefunction of three colliding atoms. Recent progress in the quantum three-body problem for the case where only zero orbital angular momenta of particle motion are important [65] opens a possibility for rigorous calculations of three-body recombination in ultra-cold atomic gases. In this Section we consider the extraordinary case of recombination (induced by elastic interaction between atoms) to a weakly bound s level. The term "weakly bound" means that the size l of the diatomic molecule in this state is much larger than the characteristic radius of interaction R_e (the phase shift for s-wave scattering comes from distances $r < R_e$). In this case the scattering length is positive and related to the binding energy ε_0 by (see, e.g., [66])

$$a = \hbar/\sqrt{m\varepsilon_0} \sim l \gg R_e \tag{3.1.1}$$

(m is the atom mass), and elastic (s-wave) scattering in pair collisions is resonantly enhanced at collision energies $E \ll \varepsilon_0$. As we show, large a and l imply a rather large recombination rate constant $\alpha_{\rm rec}$. At the same time, for large positive a we find a repulsive effective potential for three-body collisions, which strongly reduces $\alpha_{\rm rec}$. In the limit of ultra-low initial energies $E \ll \varepsilon_0$ we obtain a universal relation independent of the detailed shape of the interaction potential: $\alpha_{\rm rec} = 3.9\hbar a^4/m$.

The dependence $\alpha_{\rm rec} \propto a^4$ can be understood from qualitative arguments. For atoms of equal mass the energy conservation law for the recombination process reads

$$3\hbar^2 k_f^2/4m = \varepsilon_0, \tag{3.1.2}$$

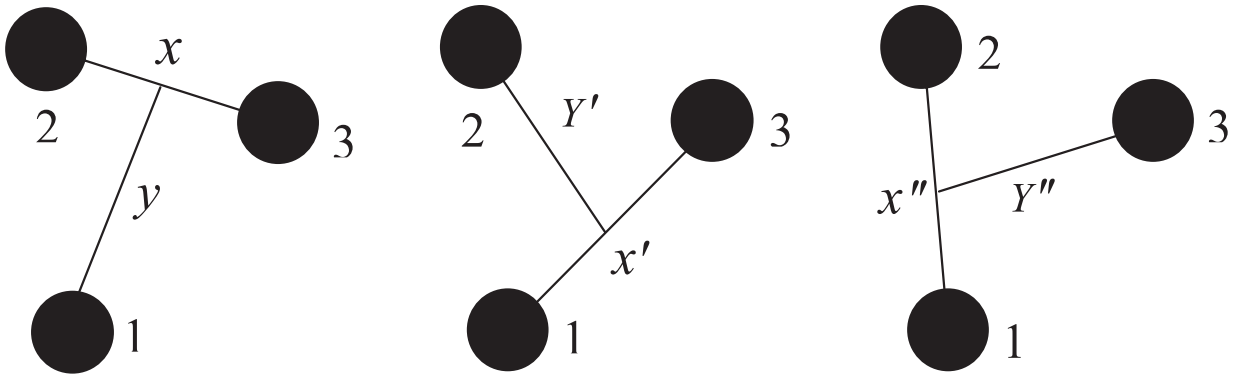

FIGURE 3.1.1. Three possible sets of coordinates for a three-body system. The relative coordinates are **x**, between two particles, and **y**, between their center of mass and the third particle.

where $k_f \sim 1/a$ is the final-state momentum of the third atom relative to the center of mass of the molecule. Recombination to a weakly bound s level occurs in a collision between two atoms, when a third atom is located inside a sphere of radius $l \sim a$ around the colliding pair. For such locations of the third atom, characterized by a statistical weight $w \sim nl^3$ (n is the gas density), this atom and one of the colliding atoms form the weakly bound state with probability of order unity. The number of recombination events per unit time and unit volume, $\nu_{\text{rec}} = \alpha_{\text{rec}} n^3$, can be estimated as $n^2 \sigma v (nl^3)$, where $\sigma = 8\pi a^2$ is the cross section for pair collisions. One may put velocity $v \sim \hbar k_f/m$, which gives $\alpha_{\text{rec}} \sim 8\pi\hbar a^4/m$.

One can also understand qualitatively the existence of a repulsive effective potential for three-body collisions and the reduction of α_{rec}. In the mean field picture the interaction in a three-body system at (maximum of the three) interparticle separations $r \gg R_e$ can be written as $4\pi\hbar^2 n_* a/m$, where $n_* \sim 1/r^3$ is the "particle density" inside a sphere of radius r. For $a > 0$ this interaction is repulsive, which makes the statistical weight w smaller than nl^3 and decreases the numerical coefficient in the above estimate for α_{rec}. The tail of the three-body effective potential at $r \gg a$ was found in [67]. Arguments clearly showing the absence of any "kinematic" repulsion independent of the value and sign of a are given in [68].

A particular system that should exhibit three-body recombination to a weakly bound s level is a gas (or a beam) of helium atoms. The He-He potential of interaction $V(r)$ has a well with a depth of 11 K. There is only one bound state in this well, with orbital angular momentum $j = 0$ and binding energy $\varepsilon_0 \approx 1.3$ mK (see [69] and references therein). The scattering length $a \approx 100$ Å found for this potential satisfies criterion (3.1.1). The existence of the He_2 dimer, the world's largest diatomic molecule ($l \approx 50$ Å), has been established experimentally [70]. Another system which is likely to have three-body recombination to a weakly bound s level is spin-polarized metastable triplet helium, a gas of helium atoms in the 2^3S state with spins aligned. The interaction potential [71] for a pair of spin-polarized He(2^3S) atoms supports an s level with binding energy $\varepsilon_0 \approx 2$ mK, which leads to $a \sim 100$ Å and important consequences for the decay kinetics of this system [72, 73].

We confine ourselves to three-body recombination of identical atoms at collision energies $E \ll \varepsilon_0$ to a weakly bound molecular s level. In this case the recombination rate constant α_{rec} can be found from the equation

$$\nu_{\text{rec}} = \alpha_{\text{rec}} n^3 = \frac{2\pi}{\hbar} \int \frac{d^3k_f}{(2\pi)^3} |T_{if}|^2 \delta\left(\frac{3\hbar^2 k_f^2}{4m} - \varepsilon_0\right) \times \frac{n^3}{6}. \tag{3.1.3}$$

Here $n^3/6$ stands for the number of triples in the gas, $T_{if} = \int \psi_i \tilde{V} \psi_f^{(0)*} d^3x d^3x'$ is the T-matrix element for three-body recombination, the coordinates $(\mathbf{x}, \mathbf{x}')$ are specified in Fig. 3.1.1, ψ_i is the true

wavefunction of the initial state of the triple, and $\psi_f^{(0)}$ is the wavefunction of free motion of the third atom relative to the center of mass of the molecule formed in the recombination event. Both ψ_i and $\psi_f^{(0)}$ can be written as a sum of three components, each expressed in terms of one of the three different sets of coordinates (see Fig. 3.1.1):

$$\psi_i = \tilde{\psi}(\mathbf{x},\mathbf{y}) + \tilde{\psi}(\mathbf{x}',\mathbf{y}') + \tilde{\psi}(\mathbf{x}'',\mathbf{y}''), \tag{3.1.4}$$

$$\begin{aligned} \psi_f^{(0)} = \quad & (1/\sqrt{3})[\phi(\mathbf{x},\mathbf{y}) + \phi(\mathbf{x}',\mathbf{y}') + \phi(\mathbf{x}'',\mathbf{y}'')], \\ & \phi(\mathbf{x},\mathbf{y}) \equiv \psi_0(x)\exp(i\mathbf{k}_f\mathbf{y}), \end{aligned} \tag{3.1.5}$$

where ψ_0 is the wavefunction of the weakly bound molecular state. The interaction between colliding atoms is regarded as a sum of pair interactions $V(r)$. The quantity $\tilde{V}$ is the part of the interaction which is not involved in constructing the wavefunction (3.1.5), i.e., if the molecule is formed by atoms 1 and 2 (the first term in Eq.3.1.5), then $\tilde{V} = V(\mathbf{r}_1 - \mathbf{r}_3) + V(\mathbf{r}_2 - \mathbf{r}_3)$, et cet. Using Eq.(3.1.5),

$$T_{if} = 2\sqrt{3}\int d^3x d^3x' \psi_0(x)\cos\left(\frac{\mathbf{k}_f\mathbf{x}}{2}\right)V(x')\exp(-i\mathbf{k}_f\mathbf{x}')\psi_i. \tag{3.1.6}$$

The initial wavefunction of the triple is best represented in hyperspherical coordinates. The hyperradius, defined as $\rho = (x^2/2 + 2y^2/3)^{1/2}$, is invariant with respect to the transformations $x, y \to x', y' \to x'', y''$. The hyperangles are defined as $\alpha = \arctan(\sqrt{3}x/2y)$, and similarly for α' and α''. For $E \ll \varepsilon_0$ only zero orbital angular momenta of the particle motion are important, and the wavefunction $\tilde{\psi}$ can be written as [65]

$$\tilde{\psi} = \sum_\lambda \frac{F_\lambda(\rho)}{\sqrt{6}} \frac{\Phi_\lambda(\alpha,\rho)}{\sin\alpha\cos\alpha}. \tag{3.1.7}$$

The functions $\Phi_\lambda(\alpha,\rho)$ are determined by the equation

$$\frac{\partial^2\Phi_\lambda(\alpha,\rho)}{\partial\alpha^2} + \frac{2m}{\hbar^2}V(\sqrt{2}\rho\sin\alpha)\rho^2\left(\Phi_\lambda(\alpha,\rho) + \frac{4}{\sqrt{3}}\int_{|\pi/3-\alpha|}^{\pi/2-|\pi/6-\alpha|} d\alpha'\Phi_\lambda(\alpha',\rho)\right) = \lambda(\rho)\Phi_\lambda(\alpha,\rho), \tag{3.1.8}$$

with boundary conditions $\Phi_\lambda(0,\rho) = \Phi_\lambda(\pi/2,\rho) = 0$ and normalization $\int_0^{\pi/2}|\Phi_\lambda(\alpha,\rho)|^2 d\alpha = \pi/4$. The sum in Eq.(3.1.7) is over all eigenvalues λ corresponding to three free atoms at infinite interparticle separation. At ultra-low collision energies the lowest such $\lambda(\rho)$ alone gives a very good approximation, and we can confine ourselves to this λ. Then the function $F_\lambda(\rho)$ can be found from the (hyper)radial equation in which the quantity $\lambda(\rho)$ serves as an effective potential [65]. Under the condition $E \ll \varepsilon_0$ at interparticle distances much smaller than their De Broglie wavelength this equation reads

$$\left(-\frac{\partial^2}{\partial\rho^2} - \frac{5}{\rho}\frac{\partial}{\partial\rho} + \frac{\lambda(\rho)-4}{\rho^2}\right)F_\lambda(\rho) = 0. \tag{3.1.9}$$

The function $F_\lambda(\rho)$ should be finite for $\rho \to 0$ and is normalized such that $F_\lambda(\rho) \to 1$ for $\rho \to \infty$.

In our case the pair interaction potential $V(r)$ supports a weakly bound s level, and the scattering length is positive and much larger than the characteristic radius of interaction R_e for this potential. For $\rho \gg R_e$ the function $\Phi_\lambda(\alpha,\rho)$ takes the form (cf. [65])

$$\Phi_\lambda(\alpha,\rho) = \begin{cases} g(\rho)\alpha\left[\left(\sqrt{2}\rho/a\right)\sin(\pi\sqrt{\lambda}/2)\chi_0(\sqrt{2}\rho\alpha) + (8/\sqrt{3})\sin(\pi\sqrt{\lambda}/6)\right], \alpha < R_e/\rho \\ g(\rho)\sin\left[\sqrt{\lambda}\,(\alpha - \pi/2)\right], \alpha > R_e/\rho, \end{cases} \tag{3.1.10}$$

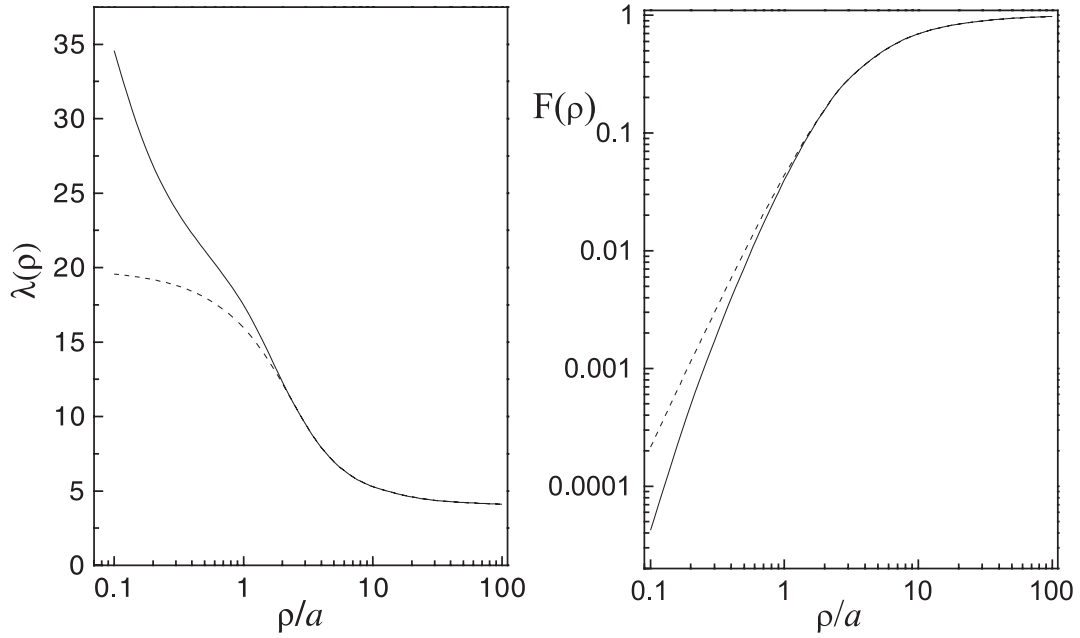

FIGURE 3.1.2. (left) The "effective potential" λ as a function of ρ/a. The solid curve is obtained from Eq.(3.1.8) using the ground state He-He potential ($a = 100$Å), and the dashed from Eq.(3.1.12). (right) The wavefunction $F_\lambda(\rho/a)$ obtained from Eq.(3.1.9). The solid curve corresponds to $\lambda(\rho)$ for the ground state He-He potential, and the dashed curve to $\lambda(\rho)$ from Eq.(3.1.12).

where $g(\rho) = [1 + \sin(\pi\sqrt{\lambda})/\pi\sqrt{\lambda}]^{-1/2}$ and $\chi_0(r)$ is the solution of the Schrödinger equation for the relative motion of a pair of particles,

$$\left[-\frac{\hbar^2}{m}\left(\frac{\partial^2}{\partial r^2} + \frac{2}{r}\frac{\partial}{\partial r}\right) + V(r)\right]\chi_0(r) = 0, \tag{3.1.11}$$

normalized such that $\chi_0 \to 1 - a/r$ as $r \to \infty$. Matching the wavefunctions (3.1.10) at $\alpha = R_e/\rho \ll 1$, to zero order in R_e/ρ we obtain the following relation for $\lambda(\rho)$ at distances $\rho \gg R_e$ (cf. [65]):

$$\frac{\sqrt{2}\rho}{a}\sin\left(\sqrt{\lambda}\frac{\pi}{2}\right) + \frac{8}{\sqrt{3}}\sin\left(\sqrt{\lambda}\frac{\pi}{6}\right) = \sqrt{\lambda}\cos\left(\sqrt{\lambda}\frac{\pi}{2}\right). \tag{3.1.12}$$

For $\rho \gg a$ this equation yields $\lambda(\rho) = 4 + 48a/\sqrt{2}\pi\rho$, and thus the potential term in Eq.(3.1.9) varies as a/ρ^3. Eq.(3.1.12) is universal in the sense that λ depends only on the ratio ρ/a, but not on the detailed shape of $V(r)$. The same statement holds for $F_\lambda(\rho)$ at distances $\rho \gg R_e$.

For infinite separation between particles, i.e., for $\rho \to \infty$ and all hyperangles larger than R_e/ρ, we have $\sqrt{\lambda} \approx 2$ and $\Phi_\lambda(\alpha, \rho) \approx \sin 2\alpha$. Accordingly, from Eq.(3.1.7) with $F_\lambda(\rho) \to 1$, each $\tilde{\psi}$ in Eq.(3.1.4) becomes equal to $\sqrt{2/3}$, and the initial wavefunction $\psi_i \to \sqrt{6}$.

The "effective potential" $\lambda(\rho)$ and the function $F_\lambda(\rho)$ for three ground-state He atoms ($a \approx 100$Å) are presented in Fig. 3.1.2. The potential $V(r)$ was taken from [69]. For $\rho > 100$Å our numerically calculated $\lambda(\rho)$ coincides (within 10%) with that following from Eq.(3.1.12), ensuring a universal dependence of F_λ on ρ/a. As $\lambda(\rho)$ is repulsive, F_λ is strongly attenuated at $\rho < a$ (see Fig. 3.1.2). This leads to a strong reduction of ψ_i when all three particles are within a sphere of radius $\sim a$.

We first consider the theoretical limit of weak binding, where the scattering length a and the binding energy ε_0 are related by Eq.(3.1.1), the wavefunction of the bound molecular state at distances

$x \gg R_e$ is

$$\psi_0(x) = \frac{1}{\sqrt{2\pi a}} \frac{1}{x} \exp\left(-\frac{x}{a}\right), \tag{3.1.13}$$

and the final momentum $k_f = 2/\sqrt{3}a$. From Eq.(3.1.13) one can see that the distance between the two atoms which will form the bound state should be of order a. To take away the binding energy the third atom should approach one of them to a distance of order R_e. The main contribution to the integral in Eq.(3.1.6) comes from distances $x \sim a$ and $x' \sim R_e \ll a$. Therefore we may put $\rho \approx \sqrt{2/3}x$, $\alpha = \alpha'' \approx \pi/3$, and $\alpha' \approx \sqrt{3}x'/2x$. Then the initial wavefunction takes the form

$$\psi_i \approx (1/\sqrt{3})\chi_0(x')\tilde{F}_\lambda(\sqrt{2}x/\sqrt{3}a), \tag{3.1.14}$$

with $\tilde{F}_\lambda(z) = zF_\lambda(z)g(z)\sin(\sqrt{\lambda(z)}\pi/2)$ and $z = \rho/a$. Putting $\mathbf{k}_f\mathbf{x}' \approx 0$ and using $\int d^3x' V(x')\chi_0(x') = 4\pi\hbar^2 a/m$, from Eq.(3.1.6) we obtain $T_{if} = 48\pi^{3/2}\hbar^2 a^{5/2} G/m$, where

$$G = \int_0^\infty dz \sin(z/\sqrt{2}) \exp(-z\sqrt{3/2})\tilde{F}_\lambda(z). \tag{3.1.15}$$

The main contribution to this integral comes from $z \sim 1$ ($\rho \sim a$), where λ and F_λ (and, hence, $\tilde{F}_\lambda$) are universal functions of ρ/a. Therefore G is a universal number independent of the potential $V(r)$. Direct calculation yields $G = 0.0364$. With the above T_{if} and G, from Eq.(3.1.3) we arrive at the recombination rate constant

$$\alpha_{\rm rec} = \frac{512\pi^2 G^2}{\sqrt{3}} \frac{\hbar}{m} a^4 \approx 3.9 \frac{\hbar}{m} a^4. \tag{3.1.16}$$

The dependence $\alpha_{\rm rec} \propto a^4$, instead of $\alpha_{\rm rec} \propto a^2$, is a consequence of the recombination to a weakly bound s level and can be also obtained within the Jastrow approximation for the initial wavefunction: $\psi_{iJ} = \sqrt{6}\chi_0(\mathbf{r}_1 - \mathbf{r}_2)\chi_0(\mathbf{r}_2 - \mathbf{r}_3)\chi_0(\mathbf{r}_3 - \mathbf{r}_1)$. This approximation was proved to be a good approach for atomic hydrogen [61–63] and was later used for alkali atoms [64]. In our case, instead of Eq.(3.1.14), we obtain $\psi_{iJ} \approx \sqrt{6}\chi_0(x')\chi_0^2(x)$ and arrive at Eq.(3.1.16), with 4 orders of magnitude larger numerical coefficient. Such a very large discrepancy occurs because both results are determined by distances $x \sim a$, where in our (rigorous) theory ψ_i is strongly reduced by the repulsive effective potential (see above). In the Jastrow approximation this reduction is not present. Moreover, ψ_{iJ} is resonantly enhanced at distances $x < a$. Thus, for large a the Jastrow approximation gives a wrong picture of three-body collisions and is absolutely inadequate to describe recombination to a weakly bound s level.

The strong reduction of $\alpha_{\rm rec}$ due to the presence of a repulsive effective potential for three-body collisions can be treated as "quantum suppression" of three-body recombination (see related discussions in [68, 74]). Nevertheless, $\alpha_{\rm rec}$ remains finite in the zero temperature limit. In fact, due to large values of a, it is rather large. It is also worth noting that for large and *negative* scattering length the quantity $\lambda(\rho)$ should have the form of a potential well, with a repulsive core at small ρ, and the picture of recombination collisions can be completely different.

In trapped gases the kinetic energy of the third atom acquired in the recombination process usually exceeds the trap barrier, and such atoms escape from the trap. Thus, the loss rate for atoms is $\dot{n} = -Ln^3$, with $L = 3\alpha_{\rm rec}$. For three-body recombination of ground-state He atoms Eq.(3.1.16) gives $L \approx 2 \cdot 10^{-27}$ cm^6/s. As the He-He interaction has $R_e \sim 15$Å$\ll a$, this value of L is a very good approximation. More accurate calculation, using $\lambda(\rho)$ and $F_\lambda(\rho)$ determined for the He-He interaction (solid curves in Fig. 3.1.2), gives a correction of 10%. The same L is obtained for three-body recombination of spin-polarized He(2^3S) atoms. In this case the result is less accurate, since the characteristic radius of interaction is somewhat larger ($R_e \sim 35$Å).

Qualitatively, the picture of an effective repulsion in three-body collisions, implying a strong reduction in the recombination rate constant, can be valid for systems with positive scattering length $a \sim R_e$. One can find such systems among the ultra-cold alkali atom gases.

3.2. Influence of resonant light on the scattering length in ultra-cold gases.

We develop the idea of manipulating the scattering length a in low-temperature atomic gases by using nearly resonant light. As found, if the incident light is close to resonance with one of the bound p levels of electronically excited molecule, then virtual radiative transitions of a pair of interacting atoms to this level can significantly change the value and even reverse the sign of a. The decay of the gas due to photon recoil, resulting from the scattering of light by single atoms, and due to photoassociation can be minimized by selecting the frequency detuning and the Rabi frequency. Our calculations show the feasibility of optical manipulations of trapped Bose condensates through a light-induced change in the mean field interaction between atoms, which is illustrated for $^7\mathrm{Li}$.

The recent successful experiments on Bose-Einstein condensation (BEC) in magnetically trapped gases of Rb [3], Li [5] and Na [4] have generated a lot of interest in macroscopic quantum behavior of atomic gases at ultra-low temperatures. These experiments were enabled by efficient evaporative [22, 23] and optical cooling [20, 21] methods combined to reach the necessary temperatures ($T < 1\mu$ K) and densities $10^{12} < n < 10^{14}$ cm^{-3}.

A principal question for BEC in atomic gases concerns the sign of the scattering length a for the pair elastic interaction. For $a > 0$ elastic interaction between atoms is repulsive and the Bose condensate is stable with respect to this interaction. If $a < 0$ elastic interaction is attractive and this is the origin of a collapse of the condensate in a homogeneous gas [31]. For trapped gases with $a < 0$ the situation is likely to be the same, provided the interaction between particles exceeds the level spacing in the trapping field [32, 33]. If this interaction is much smaller than the level spacing, there is a gap for one-particle excitations and it is possible to form a metastable Bose-condensed state [33]. Among the alkalis there are atomic gases with positive as well as with negative a [34]. Also the magnetic field dependence of a was predicted [35].

In this Section we develop the idea of manipulating the value and the sign of the scattering length by using nearly resonant light. Since changing a directly affects the mean field interaction between the atoms, this offers a possibility to investigate macroscopic quantum phenomena associated with BEC by observing the evolution of a Bose condensed gas in response to light. Also optical control of cold elastic collisions is attracting interest [75, 76]. The physical picture of the influence of the light field on the elastic interaction between atoms is the following: A pair of atoms absorbs a photon and undergoes a virtual transition to an electronically excited quasimolecular state. Then it reemits the photon and returns to the initial electronic state at the same kinetic energy. As the interaction between atoms in the excited state is much stronger than in the ground state, already at moderate light intensities the scattering amplitude can be significantly changed.

The presence of the light field also induces inelastic processes, such as photon recoil and light absorption in pair collisions (with regard to cold collisions see refs. [77, 78] for review). Photon recoil is the result of the scattering of light by single atoms. At subrecoil temperatures, typical for achieving BEC, recoiling atoms are lost as they overcome the confining barrier and escape from the trap. The probability of light scattering by single atoms is proportional to $(\Omega/\delta)^2$, where Ω is the Rabi frequency and δ is the frequency detuning of the light with respect to a single atom at rest. To suppress the recoil losses the ratio Ω/δ needs to be sufficiently small. Then, for positive δ, where the light is at resonance with continuum states of excited quasimolecules, the change of a will also be proportional to $(\Omega/\delta)^2$ and thus very small. To have small recoil losses in combination with a significant change of a, the detuning δ should be large and negative and not too far from a vibrational resonance with one of the bound p states of the electronically excited molecule. However, the vicinity of the resonance

will also lead to photoassociation in pair collisions, followed by spontaneous emission and loss from the trap. Hence, the frequency detuning δ_ν with respect to the ν-th (nearest) vibrational resonance should greatly exceed the line width of the resonance. We established that it is possible to change the scattering length substantially and even switch its sign without excessive recoil or photoassociation losses. This will be illustrated for ^{7}Li.

We consider low gas densities satisfying the condition

$$n\lambda^3 \ll 1, \tag{3.2.1}$$

where λ is the optical wavelength. Then collective optical effects [79,80] are absent, and at sufficiently low temperatures the line broadening of optical transitions is determined by the natural line width $\Gamma = 4d^2/3\hbar(\lambda/2\pi)^3$, where d is the transition dipole moment. We analyze the influence of incident light with large ($|\delta| \gg \Gamma$) and negative frequency detuning on the interaction in a pair of atoms, with vanishing wavevector of relative motion, $\mathbf{k} \to 0$. The light frequency is assumed to be nearly resonant with a highly excited vibrational p level (with vibrational quantum number ν and binding energy ε_ν) in the interaction potential $V(r)$ of the attractive excited electronic state of the quasimolecule, i.e., the frequency detuning with respect to this level, $\delta_\nu = \delta - \varepsilon_\nu$, is much smaller than the local vibrational level spacing $\Delta\varepsilon_\nu = \varepsilon_\nu - \varepsilon_{\nu+1}$ (hereafter all frequencies are given in energy units). Then radiative transitions of the pair from the ground electronic state to the excited level ν are most important. These transitions predominantly occur at interparticle distances r in the vicinity of the outer turning point r_t for the relative motion of atoms in the bound state v, i.e., $V(r_t) = -\varepsilon_\nu$. Unless ε_ν is very large, r_t is determined by the long-range part of $V(r)$, represented by the resonance dipole term. If ε_ν and $|\delta|$ are still much larger than the Zeeman and fine structure splitting, then at interparticle distances relevant for radiative transitions the polarization vector of the attractive excited quasimolecular state, $\mathbf{e}_\lambda$, is parallel to the internuclear axis, and $V(r) = -2d^2/r^3$. Hence, as $\varepsilon_\nu \sim |\delta| \gg \Gamma$, we have $r_t \ll \lambda$.

For sufficiently large ε_ν and δ spontaneous emission of excited molecules predominantly produces non-trapped atoms with kinetic energies of order ε_ν. These atoms practically do not interact with the driving light and escape from the trap. Therefore, the problem of finding the scattering length in the presence of light is equivalent to a scattering problem which can be be described in terms of wavefunctions of the ground and excited electronic quasimolecular states. These states are coupled by light, and spontaneous emission from the excited state can be taken into account by adding the "absorptive part" $-i\Gamma$ (the spontaneous emission rate for molecules is twice as large as that for single atoms) to the interaction potential $V(r)$.

In the Born-Oppenheimer approximation the total wavefunction of the quasimolecule in the presence of light can be written as $\phi(\mathbf{r})|g\rangle + \psi(\mathbf{r})|e\rangle$, where $|g>$ and $|e>$ are the electron wavefunctions of the ground and excited electronic states. The wavefunctions of the relative motion of atoms in these states, $\phi(\mathbf{r})$ and $\psi(\mathbf{r})$, can be found from the system of coupled Schrödinger equations:

$$-\frac{\hbar^2}{m}\,\triangle_{\mathbf{r}}\,\phi(\mathbf{r}) + U(r)\phi(\mathbf{r}) + \Omega\xi(\mathbf{r})\psi(\mathbf{r}) = 0, \tag{3.2.2}$$

$$-\frac{\hbar^2}{m}\triangle_{\mathbf{r}}\psi(\mathbf{r}) + (V(r) - i\Gamma - \delta)\psi(\mathbf{r}) + \Omega\xi(\mathbf{r})\phi(\mathbf{r}) = 0, \tag{3.2.3}$$

where $\xi(\mathbf{r}) = (\mathbf{e}_\alpha \mathbf{e}_\lambda(\mathbf{r}))$, $U(r)$ is the interaction potential in the ground electronic state, and $\mathbf{e}_\alpha$ the polarization vector of light. The Rabi frequency is defined as $\Omega = dE/\sqrt{2}$, where E is the amplitude of the electric field of light. In Eqs. (3.2.2) and (3.2.3) we neglect the light shifts at infinite separation between atoms and omit the recoil. These equations lead to the integral equation for $\phi(\mathbf{r})$:

$$\phi(\mathbf{r}) = \phi_0(\mathbf{r}) + \Omega^2 \int d\mathbf{r}'' d\mathbf{r}' G(\mathbf{r}'', \mathbf{r}) \xi(\mathbf{r}'') \tilde{G}(\mathbf{r}'', \mathbf{r}') \xi(\mathbf{r}') \phi(\mathbf{r}'). \tag{3.2.4}$$

Here $G(\mathbf{r}, \mathbf{r}')$ and $\tilde{G}(\mathbf{r}, \mathbf{r}')$ are the Green functions of Eqs. (3.2.2) and (3.2.3) with $\Omega = 0$. The wavefunction ϕ_0 describes the relative motion of atoms with zero energy for the potential $U(r)$ in the

absence of light. This function is a solution of Eq.(3.2.2) with $\Omega = 0$. The Green function $G(\mathbf{r}, \mathbf{r}')$ has the form

$$G(\mathbf{r}, \mathbf{r}') = \frac{m}{4\pi\hbar^2} \times \left\{ \begin{array}{c} \phi_0(r)\tilde{\phi}_0(r')\ r < r' \\ \tilde{\phi}_0(r)\phi_0(r'),\ r > r' \end{array} \right\} \tag{3.2.5}$$

where $\tilde{\phi}_0(r)$ is a solution of the same Schrödinger equation as that for $\phi_0(r)$, but contains only an outgoing spherical wave at large r: $\tilde{\phi}_0(r) \to 1/r$ for $r \to \infty$. As the frequency detuning of light was chosen such that $|\delta_\nu| \ll \Delta\varepsilon_\nu$, the bound state ν should give the dominant contribution to $\tilde{G}(\mathbf{r}, \mathbf{r}')$ and we may use

$$\tilde{G}(\mathbf{r}, \mathbf{r}') = -\psi_\nu(\mathbf{r})\psi_\nu^*(\mathbf{r}')/(\delta_\nu + i\Gamma), \tag{3.2.6}$$

where $\psi_\nu(\mathbf{r})$ is the wavefunction of this state in the absence of light. Accordingly, the dependence of the rhs of Eq.(3.2.4) on $\phi(\mathbf{r})$ will be only contained in the integral $I = \int d^3\mathbf{r}'\phi(\mathbf{r}')\xi(\mathbf{r}')\psi_\nu^*(\mathbf{r}')$. Multiplying both sides of Eq.(3.2.4) by $\xi(\mathbf{r})\psi_\nu^*(\mathbf{r})$ and integrating over $d^3\mathbf{r}$, we express I through the overlap integral $I_0 = \int d^3\mathbf{r}'\phi_0(\mathbf{r}')\xi(\mathbf{r}')\psi_\nu^*(\mathbf{r}')$. Then the exact solution of Eq.(3.2.4) is straightforward:

$$\phi(\mathbf{r}) = \phi_0(\mathbf{r}) - \frac{\Omega^2 I_0 \int d\mathbf{r}'\psi_\nu(\mathbf{r}')\xi(\mathbf{r}')G(\mathbf{r}, \mathbf{r}')}{\delta_\nu + (\Omega^2/\Delta\varepsilon_\nu)\beta + i\Gamma}. \tag{3.2.7}$$

The quantity $(\Omega^2/\Delta\varepsilon_\nu)\beta$ describes the light-induced shift of the ν-th vibrational resonance, and the numerical factor $\beta = \Delta\varepsilon_\nu \int d\mathbf{r}d\mathbf{r}' G(\mathbf{r},\mathbf{r}')\xi(\mathbf{r})\psi_\nu^*(\mathbf{r})\xi(\mathbf{r}')\psi_\nu(\mathbf{r}')$. As in the limit of zero energies only the s-wave contribution to $\phi(\mathbf{r})$ and $\phi_0(\mathbf{r})$ is important, the scattering length in the presence of light can be found from the asymptotic form of $\phi(\mathbf{r})$ at large distances: $\phi(\mathbf{r}) \to 1 - a/r$ for $r \to \infty$. At large r the Green function $G(\mathbf{r}, \mathbf{r}') = m\phi_0(\mathbf{r}')/4\pi\hbar^2 r$, and Eq.(3.2.7) yields

$$a = \overline{a} + \frac{(\Omega^2/\Delta\varepsilon_\nu)\tilde{\beta}}{\delta_\nu + (\Omega^2/\Delta\varepsilon_\nu)\beta + i\Gamma} r_t, \tag{3.2.8}$$

with $\overline{a}$ the scattering length in the absence of light, and the numerical factor

$$\tilde{\beta} = (m\Delta\varepsilon_\nu/4\pi\hbar^2 r_t)|I_0|^2.$$

It should be emphasized that Eq.(3.2.8) is valid for any ratio between $|\delta_\nu|$ and $(\Omega^2/\Delta\varepsilon_\nu)\beta$.

Unless ε_ν and $|\delta|$ are huge, the turning point separation r_t is large enough for ϕ_0 and $\tilde{\phi}_0$ to be smooth functions of r at distances $r \sim r_t$ where the main contribution originates to the integrals in the equations for β, I_0 and $\tilde{\beta}$. Putting $\phi_0(r) = \phi_0(r_t)$, $\tilde{\phi}_0(r) = \tilde{\phi}_0(r_t)$ in the integrands of these equations and using a linear approximation for $V(r) = -2d^2/r^3$ in the vicinity of r_t, we obtain

$$\tilde{\beta} = 0.8\pi^2\phi_0^2(r_t); \quad \beta = 0.8\pi^2 f_0(r_t)\phi_0(r_t). \tag{3.2.9}$$

The function $f_0(r) = r\tilde{\phi}_0(r)$ is tending to 1 for $r \to \infty$. For the level spacing the WKB approximation gives

$$\Delta\varepsilon_\nu = 1.9\pi\varepsilon_\nu(r_t/r_0)^{1/2} \ll \varepsilon_\nu. \tag{3.2.10}$$

The characteristic distance $r_0 = md^2/\hbar^2$. For alkali atoms r_0 greatly exceeds the optical wavelength ($r_0 > 10^5$ Å) and, hence, $r_0 \gg \lambda \gg r_t$.

The presence of other bound p levels and continuum states of the excited quasimolecule changes Eq.(3.2.6) for the Green function $\tilde{G}$. Our analysis, relying on the exact expression for $\tilde{G}$, shows that in order to omit the contribution of virtual transitions to these states and, hence, retain the validity of Eq.(3.2.8) it is sufficient to have $|\delta_\nu|$ and Ω much smaller than the level spacing $\Delta\varepsilon_\nu$. The condition $\Omega \ll \Delta\varepsilon_\nu$ leads to important physical consequences. The radiative transitions occur in a narrow range of distances near r_t, characterized by the width $\Delta r \sim r_t(r_t/r_0)^{1/3}$. As the characteristic velocity in this region $v \sim \sqrt{\varepsilon_\nu \Delta r/mr_t}$, the interaction time $\Delta t \sim \Delta r/v$ of the quasimolecule with light is such that $\Omega\Delta t \sim (\Omega/\Delta\varepsilon_\nu)(r_t/r_0)^{1/6} \ll 1$. Then, turning to a classical picture, one can say that the

"population" of the excited quasimolecular state will be small. This ensures the absence of effects analogous to power broadening in the single atom case.

The light changes the real part of the scattering length and introduces an imaginary part. The frequency dependence of Rea and Ima has a resonance structure:

$$\mathrm{Re}a = \overline{a} + \frac{\Omega^2\tilde{\beta}\zeta_\nu}{\Delta\varepsilon_\nu(\zeta_\nu^2+\Gamma^2)}r_t;\ \mathrm{Im}a = -\frac{\Omega^2\tilde{\beta}\Gamma}{\Delta\varepsilon_\nu(\zeta_\nu^2+\Gamma^2)}r_t, \tag{3.2.11}$$

where $\zeta_\nu = \delta_\nu + (\Omega^2/\Delta\varepsilon_\nu)\beta$. The real part determines the mean field interaction between atoms. The light-induced change of this interaction is given by

$$n(\tilde{U} - \overline{\tilde{U}}) \equiv \hbar\tau_a^{-1} = 4\pi\hbar^2(\mathrm{Re}a - \overline{a})n/m. \tag{3.2.12}$$

The imaginary part of a originates from the photoassociation process in pair collisions, followed by spontaneous emission. The inverse decay time due to this process is

$$\tau_{pa}^{-1} = 8\pi\hbar|\mathrm{Im}a|n/m. \tag{3.2.13}$$

Exactly at resonance ($\zeta_\nu = 0$) the mean field interaction is the same as in the absence of light, and the photoassociation rate is the largest.

For small Rabi frequency Eq.(3.2.11) goes over into the result of perturbation theory and both τ_a^{-1} and τ_{pa}^{-1} are proportional to Ω^2. The former can be treated as a "light shift" of the mean field interaction and the latter will be nothing else than the ordinary photoassociation rate at a low light power. For $(\Omega^2/\Delta\varepsilon_\nu)\beta \gg |\delta_\nu|$ the driving light shifts the interacting pair of atoms out of resonance. As the corresponding shift is proportional to Ω^2, the light-induced change of the mean field interaction becomes independent of Ω. It will be determined by Eq.(3.2.12) with $\mathrm{Re}a - \overline{a} = (\tilde{\beta}/\beta)r_t$. On the contrary, the photoassociation rate (Ima) decreases as $1/\Omega^2$.

The amplitude of binary interaction, affected by light, undergoes damped oscillations and reaches its stationary value (3.2.8) on a time scale of order Γ^{-1} (for $\Gamma \ll max\{|\delta_\nu|, \Omega\}$ it averages to Eq.(3.2.8) much faster). This is much shorter than the characteristic response time of a dilute trapped gas, which cannot be faster than τ_a. To have an appreciable modification of the mean field interaction without excessive photoassociation, τ_a should be short compared to τ_{pa}, i.e., the condition

$$|\mathrm{Re}a| \gg |\mathrm{Im}a| \tag{3.2.14}$$

should hold. As follows from Eq.(3.2.11), this is the case for $|\zeta_\nu| \gg \Gamma$. The change of the scattering length $\mathrm{Re}a - \overline{a} \approx (\Omega^2\tilde{\beta}/\Delta\varepsilon_\nu\zeta_\nu)r_t$ can exceed r_t, whereas the imaginary part of a will be much smaller. The scattering length can be changed in both directions simply by changing the sign of ζ_ν.

In addition, the time τ_a should be much smaller than the decay time τ_r due to the photon recoil of single atoms, caused by light scattering. Since $\tau_r^{-1} = (\Omega/\delta)^2\Gamma/2$, this is the case for ($|\delta| \approx \varepsilon_\nu$)

$$n\lambda^3 \gg |\zeta_\nu|/4\Delta\varepsilon_\nu, \tag{3.2.15}$$

as follows from Eqs. (3.2.11), (3.2.9) and (3.2.10) assuming $|\zeta_\nu| \gg \Gamma$ to simultaneously satisfy condition (3.2.14). As $|\zeta_\nu| \ll \Delta\varepsilon_\nu$, the inequality (3.2.15) is not in contradiction with our starting assumption (3.2.1) and can be fulfilled in alkali atom gases at densities $n \sim 10^{13} - 10^{14}$ cm^{-3} by an appropriate choice of Ω, the level ν and δ_ν.

All the above results remain valid for finite momenta of colliding atoms, $k \ll \min(r_t^{-1}, |\overline{a}|^{-1}, |a|^{-1})$.

We performed calculations for ^{7}Li by using spectroscopic information on the location of bound p levels in the excited electronic state $^3\Sigma_g^+$ [81]. The potential of interaction in the ground state $^3\Sigma_u^+$ was taken from [82], the scattering length in the absence of light being $\overline{a} \approx -14$ Å. Eq.(3.2.11) was used to calculate the scattering length a under the influence of light nearly resonant for vibrational p levels of the $^3\Sigma_g^+$ state, with quantum numbers ranging from $\nu = 77$ ($\varepsilon_\nu = 2.8$K) to $\nu = 66$ ($\varepsilon_\nu = 28.7$K). We find that for Ω in the range $5-40$ mK (light power ranging from 10 to 1000 W/cm^2) it is possible to

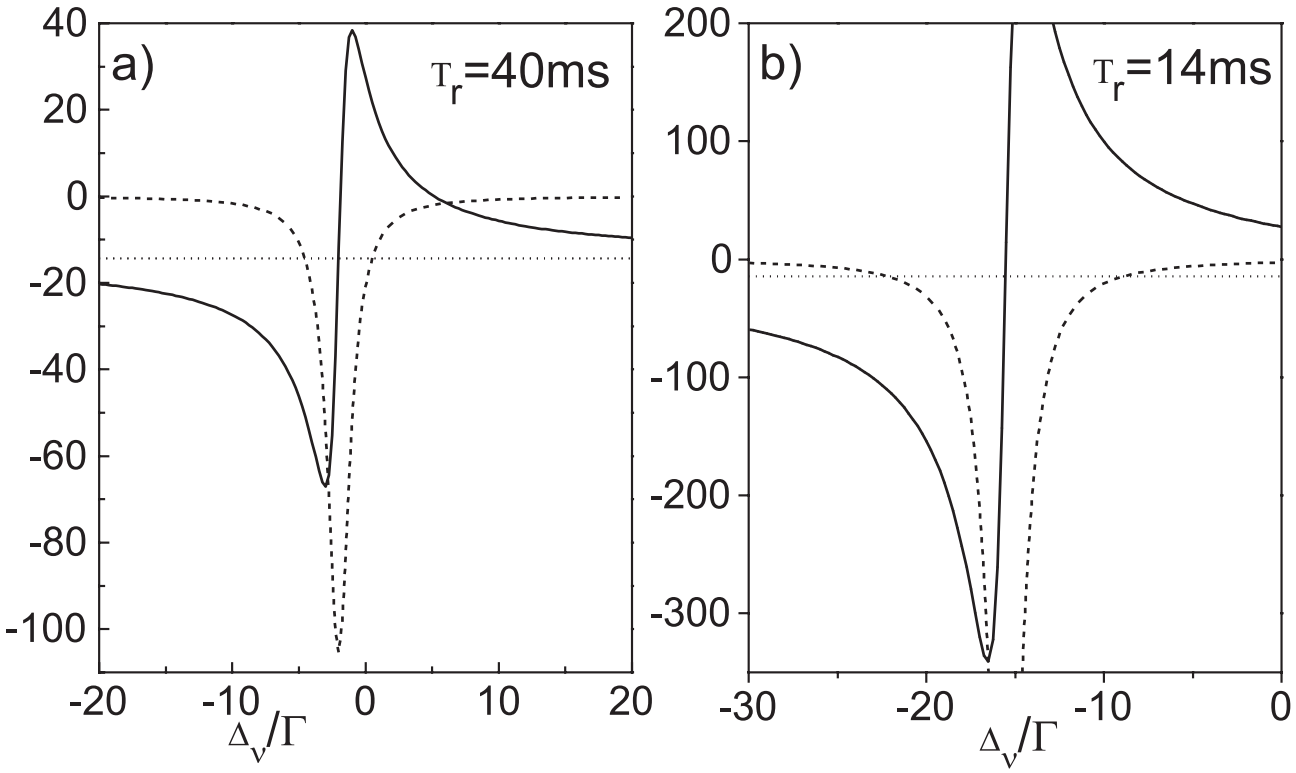

FIGURE 3.2.1. The scattering length for ^{7}Li as a function of the frequency detuning of light, δ_ν/Γ, from the excited bound p level ν: a) $\Omega = 10$ mK, $\varepsilon_\nu = 9.1$K; b) $\Omega = 40$ mK, $\varepsilon_\nu = 20.1$K. The solid curve represents the real part of a, and the dashed curve the imaginary part. The dotted line corresponds to the scattering length in the absence of light.

significantly change the scattering length and even make it positive while maintaining $|\mathrm{Im}a| \ll |\mathrm{Re}a|$ (see Fig.3.2.1). The recoil loss time τ_r varies from 100 to 1 ms.

Our results show the feasibility to optically manipulate the mean field interaction between atoms and open prospects for new optical experiments in trapped gases. For example, once a gas is in a Bose-condensed state, instantaneous switching of the sign of a changes the sign of the non-linear interaction term in the Ginzburg-Gross-Pitaevskii equation for the condensate wavefunction and causes the trapped condensate to evolve in a completely different way than a condensate set into motion by changing the trap frequency. The evolution will involve two time scales: τ_a and the inverse trap frequency ω_t^{-1}, and continue after the light is switched off. Because of the light-induced decay processes, the light should be switched on only for a time much shorter than τ_r. Hence, besides the above discussed condition $\tau_a \ll \tau_r$, experiments should be arranged such that $\omega_t \tau_r \gg 1$. This is feasible with the above values for τ_r. As in most cases τ_r will be much smaller than the characteristic time for elastic collisions, the evolving condensate will not be in equilibrium with above-condensate particles.

In trapped gases with negative scattering length one may expect a stabilization of the condensate by switching a to positive values. Of particular interest is the case where the sign of a is switched from positive to negative. In a quasihomogeneous Bose-condensed gas ($n\tilde{U} \gg \hbar\omega_t$) this should induce a "collapse" of the condensate, caused by elastic interatomic interaction. The investigation of this phenomenon is of fundamental interest.

CHAPTER 4

Dynamics of BEC at zero temperature

We analyze the dynamics of two trapped interacting Bose-Einstein condensates in the absence of thermal cloud and identify two regimes for the evolution: a regime of slow periodic oscillations and a regime of strong non-linear mixing leading to the damping of the relative motion of the condensates. We compare our predictions with an experiment recently performed at JILA.

The experimental evidence for Bose-Einstein condensation in trapped atomic gases [3–5] has attracted a lot of attention, as the presence of a macroscopically occupied quantum state makes the behavior of these gases drastically different from that of ordinary gas samples. Trapped Bose-Einstein condensates are well isolated from the environment and, at the same time, can be excited by deforming the trap or changing the interparticle interaction. The question of how the gas sample, being initially a pure condensate, subsequently reaches a new equilibrium state is directly related to the fundamental problem of the appearance of irreversibility in a quantum system with a large number of particles. Thus far the time dependent dynamics of trapped condensates has mainly been analyzed for a single condensate [32,44–46,52,83] on the basis of the Gross-Pitaevskii equation for the condensate wavefunction. Remarkably, already in this mean field approach the stochastization in the condensate evolution has been found [45], and the damping of the condensate oscillations has been observed numerically [52]. However, the question of the formation of a thermal component, addressed in [45], has not been investigated.

In this Chapter we study the evolution of a richer system, a mixture of two interacting condensates (a and b), in the situation where initially the thermal cloud is absent. The properties of a static two-component trapped condensate, including the issue of spatial separation of the a and b components due to interparticle interaction [84, 85], were investigated in [86–89]. The response of the system to small modulations of the trap frequency has also been studied numerically [90]. In our case the a and b condensates have initially the same density profile and are set into motion mostly by an abrupt displacement of the trap centers. The main goal of our work is to study the dynamics of spatial separation of the two condensates and analyze how the system can acquire statistical properties and reach a new equilibrium state. From a general point of view, we are facing the problem raised by Fermi, Pasta and Ulam [91]. They considered classical vibrations of a chain of coupled non-linear oscillators, to analyze the emergence of statistical properties in a system with a large number of degrees of freedom. As has been revealed later, the appearance of statistical properties requires a sufficiently strong non-linearity leading to stochastization of motion [92], whereas for small non-linearity the motion remains quasiperiodic (see e.g. [93]).

We consider a situation in which the two condensates a and b see harmonic trapping potentials of exactly the same shape, and the interparticle interactions characterized by the scattering lengths a_{aa}, a_{ab} and a_{bb} are close to each other. The control parameter, determining the possibilities of non-linear mixing and stochastization, is the relative displacement z_0 of the trap centers. We identify two regimes for the evolution. In the first one the relative motion of the condensates exhibits oscillations at a frequency much lower than the trap frequency ω. In the other regime there is a strong non-linear mixing leading to the damping of the relative motion, and the system has a tendency to approach a new equilibrium state. We compare our predictions with the results of the JILA experiments [94, 95] on a two-component condensate of $^{87}\mathrm{Rb}$ atoms in the $F = 1, m = -1$ and $F = 2, m = 1$ states.

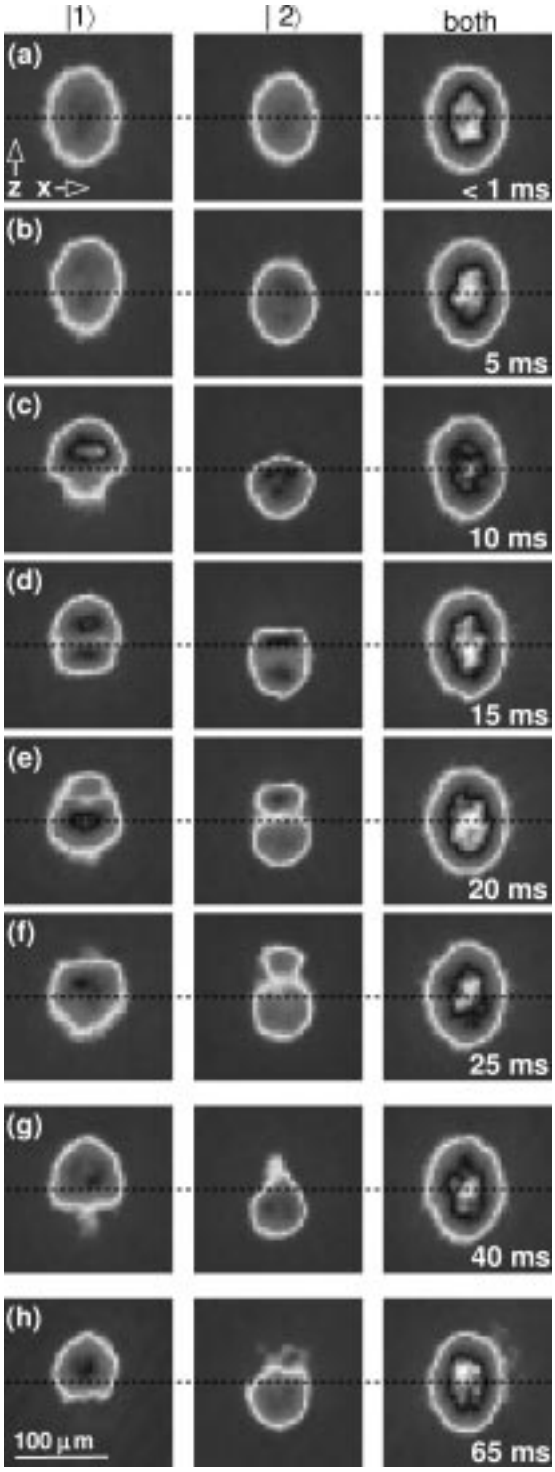

FIGURE 4.0.1. Time evolution of the binary condensate mixture [94] with a relative sag of 0.4μm (3% of the width of the combined distribution prior the expansion) and the trap frequency $59Hz$.

In these experiments the double condensate was prepared from a single condensate in the state $F = 1, m = -1$ (a) by driving a two-photon transition which coherently transfers half of the atoms to the state $F = 2, m = 1$ (b).

We mostly perform our analysis in the mean field approach relying on the Gross-Pitaevskii equations for the wavefunctions ϕ_a and ϕ_b of the a and b condensates. This approach corresponds to the

classical limit of the evolution of a quantum field, the subsequent corrections being proportional to a small parameter $(na^3_{\varepsilon\varepsilon'})^{1/2}$ (n is the gas density) and, hence, manifesting themselves only on a rather large time scale. The two coupled Gross-Pitaevskii equations for ϕ_a and ϕ_b normalized to unity read

$$i\hbar\partial_t\phi_\varepsilon = \left[-\frac{\hbar^2\Delta}{2m} + U_\varepsilon - \mu + \sum_{\varepsilon'=a,b} g_{\varepsilon\varepsilon'}N_{\varepsilon'}|\phi_{\varepsilon'}|^2\right]\phi_\varepsilon. \tag{4.0.16}$$

Here $g_{\varepsilon\varepsilon'} = 4\pi\hbar^2 a_{\varepsilon\varepsilon'}/m$ are the coupling constants for elastic interaction between atoms in the states ε and ε', m is the atom mass, and N_ε, U_ε are the number of atoms and trapping potential for the ε condensate. As in the JILA experiment, we choose the initial condition $\phi_{a,b}(0) = \phi_0$, where the (real) wavefunction ϕ_0 corresponds to the ground state of Eq.(4.0.16) with all atoms in the a state and no trap displacement. The chemical potential of this ground state is denoted as μ.

We consider the a and b condensates in the Thomas-Fermi regime ($\hbar\omega \ll \mu$) and assume the number of condensate atoms $N_a = N_b = N/2$[1] . The first set of our calculations is performed for the evolution of the condensates in a spherically symmetric trapping potential $U_0(r) = m\omega^2 r^2/2$ which at $t = 0$ is displaced along the z axis by a distance $z_0/2$ for the a atoms, and by $-z_0/2$ for the b atoms. We present the results for the time dependence of the mean separation between the condensates,

$$u(t) = \int d^3r\ z\ (|\phi_a(\mathbf{r},t)|^2 - |\phi_b(\mathbf{r},t)|^2). \tag{4.0.17}$$

For the curves in Fig.4.0.2 the coupling constants are $g_{aa} = g_{ab} = g_{bb}$, and for $z_0 = 0$ our initial state is an equilibrium state at $t \geq 0$. In this state the Thomas-Fermi radius of the condensate $R_0 = (2\mu/m\omega^2)^{1/2}$ serves as unit of length, and the shape of ϕ_0 is determined by $\mu/\hbar\omega$. Hence, for $z_0 \neq 0$ the dependence of the quantity u/R_0 on ωt is governed by the parameters $\mu/\hbar\omega$ and z_0/R_0.

Our results reveal two key features of the evolution dynamics. The first one, for a tiny displacement z_0, is a periodic motion with slow frequencies which turn out to be sensitive to small variations in the values of the coupling constants. The other feature, for much larger z_0, but still $z_0 \ll R_0$, is a strong damping in the relative motion of the two condensates, as observed at JILA [94].

In order to understand the physics behind the evolution pattern, we first perform a linear analysis of Eq.(4.0.16). For the case where $g_{aa} = g_{ab} = g_{bb} = g$, and the displacement z_0 is sufficiently small, we linearize Eq.(4.0.16) with respect to small quantities $\delta\phi_{a,b} = (\phi_{a,b} - \phi_0)$ and z_0. Then, for the quantity $\delta\phi_- = \delta\phi_a - \delta\phi_b$, describing the relative motion of the condensates, we obtain the equation

$$i\hbar\partial_t\delta\phi_- = \left[-\frac{\hbar^2\Delta}{2m} + U_0 - \mu + Ng\phi_0^2\right]\delta\phi_- + S_-, \tag{4.0.18}$$

with the source term $S_- = m\omega^2 z_0 z\phi_0$. For the quantity $\delta\phi_+ = \delta\phi_a + \delta\phi_b$ we find an equation decoupled from $\delta\phi_-$ and without source terms. Hence, the initial condition $\delta\phi_+(\mathbf{r},0) = 0$ allows us to put $\delta\phi_+(\mathbf{r},t) = 0$ for $t \geq 0$.

For $S_- = 0$ Eq.(4.0.18) is the equation for the wavefunction of a particle moving in the potential $V = U_0 - \mu + Ng\phi_0^2$. Stationary solutions of this equation provide us with the eigenmodes of oscillations of the condensates with respect to each other. In the Thomas-Fermi limit the potential V, originating from the kinetic energy of the condensate, is a smooth function of r inside the condensate spatial region $r < R_0$: $V = \hbar^2(\Delta\phi_0)/2m\phi_0 \ll \hbar\omega$. For $r > R_0$ this potential is close to $U_0 - \mu$ and is much steeper. Replacing V by an infinite square well of radius R_0 we obtain the energy spectrum of eigenmodes with large quantum numbers n: $E_{n,l} = (\pi\hbar\omega)^2(2n + l)^2/16\mu$, where l is the orbital angular momentum. This explains the appearance of oscillations at a frequency much smaller than ω in our numerical calculations (see Fig.4.0.2a), since the energy scale in the spectrum is $(\hbar\omega)^2/\mu \ll \hbar\omega$. For the latter reason we call these eigenmodes soft modes. Note that the soft modes for the

[1] We solve Eq.(4.0.16) numerically, using cylindrical symmetry, on a finite grid with a splitting technique. Numerical accuracy is tested by changing the grid and checking energy conservation ($\delta E/E < 10^{-5}$ for $t = 100$s).

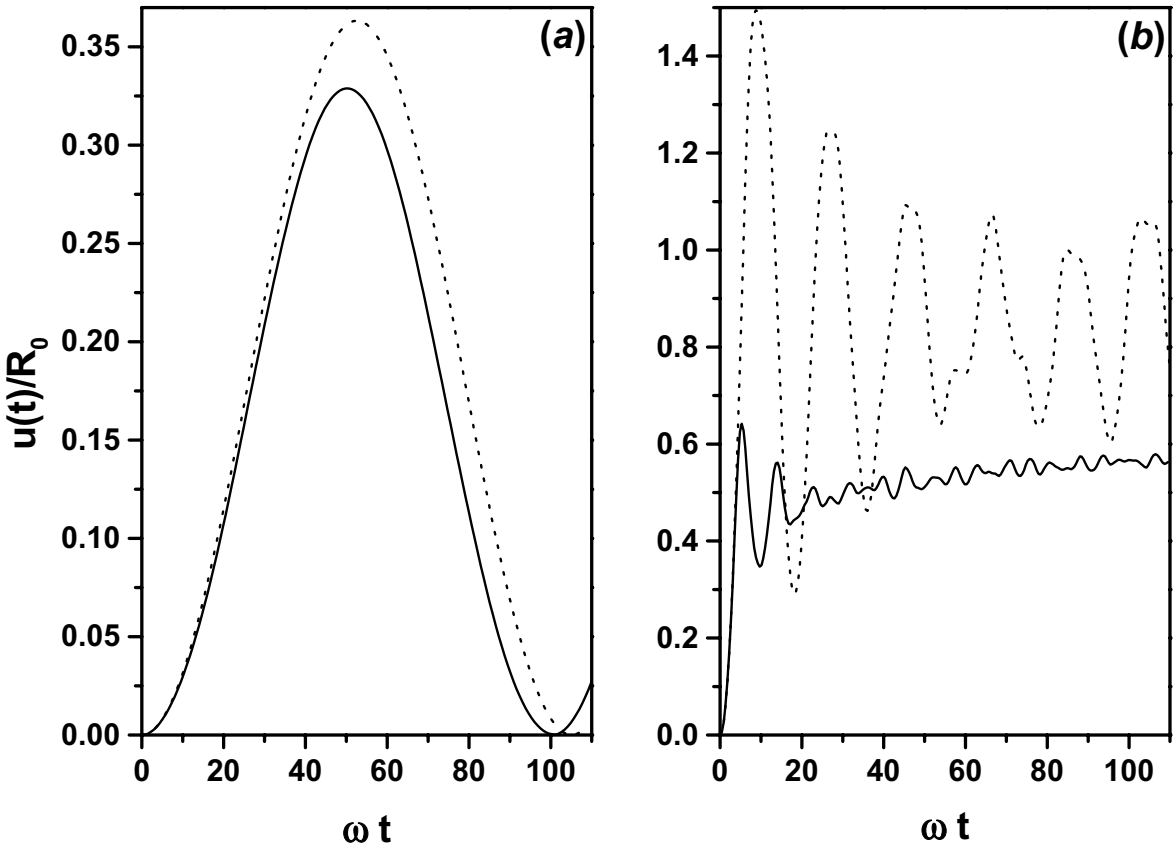

FIGURE 4.0.2. Mean separation between the condensates versus time in isotropic traps for $g_{aa} = g_{ab} = g_{bb}$ and $\mu/\hbar\omega = 29.2$. Relative displacement: $z_0 = 6.66 \times 10^{-4} R_0$ (a), and $z_0 = 7.16 \times 10^{-2} R_0$ (b). Solid curves: numerical integration of Eq.(4.0.16). Dotted curves: analytical prediction for (a) (see text), and the linear model relying on Eq.(4.0.21) for (b).

relative motion of the two condensates also exist in the spatially homogeneous case where they have a free-particle spectrum [84].

As in our linear approach we have $\delta\phi_+(\mathbf{r}, t) = 0$, Eq.(4.0.17) for the mean separation between the condensates reduces to $u(t) = 2\int d^3r\, z\, \phi_0 \mathrm{Re}\{\delta\phi_-\}$, and the contribution to $u(t)$ comes from the components of $\delta\phi_-$ with $l = 1, m_l = 0$. Solving Eq.(4.0.18) with the initial condition $\delta\phi_-(\mathbf{r}, 0) = 0$, we obtain $u(t)$ as a superposition of components, each of them oscillating at an eigenfrequency of a soft mode:

$$u(t) = z_0 \sum_{n\geq 1} \frac{2m\omega^2}{E_{n1}} \left| \int d^3r \varphi_{n1} z \phi_0 \right|^2 \left[1 - \cos\left(\frac{E_{n1} t}{\hbar} \right) \right], \tag{4.0.19}$$

where φ_{n1} is the wavefunction of the soft mode with $l = 1, m_l = 0$ and main quantum number n. Damping of oscillations of $u(t)$ could, in principle, originate from the interference between the components with different n in Eq.(4.0.19). However, the source S_- basically populates only the lowest soft mode, irrespective of the value of z_0: the amplitude of oscillations at the lowest eigenfrequency in Eq.(4.0.19) (the term with $n = 1$) greatly exceeds the sum of the amplitudes of other terms. Hence, these oscillations remain undamped. For the same reason their frequency and amplitude can be found with φ_{n1} replaced by the function $z\phi_0$ normalized to unity. Using the Thomas-Fermi approximation for the condensate wavefunction [42, 43]: $\phi_0^2(r) = 15(1 - r^2/R_0^2)/8\pi R_0^3$ for

$r < R_0$, and $\phi_0 = 0$ for $r > R_0$, we obtain $E_{11} \equiv \hbar\Omega = (7/4)(\hbar\omega)^2/\mu$ which is very close to $E_{11} = 1.62(\hbar\omega)^2/\mu$ calculated numerically. Then, retaining only the leading term ($n = 1$) in Eq.(4.0.19), we find $u(t) \approx z_0(4\mu/7\hbar\omega)^2[1-\cos(\Omega t)]$ shown in dotted line in Fig.4.0.2a. As one can see, the condition of the linear regime $u \ll R_0$ requires a very small displacement

$$z_0 \ll (\hbar\omega/\mu)^2 R_0, \tag{4.0.20}$$

and already a moderate z_0 as in Fig.4.0.2b is sufficient to drive the system out of the linear regime.

We have performed a similar linear analysis for the case where $g_{aa} \neq g_{ab} \neq g_{bb}$, but the relative difference between the coupling constants is small. Also in this case the source S_- mostly generates oscillations of the condensates relative to each other at a single frequency $\Omega' \ll \omega$. For a relative difference between the coupling constants much smaller than $(\hbar\omega/\mu)^2$, the frequency Ω' coincides with the soft-mode frequency Ω found above. Otherwise the sign of $g_- = g_{aa} + g_{bb} - 2g_{ab}$ becomes important. In particular, for positive $g_- \gg |g_{aa} - g_{bb}|$ already a moderate difference between the coupling constants strongly increases the frequency Ω' compared to Ω. In this case we obtain undamped oscillations at $\Omega' \approx (g_-/g_{aa})^{1/2}\omega$. For $g_- < 0$, already in the $z_0 = 0$ case, a breathing mode in which the two condensates oscillate out of phase becomes unstable, and the system evolves far from the initial state. Note that for a small difference between the coupling constants the condition $g_- < 0$ is equivalent to the criterion of spatial separation of the condensates in the homogeneous case, $g_{aa}g_{bb} < g_{ab}^2$ [84, 85].

We now turn to the large z_0 regime (Fig.4.0.2b) where we find a strong damping of the oscillations of the mean separation between the condensates, $u(t)$. In order to prove the key role of non-linearity in this regime, we first attempt a linear model assuming that the densities $|\phi_{\varepsilon'}|^2$ inside the square brackets of Eq.(4.0.16) are not evolving:

$$\sum_{\varepsilon'} N_{\varepsilon'} g_{\varepsilon\varepsilon'} |\phi_{\varepsilon'}|^2 \to N g |\phi_0|^2 \,. \tag{4.0.21}$$

In contrast to the analysis which led to Eq.(4.0.19), the displacement z_0 is now explicitly included in the Hamiltonian through the terms $\pm m\omega^2 z z_0/2$ in $U_{a,b}$, and the number of populated oscillation modes depends on z_0. However, for the parameters in Fig.4.0.2b we find that only a few modes are populated, and the interference between them can not account for the damping found numerically (dotted versus solid curve in Fig. 4.0.2b).

We argue that the damping in our calculations mostly originates from non-linearity of the system, which increases the number and amplitude of populated oscillation modes and provides an interaction between them. As a result, the evolution of the condensate wavefunctions ϕ_a and ϕ_b becomes chaotic. This can be seen from Fig.4.0.3 where we compare the spectral density $R_n(\nu) = |T^{-1}\int_0^T dt\, n(\mathbf{0}, t)\exp(i\nu t)|^2$ of the density at the origin $n(\mathbf{0}, t)$ with an identically defined spectral density $R_u(\nu)$ of $u(t)$ for the parameters in Fig.4.0.2b and $T = 110/\omega$. The function $R_n(\nu)$ has a smooth envelope at large ν, with peaks corresponding to the islands of regular motion. On the contrary, $R_u(\nu)$ exhibits pronounced peaks at ν of order ω, without any smooth background. This picture provides a clear signature of stochastization in the system [93] and prompts us to represent each of the condensate wavefunctions in Eq.(4.0.16) as a superposition of two constituents: (i) a slowly oscillating regular part conserving the phase coherence properties; (ii) a composition of high-energy excitations characterized by stochastic motion. Only the slow constituent contributes to such macroscopic quantities as $u(t)$, since the contribution of the fast stochastic part is averaged out.

Our analysis is consistent with the general statement that for a large population of various oscillation modes the non-linear interaction between them leads to stochastization in the motion of excitations with sufficiently high energy [93]. This allows us to employ the mechanism of stochastic heating [93] for explaining the damping of oscillations of $u(t)$: The mean field interaction between the fast stochastic and the slowly oscillating parts leads to energy transfer from the slow to the fast part.

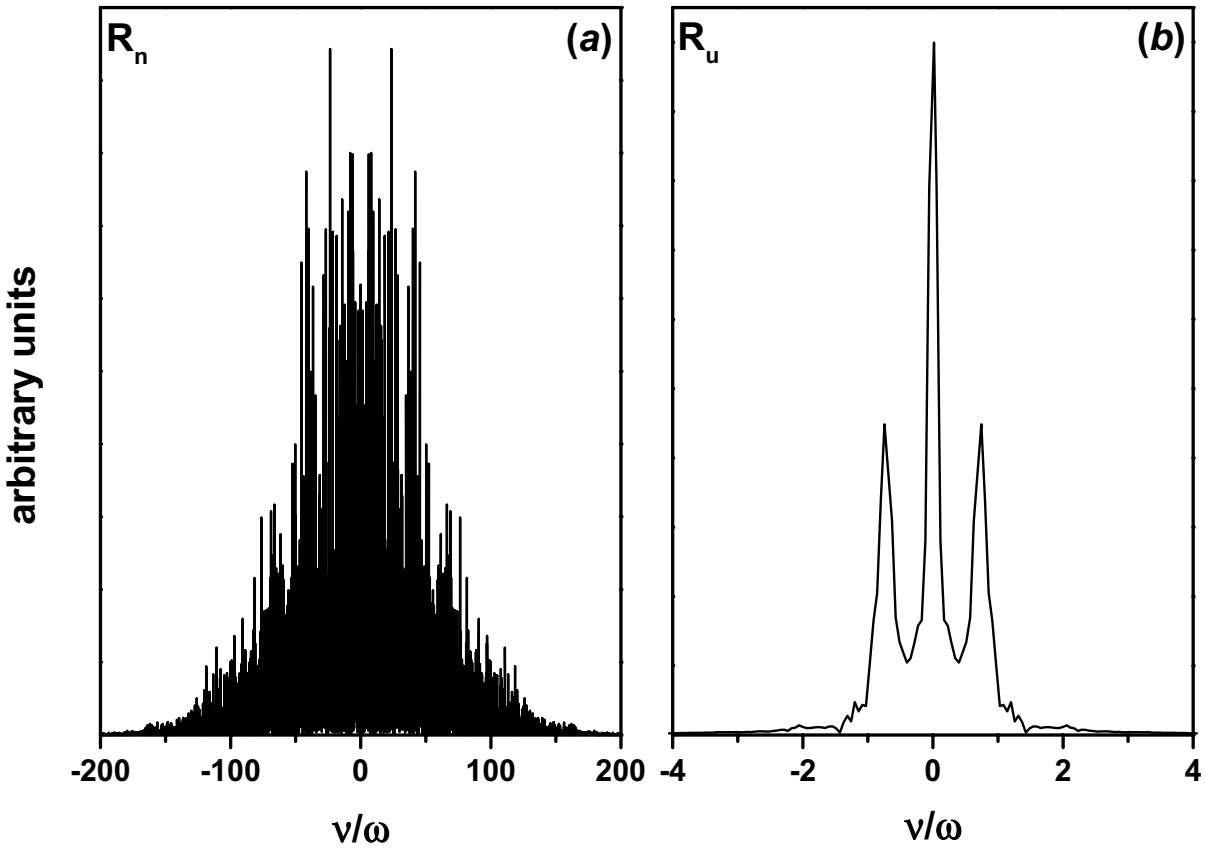

FIGURE 4.0.3. Spectral densities $R_n(\nu)$ (a) and $R_u(\nu)$ (b) for the parameters in Fig.4.0.2b and $T = 110/\omega$ (see text).

The evolution of the occupation numbers of the modes of the fast stochastic part is governed by kinetic equations [93] and eventually slows down. The rate of energy and particle exchange between the two constituents then reduces. After a sufficiently long time only small linear oscillations of the condensates survive, mostly at the lowest eigenfrequency and the gas sample as a whole could be thought as being close to a steady state. However the damping of the remaining oscillations and the ultimate evolution of the fast stochastic part towards the thermal equilibrium require an analysis beyond the mean field approach. For the parameters in Fig.4.0.2b, using the semiclassical Bogolyubov approach [96] and relying on the conservation of energy and number of particles, we find an equilibrium temperature $T_{\rm eq} \approx 0.6\mu$ and a condensed fraction $\gamma_{a,b} \approx 0.9$, for $N = 5 \times 10^5$.

The last set of our calculations relates to the recent JILA experiment [94] where the evolution of a two-component ^{87}Rb condensate has been investigated. In the conditions of this experiment we solved numerically Eq.(4.0.16) by taking $a_{ab} = 55$Å and the ratio $g_{aa} : g_{ab} : g_{bb} = 1.03 : 1 : 0.97$. We also explicitly included in these equations the 22 ms expansion of the clouds after switching off the trapping potential. The results of our calculations are presented in Fig.4.0.4. As in Fig.4.0.2b, we find a strong damping of the oscillations of the mean separation between the condensates, $u(t)$. Our numerical results are in fair agreement with the experimental data, although the damping in the experiment is somewhat larger. We extended the calculations to twice the maximum experimental time and found small oscillations which remain undamped on this time scale.

Our data for the JILA experiment [94] can be analyzed along the same lines as the results in Fig.4.0.2b, with a damping originating from stochastization in the evolution of the condensate wavefunctions. The equilibrium temperature is close to μ, corresponding to condensed fractions $\gamma_a \approx$

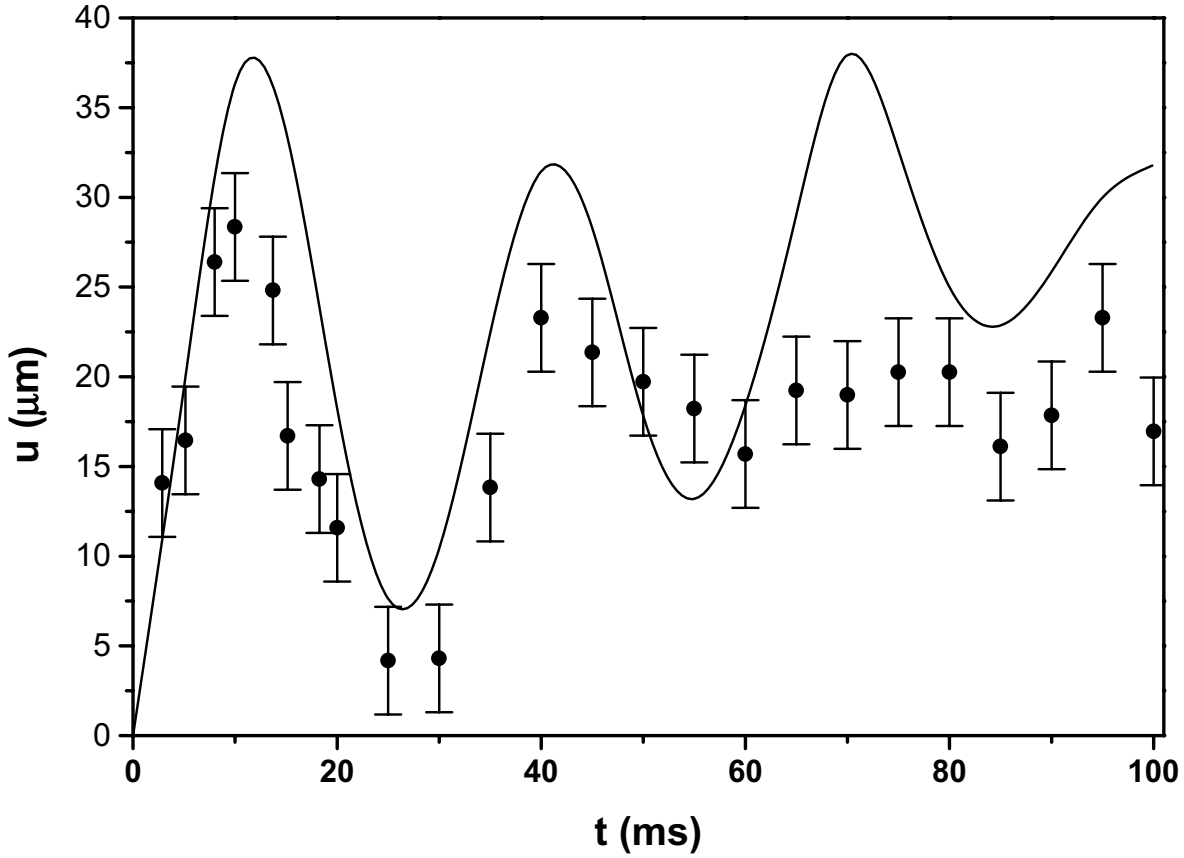

FIGURE 4.0.4. Mean separation between the condensates in the JILA experiment versus evolution time in the traps, after a 22 ms free expansion. Dots with error bars: JILA experiment. Solid curve: our numerical calculation.

$\gamma_b \approx 0.9$. The large value of the condensed fraction explains why phase coherence between the a and b components could be observed even after the damping of the motion of $u(t)$ [95]. The damping time of the small remaining oscillations, estimated along the lines of [97], will be of order 1 second.

We believe that the stochastic regime identified from our calculations is promising for investigating the loss of phase coherence and the formation of a new thermal component in initially purely Bose-condensed gas samples. An interesting possibility concerns the observation of a continuous change in the phase coherence between the a and b components with increasing the trap displacement and, hence, decreasing the final Bose-condensed fraction.

CHAPTER 5

Finite Temperature Perturbation Theory for a Bose-condensed Gas

We develop a finite temperature perturbation theory (beyond the mean field) for a Bose-condensed gas and calculate temperature-dependent damping rates and energy shifts for Bogolyubov excitations of any energy. The theory is generalized for the case of excitations in a spatially inhomogeneous (trapped) Bose-condensed gas, where we emphasize the principal importance of inhomogeneity of the condensate density profile and develop the method of calculating the self-energy functions. The use of the theory is demonstrated by calculating the damping rates and energy shifts of low-energy excitations, i.e. t excitations with energies much smaller than the mean field interaction between particles. The damping is provided by the interaction of these excitations with the thermal excitations. We emphasize the key role of stochastization in the behavior of the thermal excitations for damping in non-spherical traps. The damping rates of the lowest excitations, following from our theory, are in fair agreement with the data of recent JILA and MIT experiments. For the quasiclassical excitations the boundary region of the condensate plays a crucial role, and the result for the damping rates and energy shifts is drastically different from that in spatially homogeneous gases. We also analyze the frequency shifts and damping of sound waves in cylindrical Bose condensates and discuss the role of damping in the recent MIT experiment on the sound propagation.

5.1. Introduction

Recent developments in the physics of ultra-cold gases have led to the discovery of Bose-Einstein condensation (BEC) in trapped clouds of alkali atoms [3–5] and stimulated a tremendous boost in theoretical studies of weakly interacting Bose gases. As in previous years, these studies rely on the binary approximation for the interparticle interaction. The latter is characterized by the 2-body scattering length a, which assumes the presence of a small gaseous parameter $na^3 \ll 1$ (n is the gas density). Especially intensive are the attempts to reach beyond the ordinary mean field approach and to develop a theory which can properly describe the behavior of finite temperature elementary excitations of a trapped Bose-condensed gas and in particular, explain the JILA [50] and MIT [51] experiments on energy shifts and damping rates of the excitations.

The commonly used mean field theory (for $a > 0$) is based on the Bogolyubov quasiparticle approach developed originally for a spatially homogeneous Bose-condensed gas at $T \to 0$ [53] and employed by Lee and Yang [98] (see also [99]) at finite temperatures. The generalization of the Bogolyubov method for spatially inhomogeneous systems has been described by De Gennes [54]. In the case of a Bose-condensed gas it should be completed by the equation for the wavefunction of the spatially inhomogeneous condensate, derived by Pitaevskii [40] and Gross [38, 39].

For spatially homogeneous gases the theory beyond the mean field approach was also developed. Beliaev [100] constructed the zero-temperature diagram technique which allows one to find corrections to the energies of Bogolyubov excitations, proportional to $(n_0 a^3)^{1/2}$, where n_0 is the condensate density. The corrections are provided by the interaction between the excitations (in particular, through the condensate) and contain both real (energy shift) and imaginary (damping rate) parts. At $T = 0$ the latter originates from spontaneous decay of a given excitation (ν) to two other excitations (γ and

γ'), with smaller energies and momenta:

$$\nu \to \gamma + \gamma'. \tag{5.1.1}$$

A universal expression for the chemical potential in terms of the self-energy functions has been found by Pines and Hugenholtz [101]. It should be emphasized that the corrections proportional to $n_0 a^3$ already depend on the contribution of 3-body interactions and, hence, can not be obtained within the binary approximation.

The Beliaev approach was employed by Popov [102] at finite temperatures. In this case the corrections to the Beliaev self-energies contain infra-red singularities, i.e. they tend to infinity for momenta $p \to 0$. This prompted Popov to make a renormalization of the theory, which links the microscopic approach with phenomenological Landau hydrodynamics [31]. The Popov theory eliminates the infra-red singularities and allows one to describe the behavior of low-energy excitations (phonons) at temperatures much smaller than the mean field interparticle interaction $n_0\tilde{U}$ ($\tilde{U} = 4\pi\hbar^2 a/m$, with m being the atom mass). The damping of phonons in this temperature range is determined by the Beliaev damping processes and has also been calculated by Hohenberg and Martin [103]. A simplified approach within the dielectric formalism was used by Szepfalusy and Kondor [104] for calculating the damping rates of excitations in the phonon branch of the spectrum. They found that at temperatures $T \gg n_0\tilde{U}$ the damping rate of a given excitation (ν) originates from the scattering of thermal excitations (γ and γ') on the excitation ν through the processes:

$$\nu + \gamma \to \gamma'. \tag{5.1.2}$$

Since the characteristic energies of the thermal excitations γ, γ' turn out to be much larger than the energy of the excitation ν, this damping channel can be represented as scattering of "resonance" excitations moving in phase with the excitation ν and, hence, is exactly analogous to Landau damping. It should be noted that the damping rates can be simply found by considering the interaction between the excitations as a small perturbation and using Fermi's golden rule. This allows one to properly take into account the Bogolyubov nature of the thermal excitations. The damping rates of phonons in a spatially homogeneous Bose-condensed gas, in particular for the Szepfalusy-Kondor mechanism, have been calculated in the recent contributions [97, 105–108].

In order to reach beyond the mean field theory at $T > n_0\tilde{U}$ one should further develop the Popov approach. One can also proceed along the lines of the Beliaev theory, since any physical quantity should be determined by combinations of the Beliaev self-energies, which do not contain the infrared singularities. We choose the latter way and construct the perturbation theory for a Bose-condensed gas, which allows us to find the next to leading order terms (the terms proportional to $(n_0 a^3)^{1/2}$) in the energy spectrum of the elementary excitations. As in [104, 105, 107, 108], we consider the excitations in the so-called collisionless regime, where their De Broglie wavelength is much smaller than the mean free path of the thermal excitations.

We start with the case of a spatially homogeneous Bose-condensed gas and find temperature-dependent energy shifts and damping rates for Bogolyubov excitations of any energy. At temperatures $T \gg n_0\tilde{U}$ the small parameter of the theory proves to be

$$\frac{T}{n_0\tilde{U}}(n_0 a^3)^{1/2} \ll 1, \tag{5.1.3}$$

in contrast to $n_0 a^3 \ll 1$ for $T = 0$. The appearance of the extra factor $(T/n_0\tilde{U})$ originates from the Bose occupation numbers of thermal excitations with energies of order $n_0\tilde{U}$, which are the most important in the perturbation theory. As shown below, the damping of excitations with energies $\varepsilon_\nu \sim n_0\tilde{U}$ is determined by both the Szepfalusy-Kondor ($\nu + \gamma \leftrightarrow \gamma'$) and Beliaev ($\nu \leftrightarrow \gamma + \gamma'$) processes, and can no longer be treated as Landau damping.

The theory is generalized for the case of excitations in a spatially inhomogeneous (trapped) Bose-condensed gas. A new ingredient here is related to the inhomogeneous density profile of the condensate and the discrete structure of the excitation spectrum. We develop the method of calculating the self-energy functions and derive the equations for finding the wavefunctions and energies of the excitations (generalized Bogolyubov-De Gennes equations).

The use of the theory is demonstrated by three examples. The first one concerns quasiclassical low-energy excitations of a trapped Bose-condensed gas in the Thomas-Fermi regime. The term "low-energy" assumes that the excitation energy ε_ν is much smaller than the mean field interparticle interaction $n_{0m}\widetilde{U}$ (n_{0m} is the maximum condensate density), and the quasiclassical character of the excitations requires the condition $\varepsilon_\nu \gg \hbar\omega$, where ω is the characteristic trap frequency. We consider anisotropic harmonic traps, where the discrete structure of the excitation spectrum is not important (see below). On the contrary, the inhomogeneity of the condensate density profile has a crucial consequence for the damping rates and energy shifts of quasiclassical low-energy excitations. The most important turns out to be the boundary region of the condensate, where $n_0(\mathbf{r})\tilde{U} \sim \varepsilon_\nu$. Therefore, the result for the damping rates and energy shifts is completely different from that in spatially homogeneous gases.

Secondly, we analyze the frequency shifts and damping of axially propagating sound waves in cylindrical Bose condensates. As found, the nature of damping is similar to that in the case of phonons in spatially homogeneous Bose condensates. We show that the attenuation of axially propagating sound wave packets in the recent MIT experiment [109] can be well explained as a consequence of this damping.

Finally, we consider the damping of the lowest excitations of a trapped Bose condensate. The damping of low-energy excitations differs fundamentally from the damping of Bogolyubov excitations in an infinitely large spatially homogeneous gas. In the latter case, characterized by a continuum of excitations, any given excitation can decay into two excitations of lower energy and momentum via the Beliaev mechanism (5.1.1). In a trapped Bose-condensed gas the character of the discrete structure of the spectrum of excitations makes the Beliaev damping impossible under conservation of energy. Therefore, irrespective of the relation between T and μ, the damping of the lowest excitations has to be provided by their interaction with the thermal excitations via the Szepfalusy-Kondor (SK) process (5.1.2). As the energies E_γ of the thermal excitations are much larger than the energies $E_\nu \sim \hbar\omega$ of the lowest excitations, the SK damping mechanism of the lowest excitations can be treated as Landau damping.

Summarizing these three examples we see, that in a trapped Bose-condensed gas the damping of low-energy excitations is determined by the behavior of their wavefunctions and by the distribution of the level spacings of thermal excitations with energies $E_\gamma < \mu$, which depends on the trap symmetry. We emphasize that stochastization in the behavior of these thermal excitations plays a key role for damping in non-spherical traps. In contrast to quasiclassical ($E_\nu \gg \hbar\omega$) low-energy excitations, the damping of the lowest excitations ($E_\nu \sim \hbar\omega$) is determined by the behavior of the excitations in the entire condensate region. For this case the damping rates following from our theory are in a good agreement with the data of the JILA experiment [50] and reasonably well explain the results of the experiment at MIT [51]. In the latter case the experimental conditions correspond to a crossover between the collisionless and hydrodynamic regimes, and the measured values of the damping rates are somewhat lower than the results of our calculations.

5.2. General equations

We consider a weakly interacting Bose-condensed gas confined in an external potential $V(\mathbf{r})$. The grand canonical Hamiltonian of the gas can be written as $\hat{H} = \hat{H}_0 + \hat{H}_1$, where (hereinafter

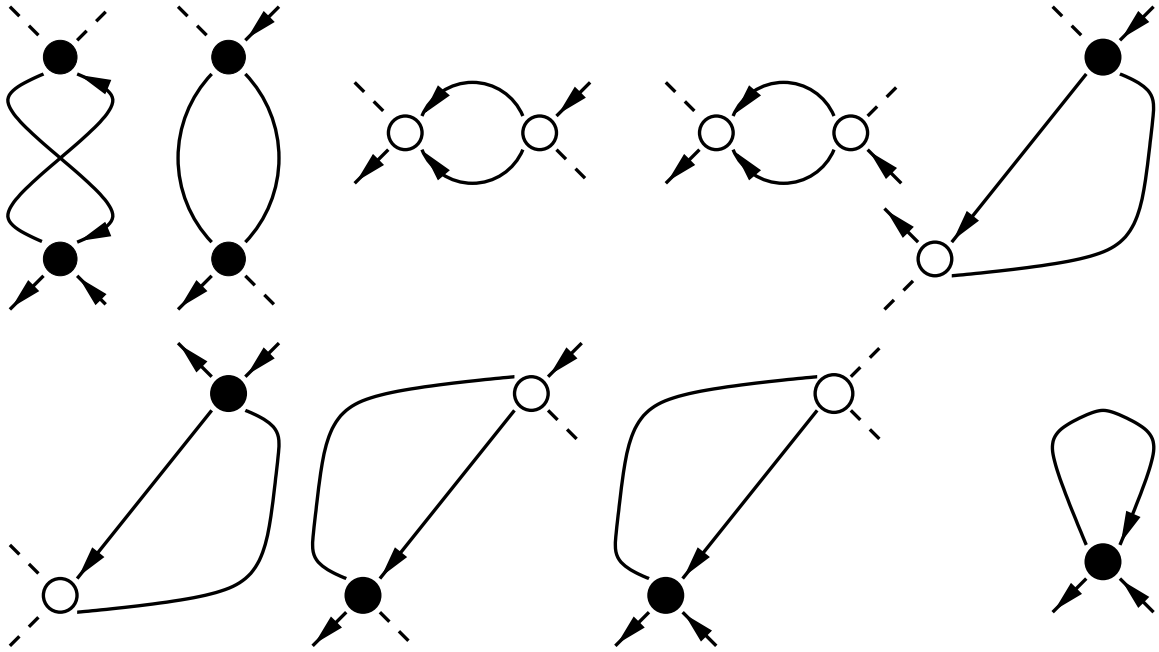

FIGURE 5.2.1. The set of diagrams contributing to the normal self-energy Σ. Here a solid line with an arrow represents the normal Green function $\mathcal{G}$, solid line without an arrow corresponds to the anomalous Green function $\mathcal{F}$, white circle stands for the interaction vertex $\tilde{U}$ and the black circle represents a sum of two white circles, one being a direct interaction and the other an exchange interaction. Dashed lines stand for the condensate wave function $\sqrt{n_0}$. The self-energy part Σ^+ can be obtained by a time-reversal(i.e. the change $t \to -t$ and $\mathbf{p} \to -\mathbf{p}$) of the graphs shown above.

$m = \hbar = 1$)

$$\hat{H}_0 = \int d^3r \hat{\Psi}^\dagger(\mathbf{r}) \left(-\frac{\Delta}{2} + V(\mathbf{r}) - \mu \right) \hat{\Psi}(\mathbf{r}), \tag{5.2.1}$$

and the term

$$\hat{H}_1 = \frac{\widetilde{U}}{2} \int d^3r \hat{\Psi}^\dagger(\mathbf{r}) \hat{\Psi}^\dagger(\mathbf{r}) \hat{\Psi}(\mathbf{r}) \hat{\Psi}(\mathbf{r}), \tag{5.2.2}$$

assumes a point interaction between atoms. The field operator of atoms $\hat{\Psi}(\mathbf{r})$ can be represented as the sum of the above-condensate part $\hat{\Psi}'$ and the condensate wavefunction $\Psi_0 = \langle \hat{\Psi} \rangle$ which is a *c*-number. As the interparticle interaction $\hat{H}_1$ contains both terms conserving the number of above-condensate particles and terms transferring two above-condensate particles to the condensate (or two condensate particles to the above-condensate part), the diagram technique should include both the normal Green function $\mathcal{G}$ and the anomalous Green function $\mathcal{F}$ (see, e.g. [100]).

The sums of the contributions of all irreducible diagrams will be represented by the normal (Σ) and anomalous (Σ_a) self-energies (see Fig.5.2.1 and 5.2.2). The former corresponds to the processes conserving the number of above-condensate particles, and the latter describes absorption (or emission) of two particles to (out of) the condensate. The Green function and self-energy operators satisfy Beliaev-Dyson equations [100, 102]

$$\mathcal{G} = G + G\Sigma\mathcal{G} + G\Sigma_a\mathcal{F}, \tag{5.2.3}$$

$$\mathcal{F} = G^+\Sigma^+\mathcal{F} + G^+\Sigma_a\mathcal{G}, \tag{5.2.4}$$

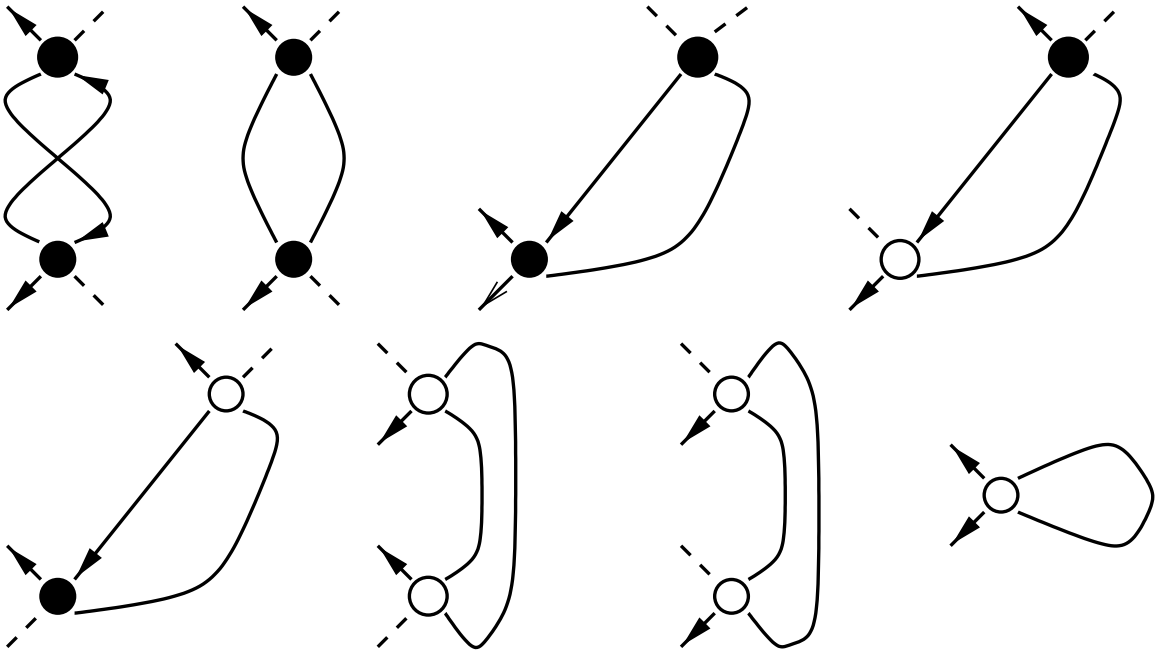

FIGURE 5.2.2. The set of graphs contributing to the anomalous self-energy Σ_a. The notations are the same as for the Fig. 5.2.1.

where the Green functions G and G^+ describe forward and backward propagation of a particle characterized by the Hamiltonian $\hat{H}_0$.

We confine ourselves to the case of repulsive interaction between the atoms ($a > 0$). To develop the finite temperature perturbation theory for calculating dynamic properties and finding the excitation spectrum of a weakly interacting Bose-condensed gas we will use the non-equilibrium generalization [110] of the Matsubara diagram technique. In Eqs. (5.2.3),(5.2.4) we perform an analytical continuation of the Matsubara frequencies $\zeta_j = 2\pi T j$ (j is an integer number) to the upper half-plane, which corresponds to the replacement $i\zeta_j \to \varepsilon + i0$. Then, multiplying both sides of Eqs. (5.2.3) and (5.2.4) by G^{-1} and $(G^+)^{-1}$, respectively, we arrive at the system of equations in the frequency-coordinate representation:

$$\varepsilon\mathcal{G}(\varepsilon;\mathbf{r},\mathbf{r}) = \left[-\frac{\Delta}{2} + V(\mathbf{r}) - \mu + \Sigma(\varepsilon)\right]\mathcal{G}(\varepsilon;\mathbf{r},\mathbf{r}') + \Sigma_a(\varepsilon)\mathcal{F}(\varepsilon;\mathbf{r},\mathbf{r}') + \delta(\mathbf{r}-\mathbf{r}'), \tag{5.2.5}$$

$$-\varepsilon\mathcal{F}(\varepsilon;\mathbf{r},\mathbf{r}') = \left[-\frac{\Delta}{2} + V(\mathbf{r}) - \mu + \Sigma^+(\varepsilon)\right]\mathcal{F}(\varepsilon;\mathbf{r},\mathbf{r}') + \Sigma_a(\varepsilon)\mathcal{G}(\varepsilon;\mathbf{r},\mathbf{r}'). \tag{5.2.6}$$

Here the action of the integral self-energy operators on the Green functions is written in a compact form $\int d^3r''\Sigma(\varepsilon;\mathbf{r},\mathbf{r}'')\mathcal{G}(\varepsilon;\mathbf{r}'',\mathbf{r}') \equiv \Sigma(\varepsilon)\mathcal{G}(\varepsilon;\mathbf{r},\mathbf{r}')$ (and similar relations for the other combinations).

The solutions of Eqs. (5.2.5),(5.2.6) can be written in the form of the Bogolyubov transformation for the Green functions

$$\mathcal{G}(\varepsilon;\mathbf{r},\mathbf{r}') = \sum_\nu \left\{\frac{u_\nu(\mathbf{r})u_\nu^*(\mathbf{r}')}{\varepsilon + i0 - \varepsilon_\nu} + \frac{v_\nu(\mathbf{r})v_\nu^*(\mathbf{r}')}{\varepsilon + i0 + \varepsilon_\nu}\right\},$$

$$\mathcal{F}(\varepsilon;\mathbf{r},\mathbf{r}') = -\sum_\nu \left\{\frac{u_\nu(\mathbf{r})v_\nu^*(\mathbf{r}')}{\varepsilon + i0 - \varepsilon_\nu} + \frac{v_\nu(\mathbf{r})u_\nu^*(\mathbf{r}')}{\varepsilon + i0 + \varepsilon_\nu}\right\},$$

where the index ν stands for the set of quantum numbers, and the eigenfunctions u_ν, v_ν and eigenenergies ε_ν satisfy generalized Bogolyubov-De Gennes equations

$$\varepsilon_\nu u_\nu(\mathbf{r}) = \left[-\frac{\Delta}{2}+V(\mathbf{r})-\mu+\Sigma(\varepsilon_\nu)\right]u_\nu(\mathbf{r})-\Sigma_a(\varepsilon_\nu)v_\nu(\mathbf{r}), \tag{5.2.7}$$

$$-\varepsilon_\nu v_\nu(\mathbf{r}) = \left[-\frac{\Delta}{2}+V(\mathbf{r})-\mu+\Sigma^+(\varepsilon_\nu)\right]v_\nu(\mathbf{r})-\Sigma_a(\varepsilon_\nu)u_\nu(\mathbf{r}). \tag{5.2.8}$$

Eqs. (5.2.7),(5.2.8) should be completed by a generalized Gross-Pitaevskii equation for the condensate wavefunction:

$$\left[-\frac{\Delta}{2}+V(\mathbf{r})-\mu+(\Sigma-\Sigma_a)|_{\varepsilon\to 0}\right]\Psi_0(\mathbf{r})=0 \tag{5.2.9}$$

and by the normalization condition

$$\int d^3r\,(n_0(\mathbf{r})+n'(\mathbf{r}))=N,$$

where $n_0(\mathbf{r})=|\Psi_0(\mathbf{r})|^2$ is the condensate density, $n'(\mathbf{r})=\left\langle\Psi'^\dagger(\mathbf{r})\Psi'(\mathbf{r})\right\rangle$ is the density of above-condensate particles, and N the total number of particles in the gas.

In the Bogolyubov-De Gennes approach only the terms bilinear in $\widehat{\Psi}'$ operators are retained in the interaction Hamiltonian $\hat{H}_1$, which assumes that the condensate density is much larger than the density of above-condensate particles. Then, the self-energy operators take the form

$$\Sigma(\varepsilon,\mathbf{r},\mathbf{r}') = 2n_0\widetilde{U}\delta(\mathbf{r}-\mathbf{r}'), \tag{5.2.10}$$

$$\Sigma_a(\varepsilon,\mathbf{r},\mathbf{r}') = n_0\widetilde{U}\delta(\mathbf{r}-\mathbf{r}'). \tag{5.2.11}$$

The result of their action on the condensate wavefunction $\Psi_0(\mathbf{r})$ and the functions $u_\nu(\mathbf{r})$, $v_\nu(\mathbf{r})$ is reduced to

$$\Sigma(\varepsilon_\nu)\Psi_0(\mathbf{r})=\int d^3r'\Sigma(\varepsilon_\nu,\mathbf{r},\mathbf{r}')\Psi_0(\mathbf{r}')=2n_0(\mathbf{r})\widetilde{U}\Psi_0(\mathbf{r})$$

and similar relations for the other combinations. Then, Eq.(5.2.9) becomes the ordinary Gross-Pitaevskii equation

$$\left[-\frac{\Delta}{2}+V(\mathbf{r})-\mu+n_0(\mathbf{r})\widetilde{U}\right]\Psi_0(\mathbf{r})=0, \tag{5.2.12}$$

and Eqs. (5.2.5),(5.2.6) are transformed to the ordinary Bogolyubov-De Gennes equations

$$\varepsilon_\nu u_\nu(\mathbf{r}) = \left[-\frac{\Delta}{2}+V(\mathbf{r})-\mu+2n_0(\mathbf{r})\widetilde{U}\right]u_\nu(\mathbf{r})-n_0(\mathbf{r})\widetilde{U}v_\nu(\mathbf{r}), \tag{5.2.13}$$

$$-\varepsilon_\nu v_\nu(\mathbf{r}) = \left[-\frac{\Delta}{2}+V(\mathbf{r})-\mu+2n_0(\mathbf{r})\widetilde{U}\right]v_\nu(\mathbf{r})-n_0(\mathbf{r})\widetilde{U}u_\nu(\mathbf{r}). \tag{5.2.14}$$

Taking into account Eq.(5.2.12), in terms of the functions $f_\nu^\pm = u_\nu \pm v_\nu$ these equations can be rewritten as

$$\varepsilon_\nu f_\nu^-(\mathbf{r}) = \left(-\frac{\Delta}{2}+\frac{\Delta\Psi_0}{2\Psi_0}\right)f_\nu^+(\mathbf{r}) \tag{5.2.15}$$

$$\varepsilon_\nu f_\nu^+(\mathbf{r}) = \left(-\frac{\Delta}{2}+\frac{\Delta\Psi_0}{2\Psi_0}+2|\Psi_0|^2\widetilde{U}\right)f_\nu^-(\mathbf{r}). \tag{5.2.16}$$

For a trapped Bose-condensed gas in the Thomas-Fermi regime, where $\mu \approx n_{0\,\max}\widetilde{U}$ is much larger then the spacing between the trap levels, the kinetic energy term in Eq. (5.2.12) can be omitted and one has [42, 43]

$$\Psi_0 = \sqrt{\frac{\mu - V(\mathbf{r})}{\widetilde{U}}}, \tag{5.2.17}$$

if the argument of the square root is positive and zero otherwise. For the low-energy excitations ($\varepsilon_\nu \ll n_{0m}\widetilde{U}$) of Thomas-Fermi condensates Eqs. (5.2.15),(5.2.16) can be reduced to hydrodynamic equations obtained by Stringari [55] and solved in the case of spherically symmetric harmonic potential $V(r)$ and for some excitations in a cylindrically symmetric potential. An analytical method of solving Eqs. (5.2.15),(5.2.16) (or the corresponding hydrodynamic equations) for the low-energy excitations of Thomas-Fermi condensates in an anisotropic harmonic potential $V(\mathbf{r})$ has been developed in [56, 111].

For a spatially homogeneous gas the generalized Gross-Pitaevskii equation (5.2.9) is equivalent to the Pines-Hugenholtz identity [101]. In the Bogolyubov approach it simply gives $\mu = n_0\widetilde{U}$, and Eqs. (5.2.13),(5.2.14) lead to the Bogolyubov spectrum

$$\varepsilon_p = \sqrt{(p^2/2)^2 + n_0\widetilde{U}p^2}, \tag{5.2.18}$$

where **p** is the momentum of the excitation.

Under the condition $n_0 \gg n'$, for which the Bogolyubov approach was originally developed, one can simply put n_0 equal to the total density n in Eq.(5.2.18). For $n' \sim n_0$, which can be the case at $T \gg \mu$, the dispersion law becomes essentially temperature dependent [98, 99]. In a spatially homogeneous gas the temperature dependence predominantly originates just from the presence of above condensate particles, with $n' \approx n(T/T_c)^{3/2}$ where $T_c = 3.31n^{2/3}$ is the BEC transition temperature. This leads to the replacement $n_0 \to n_0 + n'$ in Eq.(5.2.10) and gives $\mu = (n_0 + 2n')\widetilde{U}$. The dispersion law will be still given by Eq.(5.2.18) in which the condensate density is now temperature dependent: $n_0 = n\left[1 - (T/T_c)^{3/2}\right]$.

5.3. Spatially homogeneous Bose-condensed gas

In this section we present the results for the damping rates and energy shifts of elementary excitations in an infinitely large spatially homogeneous Bose-condensed gas. As one can see from Eqs.(5.2.13),(5.2.14), for finding the energy spectrum and wavefunctions of the excitations it is sufficient to calculate the self-energies Σ, Σ^+ and Σ_a. We will perform the calculations in the frequency-momentum representation and for physical transparency consider temperatures

$$T \gg n_0\tilde{U} \tag{5.3.1}$$

(the opposite limiting case has been discussed by Popov [102] with regard to the phonon branch of the excitation spectrum). In the zero order approximation in the parameter $(n_0a^3)^{1/2}$ we have the well-known mean field result: $\Sigma^{(0)} = \Sigma^{(0)+} = 2(n_0 + n'^{(0)})\widetilde{U}$, $\Sigma_a^{(0)} = n_0\widetilde{U}$, with $n'^{(0)} = n(T/T_c)^{3/2}$ (see above). In this approach we obtain the Bogolyubov quasiparticle excitations with the spectrum (5.2.18), which we use in order to calculate the next order in $(n_0a^3)^{1/2}$. The latter is determined by the contribution of diagrams containing one quasiparticle loop [102] (see Figures 5.2.1 and 5.2.2). Actually in this approach we represent the Hamiltonian as the sum of the (diagonalized) Bogolyubov Hamiltonian and the perturbation $\widehat{H}_{\text{int}}$ originating from $\widehat{H}_1$ (5.2.2) and containing the terms proportional to $\Psi_0\hat{\Psi}'^3$ and $\hat{\Psi}'^4$:

$$\hat{H}_{\text{int}} = \tilde{U}\int d^3r[\Psi_0(\mathbf{r})\hat{\Psi}'^\dagger(\mathbf{r})\{\hat{\Psi}'^\dagger(\mathbf{r}) + \hat{\Psi}'(\mathbf{r})\}\hat{\Psi}'(\mathbf{r}) + (1/2)\hat{\Psi}'^\dagger(\mathbf{r})\hat{\Psi}'^\dagger(\mathbf{r})\hat{\Psi}'(\mathbf{r})\hat{\Psi}'(\mathbf{r})]. \tag{5.3.2}$$

Retaining only the temperature-dependent contributions, after laborious calculations for the normal self-energy we obtain $\Sigma = \Sigma^{(0)} + \Sigma^{(1)}$, where

$$\Sigma^{(1)}(P) = \Sigma^n(P) + \Sigma^r(P),$$

$$\Sigma^n(P) = 2\widetilde{U}^2 n_0 \int \frac{d^3q}{(2\pi)^3}(n_q + n_k)\left(\frac{2A_kB_q + A_qA_k - 4A_kC_q + 2C_qC_k}{\varepsilon - \varepsilon_q - \varepsilon_k} - \right.$$

$$\left. \frac{2A_qB_k + B_qB_k - 4B_kC_q + 2C_qC_k}{\varepsilon + \varepsilon_k + \varepsilon_q}\right) - 8(\pi n_0 a^3)^{1/2}T, \tag{5.3.3}$$

$$\Sigma^r(P) = 2\widetilde{U}^2 n_0 \int \frac{d^3q}{(2\pi)^3}\frac{n_q - n_k}{\varepsilon + \varepsilon_q - \varepsilon_k}(2A_qA_k + 2A_kB_q + 2B_kB_q + 4C_kC_q - 4A_kC_q - 4B_qC_k). \tag{5.3.4}$$

Here $P = \{\varepsilon, \mathbf{p}\}$, $\mathbf{k} = \mathbf{q} + \mathbf{p}$, $E_p = p^2/2$, ε_p is given by Eq.(5.2.18), n_q is the equilibrium occupation number, $C_p = n_0\widetilde{U}/2\varepsilon_p$ and $A_p, B_p = (\pm\varepsilon_p + E_p + n_0\widetilde{U})/2\varepsilon_p$. Similarly, the correction to the anomalous self-energy is given by

$$\Sigma_a^{(1)}(P) = \Sigma_a^n(P) + \Sigma_a^r(P),$$

$$\Sigma_a^n(P) = 2\widetilde{U}^2 n_0 \int \frac{d^3q}{(2\pi)^3}(n_k + n_q)\left(\frac{2A_kB_q - 2A_kC_q - 2B_qC_k + 3C_qC_k}{\varepsilon - \varepsilon_q - \varepsilon_k} - \right.$$

$$\left. \frac{2A_qB_k - 2B_kC_q - 2A_qC_k + 3C_kC_q}{\varepsilon + \varepsilon_k + \varepsilon_q}\right) - 4(\pi n_0 a^3)^{1/2}T, \tag{5.3.5}$$

$$\Sigma_a^r(P) = 2\widetilde{U}^2 n_0 \int \frac{d^3q}{(2\pi)^3}\frac{n_q - n_k}{\varepsilon + \varepsilon_q - \varepsilon_k} \times \tag{5.3.6}$$

$$(2A_kA_q + 2B_kB_q + 6C_kC_q - 2A_kC_q - 2A_qC_k - 2B_qC_k - 2B_kC_q). \tag{5.3.7}$$

The resonant parts Σ^r, Σ_a^r originate from the terms where one of the intermediate quasiparticles is created and another one annihilated, and the non-resonant parts Σ^n, Σ_a^n from the terms where both intermediate quasiparticles are created (annihilated). Temperature independent terms in the non-resonant parts, found by Beliaev [100], are omitted in Eqs.(5.3.3)-(5.3.6).

Each of the self-energies (5.3.3)-(5.3.6) is singular at $P \to 0$ and at least for small momenta the corrections become larger than the mean field values (5.2.10). Nevertheless, keeping in mind that any physical quantity is determined by the combinations of the self-energies, which do not contain the infra-red singularities, we will still treat $\Sigma^{(1)}$ and $\Sigma_a^{(1)}$ as perturbations.

For a spatially homogeneous gas the Pines-Hugenholtz identity $\mu = (\Sigma(P) - \Sigma_a(P))|_{P\to 0}$ gives the first order correction to the chemical potential

$$\mu^{(1)} = -\beta\sqrt{n_0}; \quad \beta = 12(\pi a^3)^{1/2}T, \tag{5.3.8}$$

and the relation between n_0 and the chemical potential, $\mu = n_0\widetilde{U} - \beta\sqrt{n_0}$, coincides with that found by Popov [102]. The u, v functions in generalized Bogolyubov-De Gennes equations (5.2.7), (5.2.8) can be written as $u_p \exp(i\mathbf{pr})$ and $v_p \exp(i\mathbf{pr})$, and in terms of the functions $f_p^{\pm} = u_p \pm v_p$ these equations take the form

$$(\varepsilon - S^-(P))f_p^- = \left(\frac{p^2}{2} + S_-^+(P)\right) f_p^+, \tag{5.3.9}$$

$$(\varepsilon - S^-(P))f_p^+ = \left(\frac{p^2}{2} + 2n_0\widetilde{U} + S_+^+(P)\right) f_p^-, \tag{5.3.10}$$

where

$$S_{\pm}^{+} = \frac{\Sigma^{(1)} + \Sigma^{+(1)}}{2} + \beta\sqrt{n_0} \pm \Sigma_a, \tag{5.3.11}$$

$$S^{-} = \frac{\Sigma^{(1)} - \Sigma^{+(1)}}{2}. \tag{5.3.12}$$

Considering the terms S^-, $S_\pm^+$ in Eqs. (5.3.9),(5.3.10) as small perturbations we put $\varepsilon = \varepsilon_p$ in the expressions for these quantities, following from Eqs. (5.3.3)-(5.3.6). Then, solving Eqs. (5.3.9),(5.3.10), for the excitation energy we obtain $\varepsilon = \varepsilon_p + \varepsilon_p^{(1)}$, where

$$\varepsilon_p^{(1)} = \left[\frac{E_p}{2\varepsilon_p} S_+^+(P) + \frac{\varepsilon_p}{2E_p} S_-^+(P) + S^-(P)\right]_{P\to(\varepsilon_p,\mathbf{p})}. \tag{5.3.13}$$

As $\Sigma^{(1)}$ and $\Sigma_a^{(1)}$ are complex, the correction to the excitation energy has both a real and an imaginary part: $\varepsilon_p^{(1)} = \delta\varepsilon_p - i\Gamma_p$. The former gives the energy shift, and the latter is responsible for damping of the excitations.

5.3.1. Phonon branch of the excitation spectrum. For the phonon branch of the excitation spectrum ($\varepsilon_p \ll n_0\tilde{U}$) we calculate analytically both $\delta\varepsilon_p$ and Γ_p on the basis of Eqs.(5.3.3)-(5.3.13). Under the condition $T \gg n_0\tilde{U}$ the Beliaev damping processes (5.1.1) can be neglected, and the non-resonant contributions to the quantities $S_\pm^+$ and $S^-$are purely real:

$$S_-^{+n} = \frac{2}{3}\beta\sqrt{n_0} - 2\tilde{U}\int \frac{d^3q}{(2\pi)^3}\frac{T\mu}{4\varepsilon_k^2\varepsilon_q^2}\times$$

$$\left\{(\varepsilon_k+\varepsilon_q)^2 - (E_k - E_q)^2 + \varepsilon^2 - \frac{\varepsilon^3}{2}\left(\frac{1}{\varepsilon-\varepsilon_k-\varepsilon_q} + \frac{1}{\varepsilon+\varepsilon_k+\varepsilon_q}\right)\right\}, \tag{5.3.14}$$

$$S^{-n} = -2\tilde{U}\int \frac{d^3q}{(2\pi)^3}\frac{T\mu}{4\varepsilon_k^2\varepsilon_q^2}(2E_k\varepsilon - 2\mu\varepsilon), \tag{5.3.15}$$

$$S_+^{+n} = -2\tilde{U}\int \frac{d^3q}{(2\pi)^3}\frac{T\mu}{4\varepsilon_k^2\varepsilon_q^2}\left\{4\mu^2 + 8E_k^2 - 4\varepsilon_k^2 + 2\mu^2\varepsilon\left(\frac{1}{\varepsilon-\varepsilon_k-\varepsilon_q} + \frac{1}{\varepsilon+\varepsilon_k+\varepsilon_q}\right)\right\}. \tag{5.3.16}$$

A part of the resonant terms acquire a non-resonant character, and it is convenient to separate each of the quantities $S_\pm^{+r}$, S^{-r} into two parts, i.e. $S_\pm^{+(rr)}$, $S^{-(rr)}$ which contain a resonant denominator $(\varepsilon + \varepsilon_q - \varepsilon_k)^{-1}$ and the parts $S_\pm^{+(rn)}$, $S^{-(rn)}$ which do not contain this denominator. Then from Eqs.(5.3.3)-(5.3.6) we obtain

$$S_-^{+rn} = 2\tilde{U}\int \frac{d^3q}{(2\pi)^3}\frac{T\mu}{4\varepsilon_k^2\varepsilon_q^2}((E_k - E_q)^2 - (\varepsilon_k - \varepsilon_q)^2 - \varepsilon^2\frac{\mu^2}{\varepsilon_k^2+\mu^2}), \tag{5.3.17}$$

$$S^{-rn} = 2\tilde{U}\int \frac{d^3q}{(2\pi)^3}\frac{T\mu}{4\varepsilon_k^2\varepsilon_q^2}(2\mu\varepsilon + \varepsilon\frac{2E_k\mu}{E_k+\mu}), \tag{5.3.18}$$

$$S_+^{+rn} = -2\tilde{U}\int \frac{d^3q}{(2\pi)^3}\frac{T\mu}{4\varepsilon_k^2\varepsilon_q^2}(8\varepsilon_k^2 + 18E_k^2 + 4\mu^2), \tag{5.3.19}$$

and

$$S_-^{+(rr)} = 2\tilde{U}\int \frac{d^3q}{(2\pi)^3}\frac{T\mu}{4\varepsilon_k^2\varepsilon_q^2}\frac{\varepsilon^3}{(\varepsilon+\varepsilon_q-\varepsilon_k)}\frac{\mu^2}{\varepsilon_k^2+\mu^2}, \tag{5.3.20}$$

$$S^{-(rr)} = -2\tilde{U}\int \frac{d^3q}{(2\pi)^3}\frac{T\mu}{4\varepsilon_k^2\varepsilon_q^2}\frac{\varepsilon^2}{(\varepsilon+\varepsilon_q-\varepsilon_k)}(2\mu+\frac{2E_k\mu}{E_k+\mu}), \tag{5.3.21}$$

$$S_+^{+(rr)} = 2\tilde{U}\int \frac{d^3q}{(2\pi)^3}\frac{T\mu}{4\varepsilon_k^2\varepsilon_q^2}\frac{\varepsilon(4\mu^2+8\varepsilon_k^2+8E_k^2)}{(\varepsilon+\varepsilon_q-\varepsilon_k)}. \tag{5.3.22}$$

Only the resonant terms (5.3.20)-(5.3.22) containing the denominator $(\varepsilon+\varepsilon_q-\varepsilon_k+i0)^{-1}$ have an imaginary part and, hence, contribute to the damping rate. From (5.3.20)-(5.3.22) and (5.3.13) we find

$$\Gamma_p = -\mathrm{Im}2\tilde{U}\int \frac{d^3q}{(2\pi)^3}\frac{T\mu}{4\varepsilon_k^2\varepsilon_q^2}\frac{\varepsilon^2}{\varepsilon+\varepsilon_q-\varepsilon_k}\left\{-\frac{\mu\varepsilon_k^2}{\varepsilon_k^2+\mu^2}-\frac{2E_k\mu}{\sqrt{\varepsilon_k^2+\mu^2}}+\frac{2(\varepsilon_k^2+E_k^2)}{\mu}\right\}. \tag{5.3.23}$$

The corresponding resonant contribution $\delta\varepsilon_p^r$ to the energy shift is given by the real part of the same expression (with opposite sign). Purely real non-resonant terms (5.3.14)-(5.3.19) only contribute to the energy shifts in Eq.(5.3.13). There is a contribution $\delta\varepsilon_p^n$ proportional to ε and a contribution $\delta\varepsilon_p^{ns}$ proportional to p^2/ε:

$$\delta\varepsilon_p^n = 2\tilde{U}\varepsilon\int \frac{d^3q}{(2\pi)^3}\frac{T\mu}{4\varepsilon_k^2\varepsilon_q^2}\left\{\frac{\mu\varepsilon_k^2}{\varepsilon_k^2+\mu^2}+\frac{2E_k\mu}{E_k+\mu}-2\frac{(\varepsilon_k^2+E_k^2)}{\mu}-\frac{E_k^2}{\mu}\right\}, \tag{5.3.24}$$

$$\delta\varepsilon_p^{ns} = 2\tilde{U}\int \frac{d^3q}{(2\pi)^3}\frac{T\mu}{4\varepsilon_k^2\varepsilon_q^2}\frac{2(E_k-E_q)^2\mu}{\varepsilon}, \tag{5.3.25}$$

where $(E_k-E_q)^2=(\mathbf{pq}+p^2/2)^2/m^2$.

Performing the integration in Eqs.(5.3.23)-(5.3.25) and setting $\varepsilon=\varepsilon_p$, we obtain

$$\delta\varepsilon_p^r \approx 2\varepsilon_p(n_0a^3)^{1/2}T/\mu,$$

$$\delta\varepsilon_p^n = (-8.41-\sqrt{\pi})\varepsilon_p(n_0a^3)^{1/2}T/\mu$$

and

$$\delta\varepsilon_p^{ns} = -2\sqrt{\pi}/3\times\varepsilon_p(n_0a^3)^{1/2}T/\mu.$$

For the damping rate Γ_p and the total shift $\delta\varepsilon_p=\delta\varepsilon_p^r+\delta\varepsilon_p^n+\delta\varepsilon_p^{ns}$ we find

$$\delta\varepsilon_p \approx -7\varepsilon_p\frac{T}{n_0\widetilde{U}}(n_0a^3)^{1/2}, \tag{5.3.26}$$

$$\Gamma_p = \varepsilon_p\frac{3\pi^{3/2}T}{4n_0\widetilde{U}}(n_0a^3)^{1/2}. \tag{5.3.27}$$

The damping rate Γ_p, described solely by the resonant contributions, originates from quasi-resonant scattering of thermal excitations from a given excitation (Landau damping) and is absent at $T=0$. Both the energy shift and the damping rate are determined by the interaction of a given excitation with intermediate quasiparticles having energies $\varepsilon_q\sim n_0\widetilde{U}$. The damping rate Γ_p (5.3.27) coincides with that found in recent contributions [105, 107, 108] and contains a slight numerical difference from the earlier Szepfalusy-Kondor result [104]. The energy shift for the phonon branch of the spectrum was also calculated in [105]. In the latter work the expansion of the self-energy functions near the point $\varepsilon=\varepsilon_p$ was used and formally divergent integrals were canceling each other in the final expression for the energy shift, which have led to the result by approximately factor 6 smaller then the shift (5.3.26) obtained by the exact integration.

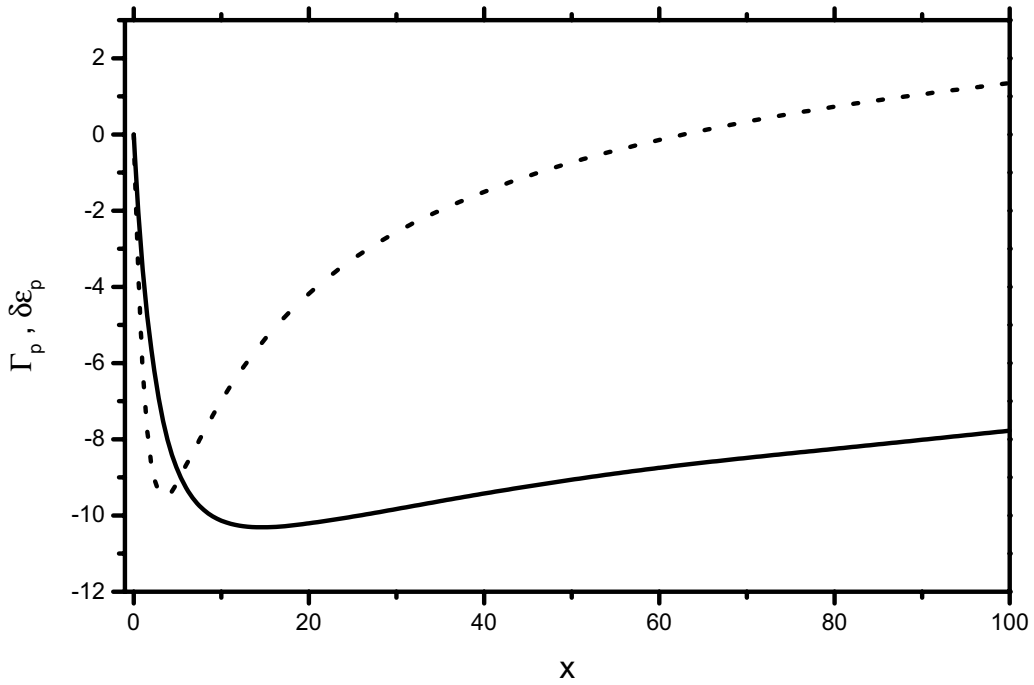

FIGURE 5.3.1. The damping rate Γ_p (solid line) and the energy shift $\delta\varepsilon_p$ (dashed line) versus $x = (\varepsilon_p/n_0\widetilde{U})$. Both Γ_p and $\delta\varepsilon_p$ are given in the units of $T(n_0a^3)^{1/2}$.

5.3.2. General case (arbitrary excitation energies). Eqs.(5.3.26),(5.3.27) clearly show that the small parameter of the theory is $(T/n_0\tilde{U})(n_0a^3)^{1/2} \ll 1$ (see Eq.(5.1.3)), whereas in the zero temperature approach [100] the small parameter is $(n_0a^3)^{1/2} \ll 1$. The presence of an additional large factor $T/n_0\widetilde{U}$ at finite temperatures $T \gg n_0\widetilde{U}$ originates from the Bose enhancement of diagrams containing one quasiparticle loop: Compared to the zero-temperature case the contribution of each of these diagrams is multiplied by the Bose factor $n_q = [\exp(\varepsilon_q/T) - 1]^{-1}$ (or $1 + n_q$). As the most important are intermediate quasiparticles with energies $\varepsilon_q \sim n_0\widetilde{U}$, for $T \gg n_0\widetilde{U}$ the Bose factor $n_q \sim T/n_0\widetilde{U}$. A criterion similar to Eq.(5.1.3) was found by Popov [99, 102] as the condition which allows one to use the mean-field approach at finite temperatures and to renormalize the theory for reaching beyond this approach.

Remarkably, the criterion (5.1.3) is fulfilled even at temperatures very close to T_c. For $\Delta T = T_c - T \ll T_c$ we have $n_0 \sim n\Delta T/T_c$, and Eq.(5.1.3) gives $\Delta T/T_c \gg (n_0a^3)^{1/3}$, which coincides with the well known Ginzburg criterion [112] for the absence of critical fluctuations. The criterion (5.1.3) also ensures that the main contribution to the damping rate originates from the interaction of a given excitation with thermal excitations through the condensate, i.e., from the first term in $\hat{H}_{\rm int}$ (5.3.2).

For any excitation energy $\varepsilon_p \ll T$ the energy shift and damping rate, being expressed in units of $T(n_0a^3)^{1/2}$, turn out to be universal functions of the parameter $\varepsilon_0/n_0\widetilde{U}$. These functions, calculated numerically from Eq.(5.3.13) on the basis of Eqs. (5.3.3)-(5.3.6) and (5.3.11),(5.3.12), are presented in Fig. 5.3.1. One can easily check that under condition (5.1.3) both the damping rate and energy shift are always much smaller than ε_p. In the phonon branch of the excitation spectrum ($\varepsilon_p \ll n_0\widetilde{U}$) the results of the numerical calculations coincide with those following from Eqs. (5.3.26), (5.3.27).

For $\varepsilon_p \lesssim n_0\widetilde{U}$ the damping rate $(-\Gamma_p)$ increases with ε_p, reaches its maximum at $\varepsilon_p \sim 10n_0\widetilde{U}$, and then slowly decreases with further increase of ε_p. The energy shift for $\varepsilon_p \lesssim n_0\widetilde{U}$ is negative. The modulus of the shift increases with ε_p and reaches its maximum at $\varepsilon_p \approx 4n_0\widetilde{U}$. Further increase of ε_p decreases $|\delta\varepsilon_p|$. The latter is equal to zero for $\varepsilon_p \approx 60n_0\widetilde{U}$, and becomes positive at larger ε_p.

For single-particle excitations ($\varepsilon_p = p^2/2 \gg n_0\widetilde{U}$), calculating the self-energy functions (5.3.11) and (5.3.12), from Eq.(5.3.13) we obtain

$$\delta\varepsilon_p = 4(\pi n_0 a^3)^{1/2} T \left[1 - 12.6 \left(\frac{n_0\widetilde{U}}{2\varepsilon_p}\right)^{1/2}\right], \tag{5.3.28}$$

$$\Gamma_p = 16(\pi n_0 a^3)^{1/2} T \left(\frac{n_0\widetilde{U}}{2\varepsilon_p}\right)^{1/2} \ln\left(\frac{2\varepsilon_p}{n_0\widetilde{U}}\right). \tag{5.3.29}$$

The damping rate can be written as $\Gamma_p \sim (T/\varepsilon_p) n_0 \sigma v_p$, where $\sigma = 8\pi a^2$ is the elastic cross section, and v_p the particle velocity. This damping rate exceeds the Beliaev temperature-independent term $n\sigma v_p$ even at T close to T_c, if $\Delta T = T_c - T \gg \varepsilon_p$. In contrast to the phonon branch of the spectrum, for $\varepsilon_p \gtrsim n_0\widetilde{U}$ the damping is provided by both the Szepfalusy-Kondor ($\nu + \gamma \leftrightarrow \gamma'$) and Beliaev ($\nu \leftrightarrow \gamma + \gamma'$) processes and, hence, can no longer be treated as Landau damping. The small parameter of the theory is still given by Eq.(5.1.3), since even at $\varepsilon_p \gg n_0\widetilde{U}$ the energy of at least one of the thermal excitations is of order $n_0\widetilde{U}$.

The above results for the damping rate and energy shift of a given excitation are obtained in the so called collisionless regime: We assume that the de Broglie wavelength of the excitation, $1/p$, is much larger than the mean free path of thermal quasiparticles with energies $\sim n_0\widetilde{U}$, which are mostly responsible for the damping and shifts. It is also assumed that the excitation energy ε_p greatly exceeds the damping rate of these thermal excitations. The latter is of order $T(n_0a^3)^{1/2}$ (see Fig. 5.3.1), and for $\varepsilon_p \lesssim n_0\widetilde{U}$ the two requirements of the collisionless regime are well satisfied under condition (5.1.3). In the phonon branch of the excitation spectrum ($\varepsilon_p \ll n_0\widetilde{U}$) these requirements are equivalent to each other, and the collisionless criterion can be simply written as

$$\varepsilon_p \gg T(n_0a^3)^{1/2}. \tag{5.3.30}$$

As clearly seen, in the phonon branch one can always find excitations which do not satisfy Eq.(5.3.30) and, hence, require a hydrodynamic description with regard to their damping rates and energy shifts.

The collisionless criterion (5.3.30) provides an additional argument on support of the above used perturbative approach for solving Eqs. (5.3.9), (5.3.10). Under condition (5.3.30) the term $S^- \lesssim T(n_0a^3)^{1/2} \ll \varepsilon_p$, $S_-^+ \lesssim \varepsilon_p(T/n_0\widetilde{U})(n_0a^3)^{1/2} \ll p^2$, and $S_+^+ \lesssim (n_0\widetilde{U}/\varepsilon_p)T(n_0a^3)^{1/2} \ll n_0\widetilde{U}$.

The non-mean-field shift $\delta\varepsilon_p$ is actually the shift of the excitation energy ε_p at a given condensate density n_0. On the other hand, ε_p is determined by the Bogolyubov dispersion law (5.2.18), with the temperature-dependent condensate density $n_0(T)$, and, hence, is temperature-dependent by itself. Therefore, at a given T one will also have the mean-field temperature-dependent energy shift $\delta\varepsilon_p^{\rm mf} = \varepsilon_p(T) - \varepsilon_p(0)$. As the condensate density decreases with increasing temperature, $\delta\varepsilon_p^{\rm mf}$ is always negative. For $T \gg n_0\widetilde{U}$ it greatly exceeds the above calculated shift $\delta\varepsilon_p$ at any p. The ratio $(\delta\varepsilon_p^{\rm mf}/\delta\varepsilon_p)$ decreases with temperature, but even for $n' \ll n_0$ one has

$$\delta\varepsilon_p^{\rm mf} = -\varepsilon_p(0)\frac{n'(T)\widetilde{U}}{p^2/2 + 2n_0(0)\widetilde{U}}, \tag{5.3.31}$$

and $(\delta\varepsilon_p^{\rm mf}/\delta\varepsilon_p) \sim (T/n_0\widetilde{U})^{1/2} \gg 1$.

5.4. Spatially inhomogeneous Bose-condensed gas

We now generalize the above obtained results for the case of elementary excitations in a spatially inhomogeneous (trapped) Bose-condensed gas. As already mentioned in the introduction, a new ingredient here is related to the inhomogeneous density profile of the condensate and the discrete structure of the excitation spectrum. This requires us to develop a new method of calculating the self-energy functions in generalized Bogolyubov-De Gennes equations (5.2.7), (5.2.8). The self-energy operators in these equations are the sums of the zeroth and first order terms:

$$\Sigma_a(\varepsilon,\mathbf{r},\mathbf{r'}) = n_0(\mathbf{r})\widetilde{U}\delta(\mathbf{r}-\mathbf{r'}) + \Sigma_a^{(1)}, \tag{5.4.1}$$

$$\Sigma(\varepsilon,\mathbf{r},\mathbf{r'}) = 2(n_0(\mathbf{r}) + n'^{(0)})\widetilde{U}\delta(\mathbf{r}-\mathbf{r'}) + \Sigma^{(1)}, \tag{5.4.2}$$

and a similar relation for Σ^+. At temperatures $T \gg n_{0m}\widetilde{U}$ the zero order value of the above-condensate density in the condensate spatial region is coordinate independent and equal to the above-condensate density in the ideal gas approach: $n'^{(0)}(T) = 2.6(T/2\pi)^{3/2}$. On the contrary, the self-energies $\Sigma^{(1)}$, $\Sigma_a^{(1)}$ depend explicitly on the condensate density. Due to the discrete structure of the energy spectrum of excitations the expressions for these quantities should be written in the form of sums over the discrete states of intermediate quasiparticles γ,γ'. In the frequency-coordinate representation we have

$$\Sigma(\varepsilon_\nu,\mathbf{r},\mathbf{r}') = \Sigma^n(\varepsilon_\nu,\mathbf{r},\mathbf{r}') + \Sigma^r(\varepsilon_\nu,\mathbf{r},\mathbf{r}'),$$

$$\Sigma^n(\varepsilon_\nu,\mathbf{r},\mathbf{r}') = 2\Psi_0(\mathbf{r})\Psi_0(\mathbf{r}')\tilde{U}^2\sum_{\gamma,\gamma'}(n_\gamma+n_{\gamma'})\left(\frac{2u_\gamma(\mathbf{r})u_\gamma(\mathbf{r}')v_{\gamma'}(\mathbf{r})v_{\gamma'}(\mathbf{r}') + u_\gamma(\mathbf{r})u_\gamma(\mathbf{r}')u_{\gamma'}(\mathbf{r})u_{\gamma'}(\mathbf{r}')}{\varepsilon-\varepsilon_\gamma-\varepsilon_{\gamma'}}\right.$$

$$+\frac{-4u_\gamma(\mathbf{r})u_\gamma(\mathbf{r}')u_{\gamma'}(\mathbf{r})v_{\gamma'}(\mathbf{r}) + 2u_\gamma(\mathbf{r})v_\gamma(\mathbf{r}')u_{\gamma'}(\mathbf{r})v_{\gamma'}(\mathbf{r}')}{\varepsilon-\varepsilon_\gamma-\varepsilon_{\gamma'}} -$$

$$\frac{2v_\gamma(\mathbf{r})v_\gamma(\mathbf{r}')u_{\gamma'}(\mathbf{r})u_{\gamma'}(\mathbf{r}') + v_\gamma(\mathbf{r})v_\gamma(\mathbf{r}')v_{\gamma'}(\mathbf{r})v_{\gamma'}(\mathbf{r}') - 4v_\gamma(\mathbf{r})v_\gamma(\mathbf{r}')u_{\gamma'}(\mathbf{r})v_{\gamma'}(\mathbf{r}')}{\varepsilon+\varepsilon_\gamma+\varepsilon_{\gamma'}}$$

$$\left.\frac{2u_\gamma(\mathbf{r})v_\gamma(\mathbf{r}')u_{\gamma'}(\mathbf{r})v_{\gamma'}(\mathbf{r}')}{\varepsilon+\varepsilon_\gamma+\varepsilon_{\gamma'}}\right) - 8(n_0\pi a^3)^{1/2}T\delta(\mathbf{r}-\mathbf{r}'), \tag{5.4.3}$$

$$\Sigma^r(\varepsilon_\nu,\mathbf{r},\mathbf{r}') = 2\Psi_0(\mathbf{r})\Psi_0(\mathbf{r}')\tilde{U}^2\sum_{\gamma,\gamma'}\frac{n_{\gamma'}-n_\gamma}{\varepsilon+\varepsilon_{\gamma'}-\varepsilon_\gamma}$$

$$(2u_\gamma(\mathbf{r})u_\gamma(\mathbf{r}')u_{\gamma'}(\mathbf{r})u_{\gamma'}(\mathbf{r}') + 2u_\gamma(\mathbf{r})u_\gamma(\mathbf{r}')v_{\gamma'}(\mathbf{r})v_{\gamma'}(\mathbf{r}') + 2v_\gamma(\mathbf{r})v_\gamma(\mathbf{r}')v_{\gamma'}(\mathbf{r})v_{\gamma'}(\mathbf{r}')+$$

$$4u_\gamma(\mathbf{r})v_\gamma(\mathbf{r}')u_{\gamma'}(\mathbf{r})v_{\gamma'}(\mathbf{r}') - 4u_\gamma(\mathbf{r})u_\gamma(\mathbf{r}')u_{\gamma'}(\mathbf{r})v_{\gamma'}(\mathbf{r}') - 4u_\gamma(\mathbf{r})v_\gamma(\mathbf{r}')v_{\gamma'}(\mathbf{r})v_{\gamma'}(\mathbf{r}')). \tag{5.4.4}$$

$$\Sigma_a = \Sigma_a^n(\varepsilon_\nu,\mathbf{r},\mathbf{r}') + \Sigma_a^r(\varepsilon_\nu,\mathbf{r},\mathbf{r}'),$$

$$\Sigma_a^n(\varepsilon_\nu,\mathbf{r},\mathbf{r}') = 2\Psi_0(\mathbf{r})\Psi_0(\mathbf{r}')\tilde{U}^2\sum_{\gamma,\gamma'}(n_\gamma+n_{\gamma'})$$

$$\left(\frac{2u_\gamma(\mathbf{r})u_\gamma(\mathbf{r}')v_{\gamma'}(\mathbf{r})v_{\gamma'}(\mathbf{r}') - 2u_\gamma(\mathbf{r})u_\gamma(\mathbf{r}')u_{\gamma'}(\mathbf{r})v_{\gamma'}(\mathbf{r}')}{\varepsilon-\varepsilon_\gamma-\varepsilon_{\gamma'}}\right.$$

$$\left.\frac{-2u_\gamma(\mathbf{r})v_\gamma(\mathbf{r}')v_{\gamma'}(\mathbf{r})v_{\gamma'}(\mathbf{r}') + 3u_\gamma(\mathbf{r})v_\gamma(\mathbf{r}')u_{\gamma'}(\mathbf{r})v_{\gamma'}(\mathbf{r}')}{\varepsilon-\varepsilon_\gamma-\varepsilon_{\gamma'}} -\right.$$

$$\frac{2v_\gamma(\mathbf{r})v_\gamma(\mathbf{r}')u_{\gamma'}(\mathbf{r})u_{\gamma'}(\mathbf{r}') - 2v_\gamma(\mathbf{r})v_\gamma(\mathbf{r}')u_{\gamma'}(\mathbf{r})v_{\gamma'}(\mathbf{r}')}{\varepsilon+\varepsilon_\gamma+\varepsilon_{\gamma'}}$$

$$-\frac{2u_\gamma(\mathbf{r})v_\gamma(\mathbf{r}')u_{\gamma'}(\mathbf{r})u_{\gamma'}(\mathbf{r}') + 3u_\gamma(\mathbf{r})v_\gamma(\mathbf{r}')u_{\gamma'}(\mathbf{r})v_{\gamma'}(\mathbf{r}')}{\varepsilon+\varepsilon_\gamma+\varepsilon_{\gamma'}}\Bigg) - 4(n_0\pi a^3)^{1/2}T\delta(\mathbf{r}-\mathbf{r}'), \tag{5.4.5}$$

$$\Sigma_a^r(\varepsilon_\nu,\mathbf{r},\mathbf{r}') = 2\Psi_0(\mathbf{r})\Psi_0(\mathbf{r}')\tilde{U}^2\sum_{\gamma,\gamma'}\frac{n_{\gamma'}-n_\gamma}{\varepsilon+\varepsilon_{\gamma'}-\varepsilon_\gamma}$$

$$(2u_\gamma(\mathbf{r})u_\gamma(\mathbf{r}')u_{\gamma'}(\mathbf{r})u_{\gamma'}(\mathbf{r}') + 2v_\gamma(\mathbf{r})v_\gamma(\mathbf{r}')v_{\gamma'}(\mathbf{r})v_{\gamma'}(\mathbf{r}') + 6u_\gamma(\mathbf{r})v_\gamma(\mathbf{r}')u_{\gamma'}(\mathbf{r})v_{\gamma'}(\mathbf{r}') -$$

$$2u_\gamma(\mathbf{r})u_\gamma(\mathbf{r}')u_{\gamma'}(\mathbf{r})v_{\gamma'}(\mathbf{r}') - 2u_\gamma(\mathbf{r})v_\gamma(\mathbf{r}')u_{\gamma'}(\mathbf{r})u_{\gamma'}(\mathbf{r}') - 2u_\gamma(\mathbf{r})v_\gamma(\mathbf{r}')v_{\gamma'}(\mathbf{r})v_{\gamma'}(\mathbf{r}') -$$

$$2v_\gamma(\mathbf{r})v_\gamma(\mathbf{r}')u_{\gamma'}(\mathbf{r})v_{\gamma'}(\mathbf{r}')). \tag{5.4.6}$$

As we saw in the previous section, in the spatially homogeneous case all physical quantities are determined by the contribution to the self-energy functions $\Sigma^{(1)}$, $\Sigma_a^{(1)}$ from intermediate quasiparticles with energies of order the mean field interaction between particles. The same holds for a spatially inhomogeneous (trapped) Bose-condensed gas in the Thomas-Fermi regime, where the mean field interaction $n_{0m}\widetilde{U}$ greatly exceeds the level spacing in the trapping potential. The intermediate quasiparticles with energies of order $n_{0m}\widetilde{U}$ are essentially quasiclassical. With regard to the integral operator $(\Sigma^{(1)}-\Sigma_a^{(1)})_{\varepsilon\to 0}$ in the generalized Gross-Pitaevskii equation (5.2.9), which is solely determined by non-resonant contributions, this immediately allows one to replace the summation over the discrete intermediate states by integration. The kernel of this integral operator varies at distances $|\mathbf{r}-\mathbf{r'}|$ of order the correlation length $l_{\rm cor}=1/\sqrt{n_0\widetilde{U}}$ which is much smaller than the characteristic size of the condensate. Therefore, the result of the operator action on the condensate wavefunction can be written in the local density approximation and, hence, should rely on Eq.(5.3.8) with coordinate-dependent condensate density $n_0(\mathbf{r})$:

$$\left[\Sigma^{(1)}-\Sigma_a^{(1)}\right]_{\varepsilon\to 0}\Psi_0(\mathbf{r}) = \int d^3r'\left[\Sigma^{(1)}(\varepsilon,\mathbf{r},\mathbf{r'})-\Sigma_a^{(1)}(\varepsilon,\mathbf{r},\mathbf{r'})\right]_{\varepsilon\to 0}\Psi_0(\mathbf{r'}) = -\beta\Psi_0^2(\mathbf{r}). \tag{5.4.7}$$

This result can be easily obtained from Eqs. (5.4.3)-(5.4.6), where one should put $\varepsilon_\nu=0$, neglect the difference between ε_γ and $\varepsilon_{\gamma'}$, and make a summation over γ'. Replacing the summation over γ by integration one should also take into account that for quasiclassical excitations the functions $f_\gamma^\pm$ can be represented in the form

$$f_\gamma^{\pm(0)}(\mathbf{r}) = \left(\frac{\sqrt{\varepsilon_\gamma^2+(n_0(\mathbf{r})\tilde{U})^2}-n_0(\mathbf{r})\tilde{U}}{\varepsilon_\gamma}\right)^{\mp 1/2} f_\gamma(\mathbf{r}), \tag{5.4.8}$$

where $|f_\gamma(\mathbf{r})|^2$ is the ratio of the local to total density of states for Bogolyubov quasiparticles of a given symmetry, described by the classical Hamiltonian

$$H(\mathbf{p},\mathbf{r}) = \sqrt{(p^2/2)^2+\tilde{n}_0(\mathbf{r})\tilde{U}p^2}. \tag{5.4.9}$$

On the basis of Eq.(5.4.7) we obtain the generalized Gross-Pitaevskii equation in the form

$$\left(-\frac{\Delta}{2}+V(\mathbf{r})-\tilde{\mu}+\widetilde{U}|\Psi_0|^2-\beta\Psi_0\right)\Psi_0 = 0, \tag{5.4.10}$$

where $\tilde{\mu} = \mu - 2n'^{(0)}(T)\tilde{U}$ is coordinate independent. Compared to the ordinary Gross-Pitaevskii equation (5.2.12), Eq.(5.4.10) contains an extra term $[2n'^{(0)}\widetilde{U} - \beta\Psi_0]\Psi_0$ in the lhs. One can easily check that Eq.(5.4.10) coincides with the equation

$$\left[-\frac{\Delta}{2} + V(\mathbf{r}) - \mu + \widetilde{U}|\Psi_0|^2 + \widetilde{U}(2\langle\hat{\Psi}'^{\dagger}\hat{\Psi}'\rangle + \langle\Psi'\Psi'\rangle)\right]\Psi_0 = 0$$

obtained by averaging the non-linear Schrödinger equation for the field operator (see [113]). As mentioned above, for $T \gg n_0\widetilde{U}$ the above-condensate density $n' = \langle\Psi'^{\dagger}\Psi'\rangle$ in the condensate spatial region is mainly determined by the coordinate-independent (ideal gas) contribution $n'^{(0)}(T)$. The coordinate-dependent correction to the above-condensate density, $n'^{(1)}(\mathbf{r}) = \langle\hat{\Psi}'^{\dagger}(\mathbf{r})\hat{\Psi}'(\mathbf{r})\rangle - n'^{(0)}$, turns out to be equal to the anomalous average $\langle\Psi(\mathbf{r})\Psi(\mathbf{r})\rangle$:

$$n'^{(1)}(\mathbf{r}) = \langle\Psi(\mathbf{r})\Psi(\mathbf{r})\rangle = -\frac{\beta\sqrt{n_0(\mathbf{r})}}{3\widetilde{U}}.$$

Accordingly, the quantity $[2n'^{(0)}\widetilde{U} - \beta\Psi_0]\Psi_0 = \widetilde{U}(2\langle\hat{\Psi}'^{\dagger}\hat{\Psi}'\rangle + \langle\Psi'\Psi'\rangle)$.

Taking advantage of Eqs (5.4.1), (5.4.2) and (5.4.10), the generalized Bogolyubov-De Gennes equations (5.2.7), (5.2.8) are reduced to

$$(\varepsilon_\nu - S^-)f_\nu^-(\mathbf{r}) = \left(-\frac{\Delta}{2} + \frac{\Delta\Psi_0}{2\Psi_0} + S_-^+\right)f_\nu^+(\mathbf{r}) \tag{5.4.11}$$

$$(\varepsilon_\nu - S^-)f_\nu^+(\mathbf{r}) = \left(-\frac{\Delta}{2} + \frac{\Delta\Psi_0}{2\Psi_0} + 2|\Psi_0|^2\widetilde{U} + S_+^+\right)f_\nu^-(\mathbf{r}), \tag{5.4.12}$$

where the quantities $S_\pm^+$, S^- are given by Eqs. (5.3.11), (5.3.12), and ε_ν is the exact value of the excitation energy. Eqs. (5.4.10), (5.4.11) and (5.4.12) represent a complete set of equations for finding the energy shifts and damping rates of the elementary excitations.

A precise calculation of the self-energy functions in Eqs. (5.4.11), (5.4.12) depends on the value of ε_ν and on the trapping geometry. In this section we will make general statements on how the calculation can be performed. In most of the cases (except the case of the lowest excitations with zero orbital angular momentum in spherically symmetric traps) the characteristic time scale in the self-energy operators, $1/\varepsilon_\nu$, is much smaller than the inverse level spacing in the trap. Therefore, the summation over the discrete intermediate states can be replaced by integration. This is a direct consequence of the general statement that the time-dependent discrete Fourier sum can be replaced by its integral representation at times much smaller than the inverse frequency spacing (see e.g., [114]).

The kernels of the non-resonant parts of the self-energy operators, $S_\pm^{+n}$ and S^{-n}, vary at distances $|\mathbf{r} - \mathbf{r'}|$ which do not exceed the correlation length $l_{\rm cor} = 1/\sqrt{n_0\widetilde{U}}$. As $l_{\rm cor}$ is much smaller than the characteristic size of the condensate, the non-resonant parts of the self-energies can be calculated in the local density approximation. The same statement holds for the quantities $S_\pm^{+rn}$ and S^{-rn} originating from the resonant parts of the self-energy operators. This approach gives the energy shift $\delta\varepsilon_p^n$ (5.3.24), with n_0 replaced by by the coordinate-dependent density $n_0(\mathbf{r})$. For quasiclassical excitations we also obtain Eq.(5.3.25) for the shift $\delta\varepsilon_p^{ns}$ (for the lowest excitations the calculation of this shift, analogous to p^2/ε in the spatially homogeneous case, requires some more investigation).

The calculation of the resonant contributions $S_\pm^{+rr}$ and S^{-rr} to the self-energies is more subtle. Using Eq.(5.4.8) for the functions $u_\nu, v_\nu = f_\nu^\pm$ in Eqs. (5.4.4), (5.4.6), one can see that all resonant contributions contain the quantity

$$Q(\mathbf{r},\mathbf{r}') = \sum_{\gamma'}\frac{f_\gamma(\mathbf{r})f_\gamma(\mathbf{r}')f_{\gamma'}(\mathbf{r})f_{\gamma'}(\mathbf{r}')}{\varepsilon_\nu + \varepsilon_\gamma - \varepsilon_{\gamma'} + i0}.$$

Writing $(\varepsilon_\nu + \varepsilon_\gamma - \varepsilon_{\gamma'} + i0)^{-1}$ as the integral over time $\int_0^\infty dt \exp\{i(\varepsilon_\nu + \varepsilon_\gamma - \varepsilon_{\gamma'} + i0)t\}$, we obtain

$$Q(\mathbf{r}, \mathbf{r}') = i \int_0^\infty dt \exp(i\varepsilon_\nu t) K_\gamma(\mathbf{r}, \mathbf{r}', t), \tag{5.4.13}$$

where the quantum-mechanical correlation function

$$K_\gamma(\mathbf{r}, \mathbf{r}', t) = \sum_{\gamma'} f_\gamma(\mathbf{r}) f_\gamma(\mathbf{r}') f_{\gamma'}(\mathbf{r}) f_{\gamma'}(\mathbf{r}') \exp\{i(\varepsilon_\gamma - \varepsilon_{\gamma'} + i0)t\}. \tag{5.4.14}$$

We will turn from the integration over the quantum states γ' of the quasiclassical thermal excitations to the integration along the classical trajectories of motion of Bogolyubov-type quasiparticles in the trap. Following a general method (see [115–117]) , we obtain

$$K_\gamma(\mathbf{r}, \mathbf{r}', t) = g_\gamma^{-1} \int \delta(\mathbf{r}'' - \mathbf{r}) \delta(\mathbf{r}_p''(t) - \mathbf{r}') \delta(\varepsilon_\gamma - H(\mathbf{p}, \mathbf{r}'')) \frac{d^3 r'' d^3 p}{8\pi^3}, \tag{5.4.15}$$

where $\mathbf{r}_p(t)$ is the coordinate of the classical trajectory with initial momentum $\mathbf{p}$ and coordinate $\mathbf{r}$. Eq.(5.4.15) will be used in the next sections where we demonstrate the facilities of the theory.

Concluding this section, we emphasize the key role of harmonicity of the trapping potential for temperature-dependent energy shifts of the excitations. As mentioned in the previous section, in the spatially homogeneous case at a given temperature the non-mean-field shift is much smaller than the shift $\delta\varepsilon^{\rm mf}$ appearing in the mean field approach simply due to the temperature dependence of the condensate density in the Bogolyubov dispersion law (5.2.18). For the Thomas-Fermi condensate in a harmonic confining potential the situation is different. In this case the spectrum of low-energy ($\varepsilon_\nu \ll n_{0m}\widetilde{U}$) excitations is independent of the mean field interparticle interaction $n_{0m}\widetilde{U}$ (chemical potential) and the condensate density profile [55, 56, 111]. Hence, the temperature-dependent energy shifts can only appear due to non-Thomas-Fermi corrections. For finding these corrections one should use the mean field self-energies $\Sigma_a(\varepsilon, \mathbf{r}, \mathbf{r'}) = n_0(\mathbf{r})\widetilde{U}\delta(\mathbf{r}-\mathbf{r'})$, $\Sigma(\varepsilon, \mathbf{r}, \mathbf{r'}) = 2(n_0(\mathbf{r})+n'^{(0)})\widetilde{U}\delta(\mathbf{r}-\mathbf{r'})$, where the only difference from the $T = 0$ case is related to the presence of above-condensate particles in the condensate spatial region at finite T through the coordinate-independent term $2n'^{(0)}\widetilde{U}$ in Σ. Then Eqs. (5.4.11), (5.4.12) take the form of ordinary Bogolyubov-De Gennes equations (5.2.15),(5.2.16), and Eq.(5.4.10) becomes the ordinary Gross-Pitaevskii equation (5.2.12), with the chemical potential μ replaced by $\tilde{\mu}$. The latter circumstance changes the condensate wavefunction compared to that at $T = 0$ and ensures the temperature dependence of Ψ_0. Accordingly, the excitation energies ε_ν in Eqs. (5.2.15),(5.2.16) also become temperature dependent. This type of approach, which for a spatially homogeneous gas would immediately lead to the result of Lee and Yang [98], has been used in recent numerical calculations of the energy shifts of the lowest quadrupole excitations in spherically symmetric [118] and cylindrically symmetric [119, 120] harmonic traps. The presence of the coordinate-dependent part of the above-condensate density, $n'^{(1)}(\mathbf{r})$, in these calculations is not adequate, since the anomalous average equal to this part was omitted and equations for the excitations did not contain the corrections to the self-energies, also proportional to $(n_0 a^3)^{1/2}$. However, at $T \gg n_0\widetilde{U}$, where $n'^{(1)} \ll n'^{(0)}$, the coordinate-dependent part $n'^{(1)}(\mathbf{r})$ as itself should not significantly influence the result, and the calculations [118–120] should actually demonstrate how important are the mean field non-Thomas-Fermi effects. The results of [119, 120] show the absence of energy shifts of the excitations at temperatures $T < 0.6T_c$ in the JILA experiment [50] and in this sense agree with the experimental data, but do not describe the upward and downward shifts of the excitation energies, observed experimentally at higher temperatures (in this respect it is worth mentioning that the calculations [121] performed for the thermal cloud in the hydrodynamic regime agree surprisingly well with the experiment [50]). On the other hand, the calculation [120] shows a downward shift of the energy of the lowest quadrupole excitation with increasing temperature in the conditions of the MIT experiment [51]. This is consistent with the experimental data and indicates that for not very

small Thomas-Fermi parameter $\omega/n_{0m}\widetilde{U}$ the mean field non-Thomas-Fermi effects can be important for temperature-dependent shifts of the lowest excitations.

Below we will assume a sufficiently small Thomas-Fermi parameter $\omega/n_{0m}\widetilde{U}$ and demonstrate the use of the theory by the examples where the influence of non-Thomas-Fermi effects on the energy shifts of the excitations is not important.

5.5. Quasiclassical excitations in a trapped Bose-condensed gas

We first consider the damping and energy shifts of quasiclassical ($\varepsilon_\nu \gg \omega$) low-energy excitations of a trapped Thomas-Fermi condensate, i.e., the quasiclassical excitations with energies much smaller than the mean field interaction between particles $n_{0m}\widetilde{U}$. In this case, for the condensates in a harmonic confining potential the ground state wave function can be found on the basis of Eqs. (5.4.10), (5.4.11), (5.4.12). Neglecting the kinetic energy term in Eq.(5.4.10), we arrive at a quadratic equation for Ψ_0. Expanding the solution of this equation in powers of β and retaining only the terms independent of β and the terms linear in β, for the condensate density we obtain

$$n_0(\mathbf{r}) = \tilde{n}_0(\mathbf{r}) + \beta\sqrt{\tilde{n}_0(\mathbf{r})}/\widetilde{U}, \tag{5.5.1}$$

where $\tilde{n}_0(\mathbf{r}) = (\tilde{\mu} - V(\mathbf{r}))/\widetilde{U}$ is the density of the Thomas-Fermi condensate in the ordinary mean field approach.

For quasiclassical excitations the terms in Eqs. (5.4.11) and (5.4.12), originating from the kinetic energy of the condensate, can be omitted from the very beginning [56]. Then, using Eq.(5.5.1) and treating the terms containing S^- and $S^+_\pm$ as perturbations, we obtain $\varepsilon_\nu = \varepsilon^{(0)}_\nu + \varepsilon^{(1)}_\nu$, where $\varepsilon^{(0)}_\nu$ is the excitation energy in the mean field approach, and the correction to the excitation energy $\varepsilon^{(1)}_\nu = \delta\varepsilon_\nu - i\Gamma_\nu$ is given by the relation

$$\varepsilon^{(1)}_\nu = \langle f^-_\nu | S^- | f^+_\nu \rangle + \frac{1}{2}\left(\langle f^-_\nu | S^+_+ + 2\beta\sqrt{\tilde{n}_0} | f^-_\nu \rangle + \langle f^+_\nu | S^+_- | f^+_\nu \rangle \right). \tag{5.5.2}$$

Here $f^{\pm(0)}_\nu$ are the zero-order wavefunctions of the excitations, determined by the ordinary Bogolyubov-De Gennes equations (5.2.15), (5.2.16), with $\varepsilon_\nu = \varepsilon^{(0)}_\nu$.

In the case of quasiclassical excitations also the kernels of resonant parts of integral operators in Eq.(5.5.2) vary on a distance scale $|\mathbf{r} - \mathbf{r'}|$ which does not exceed the correlation length $l_{\rm cor}$. This can be already seen from Eqs. (5.4.13), (5.4.15): The characteristic time scale $1/\varepsilon_\nu$ in Eq.(5.4.13) is much shorter than ω^{-1} and important is only a small part of the classical trajectory, where the condensate density is practically constant and $\mathbf{r}_p(t) = \mathbf{r} + \mathbf{v}t$, with $\mathbf{v} = \partial H/\partial\mathbf{p}$. The correlation length $l_{\rm cor}$ is not only much smaller than the size of the condensate, but also smaller than the width of the boundary region of the condensate, where $n_0\widetilde{U} \sim \varepsilon_\nu$. Therefore, the action of all integral operators on the functions $f^{\pm(0)}_\nu$ in Eq.(5.5.2) can be calculated in the local density approximation. Accordingly, for each of these operators one can use the quantity following from Eqs. (5.3.3)-(5.3.6), with $n_0 = \tilde{n}_0(\mathbf{r})$ and p from the Bogolyubov dispersion law $H(\mathbf{p}, \mathbf{r}) = \varepsilon_\nu$. Then, using Eqs. (5.4.8) we can express the energy shift $\delta\varepsilon_\nu$ and the damping rate Γ_ν through the energy shift $\delta\varepsilon_{\nu h}(\mathbf{r})$ and damping rate $\Gamma_{\nu h}(\mathbf{r})$ of the excitation of energy ε_ν in a spatially homogeneous Bose-condensed gas with the condensate density equal to $\tilde{n}_0(\mathbf{r})$:

$$\delta\varepsilon_\nu = \int d^3r |f_\nu(\mathbf{r})|^2 \left\{ \delta\varepsilon_{\nu h}(\mathbf{r}) + \frac{\varepsilon_\nu \beta\sqrt{\tilde{n}_0(\mathbf{r})}}{\sqrt{\varepsilon^2_\nu + (\tilde{n}_0(\mathbf{r})\tilde{U})^2} + \tilde{n}_0(\mathbf{r})\tilde{U}} \right\}, \tag{5.5.3}$$

$$\Gamma_\nu = \int d^3r |f_\nu(\mathbf{r})|^2 \Gamma_{\nu h}(\mathbf{r}). \tag{5.5.4}$$

The second term in the integrand of Eq.(5.5.3) originates from the temperature dependence of the shape of the condensate wavefunction. For any ratio $\varepsilon_\nu/n_0(\mathbf{r})\widetilde{U}$ this positive term dominates over the negative term $\delta\varepsilon_{\nu h}(\mathbf{r})$. The latter circumstance can be easily established from the results for $\delta\varepsilon_{\nu h}$ in Fig. 5.3.1. Thus, for quasiclassical low-energy excitations the energy shift $\delta\varepsilon_\nu$ will be always positive, irrespective of the trapping geometry and the symmetry of the excitation.

We confine ourselves to the case of cylindrical symmetry, where for the states with zero angular momentum one finds

$$|f_\nu(\mathbf{r})|^2 = \frac{\tilde{\mu}}{\pi l_\rho l_z \log(2\tilde{\mu}/\varepsilon_\nu)\rho\sqrt{\varepsilon_\nu^2 + (\tilde{n}_0(\mathbf{r})\widetilde{U})^2}}, \tag{5.5.5}$$

with $l_\rho = (2\tilde{\mu}/\omega_\rho)^{1/2}$, $l_z = (2\tilde{\mu}/\omega_z)^{1/2}$ being the characteristic size of the condensate in the radial and axial direction, ω_ρ, ω_z the radial and axial frequencies, and ρ the radial coordinate. The main contribution to the integrals in Eqs.(5.5.3),(5.5.4) comes from the boundary region of the condensate, where $\tilde{n}_0(\mathbf{r}) \sim \varepsilon_\nu$. From Eqs. (5.4.11),(5.4.12) one can easily see that in this region the possibility to omit the non-Thomas-Fermi effects originating from the kinetic energy of the condensate requires the condition $\varepsilon_\nu \gg \omega^{2/3}\tilde{\mu}^{1/3}$. This condition ensures that the characteristic width of the boundary region greatly exceeds the excitation wavelength, and we arrive at the following relations for the energy shifts and damping rates of the excitations:

$$\delta\varepsilon_\nu \approx 8\sqrt{\frac{\varepsilon_\nu}{\tilde{\mu}}}\frac{T}{\log(2\tilde{\mu}/\varepsilon_\nu)}(\tilde{n}_{0m}a^3)^{1/2}, \tag{5.5.6}$$

$$\Gamma_\nu \approx 9\sqrt{\frac{\varepsilon_\nu}{\tilde{\mu}}}\frac{T}{\log(2\tilde{\mu}/\varepsilon_\nu)}(\tilde{n}_{0m}a^3)^{1/2}. \tag{5.5.7}$$

It is important to emphasize that in the boundary region of the condensate, responsible for the energy shifts and damping rates of the quasiclassical excitations, the quantities $S^{-(1)}$, $S^{+(1)}$, and $\Sigma_a^{(1)}$ are determined by the contribution of intermediate quasiparticles which have energies comparable with ε_ν. Moreover, in this spatial region the quasiparticle energies are of order the local mean field interparticle interaction. As a consequence, the energy shift $\delta\varepsilon_\nu$ (5.5.6) and the damping rate Γ_ν (5.5.7) are practically independent of the condensate density profile. For the same reason the damping rate is determined by both the Szepfalusy-Kondor and Beliaev damping processes. Therefore, similarly to the damping of excitations with energies $\varepsilon_p > n_0\widetilde{U}$ in a spatially homogeneous gas, the damping of quasiclassical low-energy excitations of a trapped Bose-condensed gas can no longer be treated as Landau damping.

5.6. Sound waves in cylindrical Bose condensates

The derivation of Eqs. (5.5.6), (5.5.7) assumes that the motion of the excitation ν is quasiclassical for all degrees of freedom. We now turn to the condensate excitations in cigar-shaped cylindrical traps, which are quasiclassical only in the axial direction and correspond to the lowest modes of the radial motion. We will consider low-energy excitations ($\varepsilon_\nu \ll n_{0m}\widetilde{U}$), i.e., the excitations with the axial wavelength much larger than the correlation length $l_{\rm cor}$. In the recent MIT experiment [109] localized excitations of this type were created in the center of the trap by modifying the trapping potential using the dipole force of a focused off-resonant laser beam. Then, a wave packet traveling along the axis of the cylindrical trap (axially propagating sound wave) was observed. In the mean field approach the sound waves propagating in an infinitely long (axially homogeneous) cylindrical Bose condensate have been discussed in [122–124].

For revealing the key features of the non-mean-field effects (damping and the change of the sound velocity) we confine ourselves to the same trapping geometry. With regard to realistic cylindrical traps this will be a good approach if the mean free path of sound waves is smaller than the characteristic

axial size of the sample. As found in [122], for axially propagating sound waves radial oscillations of the condensate are absent, and the wavefunctions $f_k^{\pm} = (2\tilde{n}_0(\rho)\widetilde{U}/\varepsilon_k)^{\pm 1/2} f_k$, with

$$f_k = \frac{1}{\sqrt{\pi l_\rho^2}} \exp(ikz) \tag{5.6.1}$$

and k being the axial momentum. The dispersion law

$$\varepsilon_k = ck \tag{5.6.2}$$

is characterized by the sound velocity equal to $(\tilde{n}_{0m}\widetilde{U}/2)^{1/2}$, where $\tilde{n}_{0m} = \tilde{\mu}/\widetilde{U}$ is the maximum density of the Thomas-Fermi condensate in the ordinary mean field approach.

It should be noted from the very beginning that, according to Eq.(5.5.1), $\tilde{n}_{0m}$ is related to the corrected value of the maximum condensate density n_{0m} as $\tilde{n}_{0m} = n_{0m} - (\beta/\widetilde{U})\sqrt{n_{0m}}$. Therefore, being interested in the sound velocity at a given value of the maximum condensate density, one should substitute this expression to Eq.(5.6.2). This immediately changes the sound velocity to

$$c = (n_{0m}\widetilde{U}/2)^{1/2} \tag{5.6.3}$$

in the leading term (5.6.2) of the dispersion law and provides a contribution to the frequency shift of the sound wave

$$\delta\overline{\varepsilon}_k = -\varepsilon_k \frac{6T}{n_{0m}\widetilde{U}} (\pi n_{0m} a^3)^{1/2}. \tag{5.6.4}$$

The damping rate and other contributions to the frequency shift can be found directly from Eq.(5.5.2) by using the wavefunctions f_k (5.6.1). The intermediate quasiparticles giving the main contribution to the damping rate and frequency shift have energies $\varepsilon \sim n_{0m}\widetilde{U}$, i.e. much larger than the frequency of the considered sound wave, ε_k (see below). Therefore, similarly to the case of phonons in a spatially homogeneous condensate, the non-resonant terms analogous to $S_{\pm}^{+n}$, S^{-n}, $S_{\pm}^{+rn}$ and S^{-rn} contribute only to the frequency shift. As already mentioned above, the characteristic distance scale $|\boldsymbol{\rho} - \boldsymbol{\rho}\prime|$ in the kernels of the corresponding self-energies is of order the correlation length l_{cor}, and the sum of their contributions to the frequency shift can be calculated by using the local density approximation for the action of the self-energy operators on the functions $f_k^{\pm}$. This gives the non-resonant contribution to the frequency shift, $\delta\varepsilon_k^n(\rho) = (-8.4 - \sqrt{\pi})(n_0 a^3)^{1/2} T/(n_0\tilde{U})$ and the non-resonant contribution $\delta\varepsilon_k^{ns}(\rho) = 2\sqrt{\pi} \times (n_0 a^3)^{1/2} T/(n_0\tilde{U})$, with $n_0 = \tilde{n}_0(\rho)$. Then, we can express the total non-resonant part $\delta\varepsilon_k^{nt}$ of the frequency shift of the sound wave through the quantity $\delta_{kh}^n(\rho) = \delta\varepsilon_k^n(\rho) + \delta\varepsilon_k^{ns}(\rho)$:

$$\delta\varepsilon_k^{nt} = \int d^2\rho |f_k|^2 \left\{ \delta_{kh}^n(\rho) + \frac{\beta\sqrt{\tilde{n}_0(\rho)}}{2\tilde{n}_0(\rho)\widetilde{U}} \varepsilon_k \right\} \approx \varepsilon_k \frac{4.5T}{n_{0m}\widetilde{U}} (\pi n_{0m} a^3)^{1/2}. \tag{5.6.5}$$

The resonant terms analogous to $S_{\pm}^{+rr}$ and S^{-rr} in Eqs.(5.3.19)-(5.3.21) contribute to both the frequency shift and damping rate. This means that the latter is determined by the Szepfalusy-Kondor scattering processes and, since the characteristic energies of intermediate quasiparticles are much larger than ε_k, can be treated as Landau damping. The resonant contributions to the frequency shift and damping rate can not be found in the local density approximation, as the characteristic distance scale $|\boldsymbol{\rho} - \boldsymbol{\rho}'|$ in the kernels of the self-energy operators in Eq.(5.5.2) is of order the radial size of the condensate. For finding these contributions one has to substitute the resonant parts of the self-energies, (5.4.3)-(5.4.6), to Eq.(5.5.2) and, by using Eqs.(5.4.13)-(5.4.15), turn from summation over quasiclassical states γ, γ' of intermediate quasiparticles to the integration along classical trajectories

of their motion. Then, a direct calculation of the quantity $\delta_k^r = \delta\varepsilon_k^{rr} - i\Gamma_k$ yields

$$\delta_k^r = i\frac{\varepsilon_k^2\tilde{U}}{2}\int d\varepsilon_\gamma \frac{dn_\gamma}{d\varepsilon_\gamma}\int_0^\infty dt\exp(i\varepsilon_k t)\int \Phi_{k\gamma}(\mathbf{r})\Phi^*_{k\gamma}(\mathbf{r}(\mathbf{p},t))\delta(\varepsilon_\gamma - H(\mathbf{p},\mathbf{r}))\frac{d^3rd^3p}{(2\pi)^3}, \tag{5.6.6}$$

where $\mathbf{r}(\mathbf{p},t)$ is the classical trajectory starting at the phase space points $(\mathbf{r},\mathbf{p})$ on the (hyper)surface of constant energy ε_γ, $\Phi_{k\gamma}(\mathbf{r}) = f_k(z)F_\gamma(\rho)$, and

$$F_\gamma(\rho) = \frac{2\varepsilon_\gamma^2 + (\tilde{n}_0(\rho)\tilde{U})^2 - \tilde{n}_0(\rho)\tilde{U}\sqrt{\varepsilon_\gamma^2 + (\tilde{n}_0(\rho)\tilde{U})^2}}{\varepsilon_\gamma\sqrt{\varepsilon_\gamma^2 + (\tilde{n}_0(\rho)\tilde{U})^2}}.$$

Generally speaking, the integration in Eq.(5.6.6) is a tedious task as it requires a full knowledge of the classical trajectories on a time scale $\sim 1/\varepsilon_k$. This is also the case in the idealized cylindrical trap, because of coupling between the radial and axial degrees of freedom. We will rely on the approach which assumes a fast radial motion of quasiparticles compared to their motion in the axial direction and, hence, requires the frequency of the sound wave, ε_k, significantly smaller than the radial frequency ω_ρ. Then on a time scale $\sim 1/\varepsilon_k$ the quasiparticles with energies $\sim \tilde{n}_0\tilde{U}$ (which are the most important for the energy shifts and damping of the sound wave) oscillate many times in the radial direction, whereas their axial variables $z(\mathbf{p},t)$, $p_z(\mathbf{p},t)$ only slightly change and, hence, can be adiabatically separated from the fast radial variables $\rho(\mathbf{p},t)$, $\mathbf{p}_\rho(\mathbf{p},t)$. In this case it is convenient to integrate Eq,(5.6.6) over $d\mathbf{p}_\rho$ and, using Eq.(5.6.1), represent it in the form

$$\delta_k^r = i\frac{\varepsilon_k^2\widetilde{U}}{4\pi^2 l_\rho^2}\int \varepsilon_k d\varepsilon_\gamma \frac{dn_\gamma}{d\varepsilon_\gamma}\int dt\exp(i\varepsilon_k t)\int \rho d\rho dp_z dz \frac{F_\gamma(\rho)F_\gamma(\rho(\mathbf{p},t))}{\sqrt{\varepsilon_\gamma^2 + (\tilde{n}_0(\rho)\widetilde{U})^2}}\exp\{i(z - z(\mathbf{p},t))\}, \tag{5.6.7}$$

where the integration is performed over the entire classically accessible region of the phase space.

Since $z(\mathbf{p},t)$ is close to z, in the exponent of the integrand we can write $z(\mathbf{p},t) - z = v_z$, where the axial velocity v_z is obtained from the exact Hamiltonian equations of motion by averaging over the fast radial variables: $v_z = \langle \partial H(\mathbf{p},\mathbf{r})/\partial p_z\rangle_\rho$. For the classical radial motion ($\varepsilon_\gamma \gg \omega_\rho$) the averaging procedure simply reduces to integration over $d\rho$ under the condition $H(\mathbf{p},\mathbf{r}) = \varepsilon_\gamma$ at fixed values of ε_γ, p_z and z, with the weight proportional to the local density of states for the radial motion:

$$\langle(...)\rangle_\rho = g^{-1}\int (...)(\varepsilon_\gamma^2 + (\tilde{n}_0(\rho)\widetilde{U})^2)^{-1/2}2\pi\rho d\rho,$$

where $g = \int(\varepsilon_\gamma^2 + (\tilde{n}_0(\rho)\widetilde{U})^2)^{-1/2}2\pi\rho d\rho$. Finally, averaging the function $F_\gamma(\rho(t))$ over the fast radial variables and integrating over dt in Eq.(5.6.7), we obtain

$$\delta_k^r = \frac{\varepsilon_k^2\widetilde{U}}{8\pi^3 l_\rho^2}\int d\varepsilon_\gamma \frac{\varepsilon_\gamma dn_\gamma}{d\varepsilon_\gamma}\int dz dp_z g\frac{\langle F(\rho)\rangle_\rho^2}{\varepsilon_k - p_z v_z + i0}. \tag{5.6.8}$$

The resonant contribution to the frequency shift, given by the real part of Eq.(5.6.8), after the integration proves to be $\delta\varepsilon_k^r \approx -2.3\varepsilon_k(T/n_{0m}\widetilde{U})(n_{0m}a^3)^{1/2}$. The sum of this quantity with the non-resonant term (5.6.5) and $\delta\overline{\varepsilon}_k$ (5.6.4) leads to the frequency shift of the sound wave

$$\delta\varepsilon_k \approx -5\varepsilon_k(n_{0m}a^3)^{1/2}\frac{T}{n_{0m}\widetilde{U}}. \tag{5.6.9}$$

The imaginary part of Eq.(5.6.8) gives the damping rate

$$\Gamma_k = 8.6\varepsilon_k(n_{0m}a^3)^{1/2}\frac{T}{n_{0m}\widetilde{U}}. \tag{5.6.10}$$

Except for the numerical coefficients, Eqs,(5.6.9), (5.6.10) are similar to Eq.(5.3.26), (5.3.27) for the damping rate and energy shift of phonons in a spatially homogeneous Bose condensate. This a consequence of the fact that the condensate boundary region practically does not contribute to the damping rate and frequency shift of axially propagating sound waves, in contrast to the case of excitations quasiclassical for both axial and radial degrees of freedom.

In the MIT experiment [109] the characteristic spatial size of created localized excitations was $\lambda \approx 20$ μm and, accordingly, so was the initial wavelength of propagating sound. According to the experimental data, the propagating pulse died out during 25 ms, and after that only the lowest quadrupole excitation characterized by a much loner damping time (~ 300 ms) was observed. We believe that the attenuation of axially propagating sound in the MIT experiment [109] on the time scale of 25 ms can be well explained as a consequence of damping. The characteristic frequency of the waves in the packet can be estimated as $\varepsilon_\nu \approx 2\pi\sqrt{n_{0m}\tilde{U}/2}/\lambda$. Then Eq.(5.6.10) gives the damping rate independent of the condensate density $\tilde{n}_{0m}$. In the MIT experiment the temperature $T \approx$0.5 μK was roughly only twice as large as $n_{0m}\widetilde{U}$, which decreases the damping rate by approximately 20% compared to that given by Eq.(5.6.10). In these conditions we obtain a characteristic damping time of 15 ms, relatively close to the measured value.

The relative change of the sound velocity, $\delta c/c = \delta\varepsilon_k/\varepsilon_k$, increases with decreasing condensate density n_{0m}. However, even at the lowest densities of the MIT experiment [109] ($n_{0m} \approx 10^{14}$ cm^{-3}) the quantity $\delta c/c$ does not exceed $\sim 5\%$ and is practically invisible.

5.7. Damping of low-energy excitations in a trapped Bose-condensed gas

In this section we use our theory for the calculation of damping of the lowest excitations (i.e. the excitations with energies $\hbar\omega \sim \varepsilon \ll \mu$) of a trapped condensate in the Thomas-Fermi regime at finite temperatures $T \gg \hbar\omega$ ranging almost up to the BEC phase transition temperature. We will again assume the inequality (5.1.3) (with $n_0 = n_{0m}$) which ensures that the main contribution to the damping rate comes from the first term in H_{int} (5.3.2), proportional to $\hat{\Psi}'^3$, and the damping is actually caused by the interaction of the lowest excitations with the thermal excitations through the condensate and is governed by the SK process (5.1.2). The damping rate is given by the part of Eq.(5.6.6) in which the functions $\Phi_{\nu\gamma}(\mathbf{r}) = f_\nu(\mathbf{r})F_\gamma(\mathbf{r})$, and the wavefunctions of the lowest excitations:

$$f_\nu = \left(\prod_i l_i\right)^{-1/2} W_\nu(r_i/l_i), \tag{5.7.1}$$

with polynomials W_ν introduced in Chapter 2.

Eq.(5.6.6) can also be found within the first order perturbation theory in H_{int}:

$$\Gamma_\nu = \mathrm{Im}\sum_{\gamma\gamma'} \frac{1}{\hbar}\frac{|<\gamma'|\hat{H}_{\mathrm{int}}|\nu\gamma>|^2}{E_\gamma - E_{\gamma'} + E_\nu + i0}(N_\gamma - N_{\gamma'}), \tag{5.7.2}$$

where $N_\gamma = [\exp(E_\gamma/T) - 1]^{-1}$ are equilibrium occupation numbers for the thermal excitations. The transition matrix element can be represented in the form

$$<\gamma'|\hat{H}_{\mathrm{int}}|\nu\gamma> = \frac{\tilde{U}}{2}\left[3H_{\nu\gamma\gamma'} - (H^{\nu\gamma}_{\gamma'} - H^{\nu\gamma'}_{\gamma} - H^{\gamma\gamma'}_{\nu})\right], \tag{5.7.3}$$

where $H_{\nu\gamma\gamma'} = \int d^3r\Psi_0(\mathbf{r})f^-_\nu(\mathbf{r})f^-_\gamma(\mathbf{r})f^{-*}_{\gamma'}(\mathbf{r})$ and $H^{\gamma\gamma'}_\nu = \int d^3r\Psi_0(\mathbf{r})f^-_\nu(\mathbf{r})f^+_\gamma(\mathbf{r})f^{+*}_{\gamma'}(\mathbf{r})$.

Since energies of the thermal excitations $E_\gamma \gg \hbar\omega$, these excitations are quasiclassical and, similarly to the spatially homogeneous case, one can write

$$f^\pm_\gamma(\mathbf{r}) = \left[E_\gamma/(\sqrt{E^2_\gamma + (n_0(\mathbf{r})\tilde{U})^2} - n_0(\mathbf{r})\tilde{U})\right]^{\pm 1/2} f_\gamma(\mathbf{r}).$$

Then, using Eq(5.7.1), from Eq.(5.7.3) we obtain

$$< \gamma' | \hat{H}_{\rm int} | \nu\gamma >= \left(\frac{E_\nu \tilde{U}}{2 \prod_i l_i} \right)^{1/2} \int d^3 r \Phi_{\nu\gamma}(\mathbf{r}) f_\gamma(\mathbf{r}) f^*_{\gamma'}(\mathbf{r}), \tag{5.7.4}$$

where $\Phi_{\nu\gamma}(\mathbf{r}) = W_\nu(r_i/l_i) F_\gamma(\mathbf{r})$, and

$$F_\gamma(\mathbf{r}) = \frac{2E^2_\gamma + (n_0(\mathbf{r})\tilde{U})^2 - n_0(\mathbf{r})\tilde{U}\sqrt{E^2_\gamma + (n_0(\mathbf{r})\tilde{U})^2}}{E_\gamma \sqrt{E^2_\gamma + (n_0(\mathbf{r})\tilde{U})^2}}. \tag{5.7.5}$$

For the distribution of energy levels of the thermal excitations with a given set of quantum numbers $\tilde{\gamma}$ determined by the trap symmetry (in cylindrically symmetric traps $\tilde{\gamma}$ is the projection M of the orbital angular momentum on the symmetry axis) we will use the statistical Wigner-Dyson [125–127] approach which assumes ergodic behavior of the excitations. Then, the quantum spectrum of the thermal excitations is random and the sum in Eq.(5.7.2) can be replaced by the integral $\int dE_\gamma dE_{\gamma'} \sum_{\tilde{\gamma}\tilde{\gamma}'} g_\gamma g_{\gamma'} R_{\gamma\gamma'}$ in which $g_\gamma(E_\gamma)$ is the density of states for the excitations with a given set $\tilde{\gamma}$, and $R_{\gamma\gamma'}$ the level correlation function. In non-spherical harmonic traps $g_\gamma E_\nu \gg 1$ and, hence, $R_{\gamma\gamma'} \approx 1$. Then, putting $N_\gamma - N_{\gamma'} = E_\nu (dN_\gamma/dE_\gamma)$ and writing $(E_\gamma - E_{\gamma'} + E_\nu + i0)^{-1}$ as the integral over time $i\int_0^\infty dt \exp\{i(E_\gamma - E_{\gamma'} + E_\nu + i0)t/\hbar\}$, from Eqs. (5.7.2), (5.7.4) we obtain:

$$\Gamma_\nu = \frac{E^2_\nu \tilde{U}}{2\hbar^2 \prod_i l_i} \mathrm{Re} \sum_{\tilde{\gamma}} \int g_\gamma dE_\gamma \int_0^\infty dt \exp i\frac{(E_\nu + i0)t}{\hbar} \int d^3 r d^3 r' \Phi_{\nu\gamma}(\mathbf{r}) \Phi^*_{\nu\gamma}(\mathbf{r}') K_\gamma(\mathbf{r}, \mathbf{r}', t) \tag{5.7.6}$$

The quantummechanical correlation function

$$K_\gamma(\mathbf{r}, \mathbf{r}', t) = \sum_{\tilde{\gamma}'} \int g_{\gamma'} dE_{\gamma'} \exp\left\{ i\frac{(E_\gamma - E_{\gamma'})t}{\hbar} \right\} f_\gamma(\mathbf{r}) f^*_\gamma(\mathbf{r}') f^*_{\gamma'}(\mathbf{r}) f_{\gamma'}(\mathbf{r}'). \tag{5.7.7}$$

and, similarly to the transformation of Eq.(5.4.14) to (5.4.15), can be written as

$$\sum_{\tilde{\gamma}} g_\gamma K_\gamma(\mathbf{r}, \mathbf{r}', t) = \int \delta(\mathbf{r}'' - \mathbf{r}) \delta(\mathbf{r}_p(t|\mathbf{r}'', \mathbf{p}) - \mathbf{r}\prime) \delta(E_\gamma - H(\mathbf{p}, \mathbf{r}'')) \frac{d^3 p d^3 r''}{(2\pi\hbar)^3}, \tag{5.7.8}$$

where again the classical Bogolyubov Hamiltonian $H(\mathbf{p}, \mathbf{r})$ is given by Eq.(5.4.9), and $\mathbf{r}_p(t|\mathbf{r},\mathbf{p})$ is the coordinate of the classical trajectory with initial momentum $\mathbf{p}$ and coordinate $\mathbf{r}$. Then, Eq.(5.7.6) is reduced to the form

$$\Gamma_\nu = \frac{E^2_\nu \tilde{U}}{2\hbar^2 \prod_i l_i} \mathrm{Re} \int dE_\gamma \frac{dN_\gamma}{dE_\gamma} \int_0^\infty dt \exp\left(i\frac{E_\nu t}{\hbar} \right) \int \Phi_{\nu\gamma}(\mathbf{r}) \Phi^*_{\nu\gamma}(\mathbf{r}_{\rm cl}(t|\mathbf{r},\mathbf{p})) \delta(E_\gamma - H(p, \mathbf{r})) \frac{d^3 r d^3 p}{(2\pi\hbar)^3}. \tag{5.7.9}$$

We first consider temperatures $T \gg \mu$, where the main contribution to the integral in Eq.(5.7.9) is provided by the thermal excitations with energies $E_\gamma < \mu$. In this case the use of the statistical approach in non-spherical traps is justified by the fact that, as shown in [57, 111], the motion of corresponding classical Bogolyubov-type quasiparticles is strongly chaotic at energies of order μ. The characteristic values of p and t in Eq.(5.7.9) are of order $(m n_0(\mathbf{r})\tilde{U})^{1/2}$ and $\hbar/E_\nu$, respectively. For the lowest excitations ($E_\nu \sim \hbar\omega$) the characteristic values of p in Eq.(5.7.9) are of order $(m\mu)^{1/2}$, and the result of integration can be represented in the form

$$\Gamma_\nu = A_\nu \frac{E_\nu}{\hbar} \frac{T}{\mu} (n_{0m} a^3)^{1/2}, \tag{5.7.10}$$

where A_ν is a numerical coefficient which depends on the form of the wavefunction of the low-energy excitation ν. In contrast to the case of $E_\nu \gg \hbar\omega$, the calculation of A_ν requires a full knowledge of

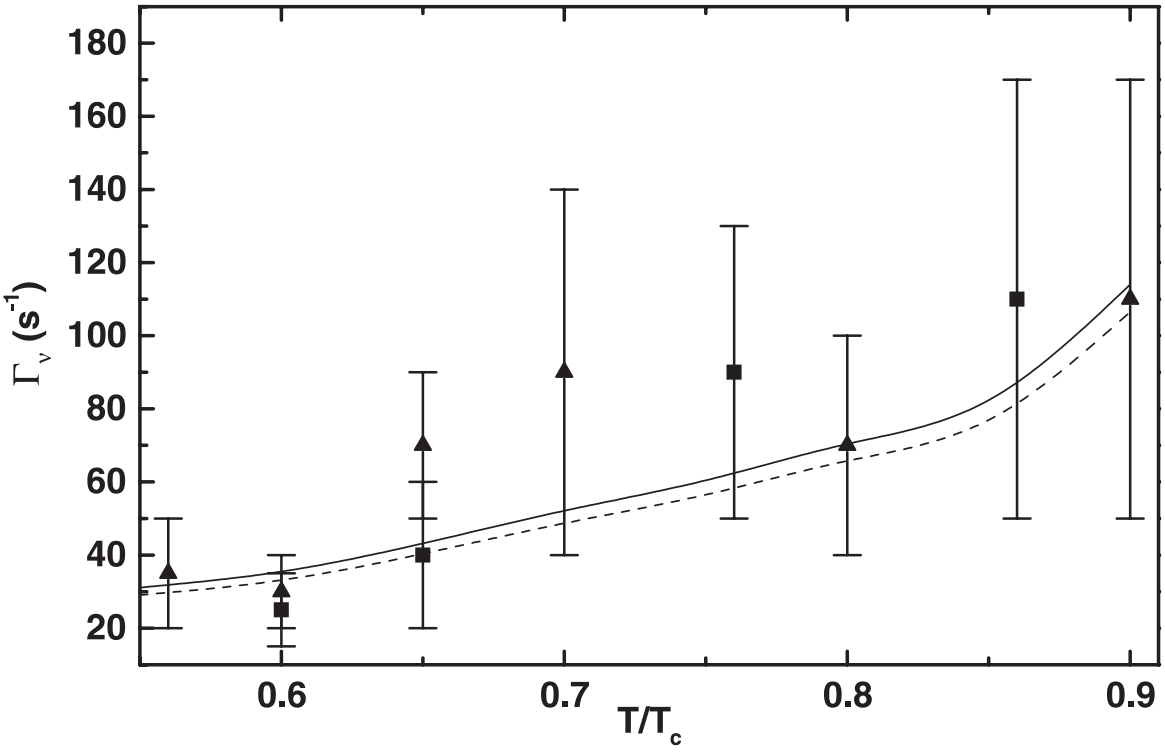

FIGURE 5.7.1. The damping rate Γ_ν versus T for the JILA trapping geometry. The solid (dashed) curve and boxes (triangles) correspond to our calculation and the experimental data [50] for the excitations with $M = 2$ ($M = 0$), respectively.

classical trajectories of (stochastic) motion of Bogolyubov-type quasiparticles in the spatially inhomogeneous Bose-condensed gas. In this respect the damping of the lowest excitations has a strongly non-local character and, hence, can not be found in any type of a local density approximation. The same statement holds for the resonant part of the shifts of the lowest excitations.

The criterion of the collisionless regime for the excitations with energies $E_\gamma \sim \mu$ assumes that their damping time Γ_μ^{-1} is much larger than the oscillation period in the trap ω^{-1} and, hence, the mean free path greatly exceeds the size of the condensate. From Eq.(5.7.10) we find $\Gamma_\mu \sim (T/\hbar)(n_{0m}a^3)^{1/2}$ and obtain the collisionless criterion

$$(T/\hbar\omega)(n_{0m}a^3)^{1/2} \ll 1. \tag{5.7.11}$$

Due to collective character of the excitations the criterion (5.7.11) is quite different from the Knudsen criterion in ordinary thermal samples.

Remarkably, both Eq.(5.7.11) and the assumption of stochastic behavior of thermal excitations with energies of order μ are well satisfied in the conditions of the JILA [50] and MIT [51] experiments, where the temperature dependent damping of the lowest quadrupole excitations in cylindrically symmetric traps has been measured at temperatures significantly larger than μ. The JILA experiment [50], where the ratio of the axial to radial frequency $\beta = \omega_z/\omega_\rho = \sqrt{8}$, concerns the damping of two quadrupole excitations: $M = 2$, $E_\nu = \sqrt{2}\omega_\rho$, and $M = 0$, $E_\nu = 1.8\omega_\rho$. Our numerical calculation of Eq.(5.7.9), with W_ν from [56], gives $A_\nu \approx 7$ for $M = 2$ and $A_\nu \approx 5$ for $M = 0$. This leads to the damping rate $\Gamma_\nu(T)$ which is in agreement with the experimental data [50] (see Fig. 5.7.1).

In the MIT experiment [51], where $\beta = 0.08$, the damping rate has been measured for the quadrupole excitation with $M = 0$, $E_\nu = 1.58\omega_z$. In this case we obtain $A_\nu \approx 10$. The corresponding damping rate $\Gamma_\nu(T)$ (5.7.10) monotonously increases with T and for the conditions of the MIT experiment [51] ranges from 4 s^{-1} at $T \approx 200$ nK to 18 s^{-1} at $T \approx 800$ nK. These results

somewhat overestimate the damping rate compared to the experimental data. In fact, the exact match between the presented theory and the measured values for the damping rates can not be expected. The reason is that the in the high temperature part of experiment ($T \gg \mu$), which can be compared with our calculations, the lhs of Eq.(5.7.11) is of order one. This means that the measurements were performed for the intermediate range of densities and temperatures, which corresponds to a crossover between the collisionless and hydrodynamic regimes. In the latter case the inequality opposite to (5.7.11) is satisfied, and the damping rates are expected to be smaller (see, e.g. [102]).

Importantly, under the condition (5.7.11) the damping rate Γ_ν of the low-energy excitations is much larger than the damping rate Γ_T of the oscillations of the thermal cloud. This phenomenon was observed at JILA [50]. One can easily find that for $T \gg \mu$ the damping rate $\Gamma_T \sim n\sigma v_T$, where $n \sim (mT/2\pi\hbar^2)^{3/2}$ is the characteristic density of the thermal cloud, $\sigma = 8\pi a^2$ the elastic cross section, and $v_T \sim \sqrt{T/m}$ the thermal velocity. Accordingly, the ratio Γ_T/Γ_ν is just of order the lhs of Eq.(5.7.11).

In spherically symmetric traps at any excitation energies one has a complete separation of variables, which means that the classical motion of Bogolyubov-type quasiparticles is regular. The excitations are characterized by the orbital angular momentum l and its projection M, and for given l, M the level spacing $g_\gamma^{-1} \sim \hbar\omega$ can greatly exceed the interactions provided by the non-Bogolyubov Hamiltonian terms proportional to Ψ'^3 and Ψ'^4. In such a situation the discrete structure of the energy spectrum of thermal excitations becomes important, and one can get nonlinear resonances instead of damping. On the other hand, stochastization of motion of thermal excitations can be provided by their interaction with each other or with the heat bath. In this case the damping rate Γ_ν(5.7.10) follows directly from Eq.(5.7.6) by using the Dyson relation for the level correlation function [127] ($g_\gamma E_\nu \sim 1$) and f_γ from the WKB analysis of Eq.(2.3.5).

For $T < \mu$ the picture of damping of low-energy excitations changes, since Γ_ν will be determined by the contribution of thermal excitations with energies $E_\gamma \sim T$. In this case, the lower is the ratio T/μ the more questionable is the assumption of ergodic behavior of the thermal excitations. But, even if the stochastization is present, at T significantly lower than μ the temperature dependent damping of the lowest excitations will be rather small. For cylindrically symmetric traps from Eqs. (5.7.6), (5.7.9) one can find $\Gamma_\nu \sim (E_\nu/\hbar)(T/\mu)^{3/2}(n_{0m}a^3)^{1/2}$.

5.8. Concluding remarks

In conclusion we have developed a finite-temperature perturbation theory (beyond the mean field) for a spatially homogeneous Bose-condensed gas and calculated temperature-dependent energy shifts and damping rates for Bogolyubov excitations of any energy. The theory is generalized for the case of excitations in a spatially inhomogeneous (trapped) Bose-condensed gas and used for calculating the energy shifts and damping rates of low-energy quasiclassical excitations. We also analyzed the frequency shifts and damping of axially propagating sound waves in cylindrical Bose condensates. For the lowest elementary excitations we used our theory to calculate the damping rates. Our results are in excellent agreement with the data of the JILA experiment [50] for the lowest quadrupole excitations in a cylindrical trap and reasonably well explain the MIT experiment [51]. In the latter case the generalization of the presented theory in the hydrodynamics domain remains to be developed (see e.g. [102] and [128, 129] for the latest developments).

There is still a question of what is the nature of temperature-dependent energy shifts on approaching T_c and how to explain the JILA [50] and MIT [51] experiments where these shifts have been measured for the lowest quadrupole excitations. Among other approaches [130, 131] we would especially mention the recent contribution [132], where the shifts where studied in an effectively local approximation. Although the results of the calculation seem to fit the experiment, we would like to emphasize that for the lowest excitations the nonlocal character of related energy shifts and damping

rates should manifest itself in any scheme of calculations and purely local calculations can not give a full account for the experimental results.

CHAPTER 6

Dissipative dynamics of a vortex state in a trapped Bose-condensed gas.

We discuss dissipative dynamics of a vortex state in a trapped Bose-condensed gas at finite temperature and draw a scenario of decay of this state in a static trap. The interaction of the vortex with the thermal cloud transfers energy from the vortex to the cloud and induces the motion of the vortex core to the border of the condensate. Once the vortex reaches the border, it immediately decays through the creation of excitations. We calculate the characteristic life-time of a vortex state and address the question of how the dissipative dynamics of vortices can be studied experimentally.

The recent successful experiments on Bose-Einstein condensation (BEC) in trapped clouds of alkali atoms [3–5] have stimulated a great interest in the field of ultra-cold gases [96]. One of the goals of ongoing studies is to investigate the nature of a superfluid phase transition in ultra-cold gases and to make a link to more complicated quantum systems, such as superfluid helium. Of particular interest is the relation between Bose-Einstein condensation and superfluidity. However, being the most spectacular manifestation of the phase transition in ^{4}He, superfluidity has not yet been observed in trapped gases. A promising way of studying superfluidity in trapped gases is the creation of quantum vortices, as quantization of circulation and the related phenomenon of persistent currents are the most striking properties of superfluids.

A widely discussed option of creating vortices in trapped gases assumes the rotation of a slight asymmetry of a cylindrical trap after achieving BEC, or cooling down the gas sample below the Bose-condensation temperature in an already rotating trap [133, 134]. Another possibility is a rapid quench of a gas sample near the critical temperature, which should lead to creation of vortices even in a non-rotating trap [135]. It is worth mentioning the ideas to create the vortex state in a Bose-condensed gas by optical means [136, 137], and the idea to form vortex rings in the regime of developed turbulence [138]. The spatial size of the vortex core in the Thomas-Fermi regime is too small to be observed, and for visualizing the vortex state it is suggested to switch off the trap and let the cloud ballistically expand. Then the size of the vortex core will be magnified approximately by the same factor as the size of the expanding condensate [139].

Similarly to the recently studied kink-wise condensates [136, 140, 141], vortices are the examples of macroscopically excited Bose-condensed states. In a non-rotating trap the vortex state has a higher energy than the ground-state Bose condensate, i.e. the vortex is thermodynamically unstable [142–144]. On the other hand, a quantum vortex with the lowest possible circulation (the vortex "charge" equal to 1), is dynamically stable (small perturbations do not develop exponentially with time; see [139, 145] and refs. therein). Therefore, the vortex state can only decay in the presence of dissipative processes.

In this Letter we discuss dissipative dynamics of a vortex state in a trapped Bose-condensed gas at finite temperatures and show how the interaction of the vortex with the thermal cloud leads to decay of the vortex state in a static trap. According to our scenario, the scattering of thermal excitations by a vortex provides the energy transfer from the vortex to the thermal cloud and induces motion of the vortex core to the border of the condensate, where the vortex decays by creating elementary excitations. We calculate the characteristic life-time of the vortex state and discuss how the dissipative dynamics of vortices can be studied experimentally.

We first briefly outline the main features of vortex behavior in a superfluid, known from studies of liquid helium. The motion of a vortex in a superfluid of density ρ_s satisfies the Magnus law (see [146–148] and refs therein):

$$\rho_s(\mathbf{v}_L - \mathbf{v}_S) \times \boldsymbol{\kappa} = \mathbf{F}. \tag{6.0.1}$$

Here $\mathbf{v}_L$ is the velocity of the vortex line, and $\mathbf{v}_S$ the velocity of superfluid at the vortex line. The vector $\boldsymbol{\kappa}$ is parallel to the vortex line and is equal to the circulation carried by the vortex. The force $\mathbf{F}$ acting on the vortex originates from the mutual friction between the normal component and the moving vortex line, and is usually small. Assuming the absence of friction ($\mathbf{F} = 0$), the vortex moves together with the superfluid component ($\mathbf{v}_L = \mathbf{v}_S$). In the presence of a vortex at the point $\mathbf{r}_0$ the superfluid velocity $\mathbf{v}_S(\mathbf{r})$ satisfies the equations

$$\mathrm{rot}\mathbf{v}_S = 2\pi\boldsymbol{\kappa}\delta(\mathbf{r} - \mathbf{r}_0);\ \mathrm{div}\mathbf{v}_S = 0 \tag{6.0.2}$$

and is related to the phase ϕ of the condensate wave-function as $\mathbf{v}_S = \boldsymbol{\nabla}\phi$. This leads to quantization of the circulation: $\kappa = Z\hbar/m$ [59], where Z is an integer (the charge of the vortex) and m is the mass of the condensate particle. Below we will consider vortex states with $Z = 1$, which are dynamically stable ([139, 145] and refs. therein).

Eqs.(6.0.2) are similar to the equations of the magnetostatic problem, with the magnetic field replaced by the velocity $\mathbf{v}_S$ and the electric current replaced by $\boldsymbol{\kappa}$. The velocity field around an infinitely long straight vortex line is analogous to the magnetic field of a straight current:

$$\mathbf{v}_S(\mathbf{r}) = [\boldsymbol{\kappa} \times \mathbf{r}]/r^2. \tag{6.0.3}$$

The vortex itself can experience small oscillations of its filament, characterized by the dispersion law $|\omega(k)| = \kappa k^2 \ln(1/ak)/2$ [31], where k is the wave vector of the oscillations, and a the radius of the vortex core. In a weakly interacting Bose-condensed gas the core radius is of order the healing length $a = (\hbar^2/m\mu)^{1/2}$, where μ is the chemical potential.

We will see that the dissipative dynamics of a vortex state is insensitive to the details of the density distribution in a gas. The spatial size of the Thomas-Fermi condensate trapped in a harmonic potential of frequency ω is $R = (2\mu/m\omega^2)^{1/2}$. Therefore, for finding the superfluid velocity $\mathbf{v}_S$ in this case, we may consider a vortex in a spatially homogeneous condensate in a cylindrical vessel of radius R, with the vortex line parallel to the axis of the cylinder. For the vortex line at distance x_0 from the axis, the velocity field can be found by using the "reflection" method [146]. In a non-rotating trap, in order to compensate the normal component of the velocity field (6.0.3) everywhere on the surface of the cylinder, we introduce a fictious vortex with opposite circulation on the other side of the vessel wall, i.e. at distance R^2/x_0 from the cylinder axis. At the position of the vortex the "reflection" induces the velocity

$$\mathbf{v}_S = \frac{[\boldsymbol{\kappa} \times \mathbf{x}_0]}{R^2 - x_0^2}. \tag{6.0.4}$$

As $v_S \approx v_L$, the vortex line will slowly drift around the axis of the trap.The characteristic time for the formation of the velocity field (6.0.4) is $\tau_R \sim R/c_s$, where $c_s = \sqrt{\mu/m}$ is the velocity of sound. Sufficiently far from the border of the Thomas-Fermi condensate, i.e. outside the spatial region where $R - x_0 \ll R$, the drift period is $\tau_{dr} \sim x_0/v_S \sim R^2/\kappa$ and greatly exceeds the time τ_R :

$$\frac{\tau_R}{\tau_{dr}} \sim \frac{R}{c_s\tau_{dr}} \sim \frac{a}{R} \ll 1.$$

This means that we can neglect retardation effects and, in particular, the emission of phonons by the moving vortex. In other words, the "cyclotron" radiation is prohibited, since the wavelength $c_s\tau_{dr}$ of sound which would be emitted exceeds the size R of the condensate.

According to the above mentioned magnetostatic analogy, in a non-rotating trap the potential energy of the system (vortex plus its reflection) can be thought as the energy of two counter flowing

currents. Since the currents attract each other, the energy is negative and decreases with displacing the vortex core towards the wall. In other words, it is energetically favorable for the vortex to move to the border of the vessel. Near the border the velocity of the vortex exceeds the Landau critical velocity, and in a homogeneous superfluid the vortex decays through the creation of phonons [146]. In a trapped gas the condensate density strongly decreases near the border, and the vortex can decay by emitting both collective and single-particle excitations. The motion of the vortex towards the wall requires the presence of dissipation, as in the frictionless approach the velocity of the vortex core coincides with the velocity (6.0.4) which does not contain a radial component. Thus, just the presence of dissipative processes provides a decay of the vortex state (see [143] and related discussion [141] of the stability of a kink state).

The dissipation originates from the scattering of elementary excitations by the vortex and is related to the friction force **F** in Eq.(6.0.1), which is nothing else than the momentum transferred from the excitations to the vortex per unit time. This force can be decomposed into longitudinal and transverse components:

$$\mathbf{F} = -D\mathbf{u} - D'\mathbf{u}\times\boldsymbol{\kappa}/\kappa, \tag{6.0.5}$$

where $\mathbf{u} = \mathbf{v}_L - \mathbf{v}_n$, $\mathbf{v}_n$ is the velocity of the normal component, and D, D' are longitudinal and transverse friction coefficients, respectively. In a static trap $\mathbf{u} = \mathbf{v}_L$, as the normal component is at rest ($\mathbf{v}_n = 0$). The friction force has been investigated in relation to the attenuation of the second sound in superfluid ^{4}He, where the the transverse component is most important [149–151] (see also [147] for review). For a straight infinite vortex line (parallel to the z-axis), a general expression for the friction force in a homogeneous superfluid is obtained in terms of the scattering amplitude $f(\mathbf{k},\mathbf{k}')$ [151]:

$$\mathbf{F} = \left[\int \frac{\partial n}{\partial E_k}\hbar(\mathbf{ku})\int(\mathbf{k}-\mathbf{k}')\frac{\delta(E_k - E_{k'})}{\delta(k_z - k'_z)}\right.$$

$$\left.|f(\mathbf{k},\mathbf{k}')|^2\frac{d^3k}{(2\pi)^3}\frac{d^3k'}{(2\pi)^3}\right] - [\mathbf{u}\times\boldsymbol{\kappa}]\rho_n. \tag{6.0.6}$$

Here ρ_n is the local mass density of the normal component, $\mathbf{k},\mathbf{k}'$ are the wave vectors of the incident and scattered excitations, $n(E_k) = (\exp(E_k/T)-1)^{-1}$are the Bose occupation numbers for the excitations, E_k is the excitation energy, and T the gas temperature. Comparing the second terms of Eqs. (6.0.5) and (6.0.6), one immediately arrives at the universal expression for the transverse friction coefficient: $D' = \kappa\rho_n$, assuming that the first term of Eq.(6.0.6) does not contribute to D' [147, 151].

We now turn to our analysis of the dissipative dynamics of the vortex state in a non-rotating trap, related to the motion of the vortex core (line) to the border of the condensate. This motion occurs on top of small oscillations of the vortex filament and a slow drift (6.0.4) of the vortex core. The radial component of the velocity of the vortex core is determined by the longitudinal friction coefficient D. For finding these quantities in dilute Bose-condensed gases, the analysis of [147, 149–151] can only be used at very low temperatures ($T \ll \mu$), where the number of thermal excitations is very small and, hence, the longitudinal friction force is extremely weak.

The situation is drastically different in the temperature range $T \gtrsim \mu$, which is the most interesting for trapped Bose-condensed gases. We will consider the limit $T \gg \mu$ and first analyze how the vortex scatters excitations with energies $E_k \gtrsim \mu$. These excitations are single particles, and their De Broglie wave length is much smaller than the spatial size R of the condensate. The most important is the interaction of the excitations with the vortex at distances from the vortex line $r \sim a \ll R$. Therefore, the corresponding friction force in a trapped condensate can be found in the local density approximation: We may use Eq.(6.0.6), derived for a homogeneous superfluid, and then replace the condensate density n_0 by the Thomas-Fermi density profile of the trapped condensate.

The Hamiltonian of the single-particle excitations is $\hbar^2\hat{\mathbf{k}}^2/2m + 2n_0(\mathbf{r})g - \mu$, where the second term originates from the mean-filed interparticle interaction, with $n_0(\mathbf{r})$ is the density of the vortex

state, $g = 4\pi\hbar^2 a_{sc}/m$, a_{sc} is the scattering length, and $\mu = n_0(\infty)g$ ($n_0(\infty) \equiv n_0$). For $r \to \infty$ we have $\hat{H}(\hat{\mathbf{k}}, \mathbf{r}) = \hbar^2\hat{\mathbf{k}}^2/2m + \mu$. Hence, the interaction Hamiltonian responsible for the scattering of excitations from the vortex can be written as

$$\hat{H}_{int} = 2\left[n_0(\mathbf{r})g - \mu\right].$$

For the vortex charge $Z = 1$, at distances $r \ll a$ the interaction Hamiltonian $\hat{H}_{int} \approx -2\mu$. For $r \gg a$ we have $n_0(\mathbf{r}) \approx (\mu - \hbar^2/2mr^2)/g$, and $\hat{H}_{int} \approx -\hbar^2/mr^2$. The scattering amplitude in Eq.(6.0.6) can be written as $f(\mathbf{k}, \mathbf{k}') = 2\pi\delta(k_z - k_z')\tilde{f}(\mathbf{k}, \mathbf{k}')$, where the 2D scattering amplitude in the Born approximation is given by

$$\tilde{f}(\mathbf{k}, \mathbf{k}') = \int d^2 r H_{int}(\mathbf{r}) e^{i\mathbf{qr}}. \tag{6.0.7}$$

Here $\mathbf{q} = \mathbf{k} - \mathbf{k}'$ is the momentum transferred from the excitation to the vortex. As the amplitude $\tilde{f}$ only depends on $|\mathbf{q}|$, the first term in Eq.(6.0.6) is purely longitudinal.

For $qa \ll 1$, which corresponds to small angle scattering, from Eq.(6.0.7) we obtain $\tilde{f} \sim (\hbar^2/m)\log(1/qa)$. For $qa \gg 1$ we find $|\tilde{f}(q)|^2 \sim (\hbar^2/m)^2 \sin^2(qa - \pi/4)/(aq)^3$. Using these results in Eq.(6.0.6), we see that the main contribution to the integral over momenta comes from energies E_k satisfying the inequality $\mu \lesssim E_k \ll T$. A direct calculation of the longitudinal friction coefficient gives

$$D \approx \kappa\rho_n(T)(n_0 g/T)^{1/2}, \tag{6.0.8}$$

where the density of the normal component

$$\rho_n = -\frac{1}{3}\int \frac{\partial n}{\partial E_p} p^2 \frac{d^3 p}{(2\pi\hbar)^3} \approx 0.1\frac{m^{5/2}T^{3/2}}{\hbar^3}.$$

A collective character of excitations with energies $E_k \sim \mu$ can influence the numerical coefficient in Eq.(6.0.8), and for this reason we did not present the exact value of this coefficient in the single-particle approximation. In cylindrical traps the behavior of excitations with energies $E \sim \mu$ (and somewhat larger) is stochastic [57, 111], and hence the discrete structure of the spectrum is not important (see Chapter 5).

The coefficient $D \propto T$, and Eq. (6.0.8) can be rewritten as $D \propto \hbar n_0 \xi$, where the quantity

$$\xi = (n_0 a_{sc}^3)^{1/2}(T/\mu) \ll 1 \tag{6.0.9}$$

is a small parameter of the finite-temperature perturbation theory at $T \gg \mu$. The inequality $\xi \ll 1$ remains valid even near the BEC transition temperature, except the region of critical fluctuations (see Chapter 5).

Relying on Eq.(6.0.8) for the longitudinal friction force, we consider the motion of the vortex line to the border of the condensate in a static trap, where the normal component is at rest. Assuming a small friction in Eqs.(6.0.1) and (6.0.5), for finding a friction-induced small quantity $\mathbf{v}_L - \mathbf{v}_S$ we only retain the terms linear in the dissipation coefficients D and D'. Then we obtain the equation

$$\rho_s[(\mathbf{v}_L - \mathbf{v}_S) \times \boldsymbol{\kappa}] = -D\mathbf{v}_S - D'[\mathbf{v}_S \times \boldsymbol{\kappa}]/\kappa$$

which has a solution of the form $v_L = v_L^{(r)}\hat{r} + v_L^{(\phi)}[\boldsymbol{\kappa} \times \mathbf{r}]/\kappa r$. For the radial ($v^{(r)}$) and tangential ($v^{(\phi)}$) components of the velocity of the vortex line we find

$$v_L^{(r)} = Dv_S/\rho_s\kappa; \quad v_L^{(\phi)} = v_S(1 - D'/\rho_s\kappa). \tag{6.0.10}$$

>From Eqs.(6.0.10) it is clear that the radial motion of the vortex is governed by the value of the longitudinal friction coefficient, whereas the transverse friction (Iordanskii force) simply slows down the drift velocity (6.0.4) of the vortex. The radial velocity $v_L^{(r)} \ll v_S$, which is guaranteed by the inequality (6.0.9).

The time dependence of the distance x_0 of the vortex line from the axis of a cylindrical trap follows from the equation of radial motion for the vortex, $dx_0/dt = v_L^{(r)}$. With Eq.(6.0.10) for $v_L^{(r)}$ and Eq.(6.0.4) for v_S, for the characteristic time of motion of the vortex from the center of the trap to the border we obtain

$$\tau \approx \int_{x_{min}}^{R} \frac{dx_0 m(R^2 - x_0^2)\rho_s}{\hbar x_0 \rho_n} \left(\frac{n_0 g}{T}\right)^{1/2}, \tag{6.0.11}$$

where x_{min} is the initial displacement of the vortex line from the axis of the trap. The vortex velocity is the smallest near the axis, and the main contribution to the integral in Eq.(6.0.11) comes from distances $x_0 \ll R$. Therefore, we can neglect x_0 in the numerator of the integrand and put $\rho_s = \rho_S(0)$, $n_0 = n_0(0)$. Then, Eq.(6.0.11) yields

$$\tau \approx \frac{mR^2\rho_s}{\hbar\rho_n} \left(\frac{n_0 g}{T}\right)^{1/2} \ln(R/x_{min}). \tag{6.0.12}$$

This result is only logarithmically sensitive to the exact value of x_{min}, and we can put $x_{min} \sim a$.

Once the vortex reaches the border of the condensate, it immediately decays. Hence, the time τ can be regarded as a characteristic life-time of the vortex state in a static trap. Interestingly, the decay rate can be written as

$$\tau^{-1} \sim \frac{E_0}{\hbar}(n_{0m}a_{sc}^3)^{1/2} \left(\frac{T}{\mu}\right), \tag{6.0.13}$$

where n_{0m} is the maximum condensate density, and $E_0 \sim \hbar^2/mR^2$ is the energy of excitation corresponding to the motion of the vortex core with respect to the rest of the condensate (excitation with negative energy, found in the recent calculations [142, 144, 145, 152, 153]). Eq.(6.0.13) is similar to the damping rate of low-energy excitations of a trapped condensate, found beyond the mean-field approach [96, 97]. Both rates are proportional to the small parameter ξ (6.0.9).

For Rb and Na condensates at densities $n_0 \sim 10^{14} cm^{-3}$ and temperatures $100 \lesssim T \lesssim 500$ nK, in the static traps with frequencies $10 \lesssim \omega \lesssim 100$ Hz the life-time τ of the vortex state ranges from 0.1 to 10 s. This range of times is relevant for experimental studies of the dissipative vortex dynamics.

A proposed way of identifying the presence of a vortex state in a trapped Bose-condensed gas assumes switching off the trap and observing a ballistically expanding gas sample [139]. As follows from the numerical simulations [139], at zero temperature the expansion of a condensate with a vortex occurs along the lines of the scaling theory [44, 46]. The shape of the Bose-condensed state is nearly preserved and its spatial size is increasing. Due to expansion the density of the condensate decreases, and the size of the vortex core increases to match the instantaneous value of the healing length. This should allow one to detect the vortex through the observation of a hole in the density profile of the condensate.

It is important to emphasize that at temperatures $T \gg \mu$ the thermal cloud will expand with the thermal velocity $v_T \sim \sqrt{T/m}$ which is much larger than the expansion velocity of the condensate (the latter is of order the sound velocity c_s). Therefore, after a short time R/v_T the thermal component flies away, and the dissipation-induced motion of the vortex core ceases. Accordingly, the expansion of the Bose-condensed state will be essentially the same as that at zero temperature. This means that the relative displacement of the vortex core from the trap center practically remains the same as before switching off the trap. Therefore, the dissipative motion of the vortex towards the border in the initial static trap can be studied by switching off the trap at different times and visualizing the position of the vortex core in a ballistically expanding condensate.

In conclusion, we have developed a theory of dissipative dynamics of a vortex state in a trapped Bose-condensed gas at finite temperatures and calculated the decay time of the vortex with charge equal to 1 in a static trap. Our theory can be further developed to analyze the motion of vortices in

rotating traps and, in particular, to calculate a characteristic time of the formation of the vortex state in a trap rotating with supercritical frequency.

Bibliography

[1] S. Bose, Z. Phys. **26**, 178 (1924).
[2] A. Einstein, Sitzber. Kgl. Preuss. Akad. Wiss. 261 (1924).
[3] M. H. Anderson *et al.*, Science **269**, 198 (1995).
[4] K. B. Davis *et al.*, Phys. Rev. Lett. **75**, 3969 (1995).
[5] C. C. Bradley, C. A. Sackett, J. J. Tolett, and R. G. Hulet, Phys. Rev. Lett. **75**, 1687 (1995).
[6] H. London and F. London, Proc. Roy. Soc. (London) **A149**, 71 (1935).
[7] S. Weinberg, *The quantum Theory of Fields II: Modern applications* (Cambridge University Press, Cambridge, 1966).
[8] A. Linde, Phys. Rev. D **49**, 748 (1994).
[9] S. Davis, A. Davis, and M. Trodden, Phys. Rev. D **57**, 5184 (1998).
[10] M. Alpar and D. Pines, *The Lives of the Neutron Star: conference proceedings*, edited by M. Alpar and J. van Paradijs (Kluwere Academic Publisher, Dordrech, 1995).
[11] K. Cheng, D. Pines, M. Alpar, and J. Shalam, ApJ **330**, 835 (1988).
[12] I. Silvera and J. Walraven, Phys. Rev. Lett. **44**, 164 (1980).
[13] I. Silvera and J. Walraven, *Progress in Low Temperature Physics*, edited by D. Brewer (Elsivier, Amsterdam, 1984), Vol. X, p. 139.
[14] T. J. Greytak and D. Kleppner, *New Trends in Atomic Physics*, edited by G. Grynberg and R. Stora (North Holland, Amsterdam, 1984).
[15] T. J. Greytak, *Bose Einstein Condensation*, edited by A. Griffin, D. W. Snoke, and S. Stringari (Cambridge University Press, Cambridge, 1995), p. 131.
[16] I. F. Silvera, *Bose Einstein Condensation*, edited by A. Griffin, D. W. Snoke, and S. Stringari (Cambridge University Press, Cambridge, 1995), p. 160.
[17] D. Fried *et al.*, Phys. Rev. Lett. **81**, 3811 (1998).
[18] A. Safonov *et al.*, Phys. Rev. Lett. **81**, 4545 (1998).
[19] S. Chu, Rev. Mod. Phys. **70**, 707 (1998).
[20] C. Cohen-Tannoudji, *Atomic Physics*, edited by C. Wieman, D. Wineland, and S. Smith (AIP, New York, 1995), Vol. 14, p. 193.
[21] W. Phillips, *Atomic Physics*, edited by C. Wieman, D. Wineland, and S. Smith (AIP, New York, 1995), Vol. 14, p. 211.
[22] J. T. M. Walraven, *Quantum dynamics of simple systems*, edited by J.-L. Oppo, S. M. Barnett, E. Riis, and M. Wilkinson (Institute of Physics Publ., London, 1996), p. 315.
[23] W. Ketterle and N. J. van Druten, *Advances in Atomic, Molecular and Optical Physics*, edited by B. Bederson and H. Walther (Academic Press, San Diego, 1996), Vol. 37, p. 181.
[24] M. Kasevich, talk at the IV Workshop on Optics and Interferometry with Atoms, 1997.
[25] D.-J. Han, R. H. Wynar, P. Courteille, and D. J. Heinzen, Phys. Rev. A **57**, R4114 (1998).
[26] U. Ernst *et al.*, Europhys. Lett. **41**, 1 (1998).
[27] T. Esslinger, L. Bloch, and T. Hansch, 1998, unpublished.
[28] L. Hau *et al.*, *Photonic, Electronic ans Atomic Collisions*, edited by F. Aumayr and H. Winter (World Scientific, Singapure, 1997), Vol. 1, p. 41.
[29] L. Hau *et al.*, Phys. Rev. A **58**, R54 (1998).
[30] R. Lutwak, 1998, unpublished.
[31] E. M. Lifshitz and L. P. Pitaevskii, *Statistical Physics, Part 2* (Pergamon Press, Oxford, 1980).
[32] P. A. Ruprecht, M. J. Holland, K. Burnett, and M. Edwards, Phys. Rev. A **51**, 4704 (1995).
[33] Y. Kagan, G. Shlyapnikov, and J. Walraven, Phys. Rev. Lett **76**, 2670 (1996).
[34] B. J. Verhaar, *Atomic Physics*, edited by C. Wieman, D. Wineland, and S. Smith (AIP, New York, 1995), Vol. 14, p. 218.
[35] E. Tiesinga, B. J. Verhaar, and H. T. C. Stoof, Phys. Rev. A **47**, 4114 (1992).
[36] E. Cornell, J. Res. Nat. Stand. Technol. **101**, 419 (1996).

[37] R. Feynman, *Statistical Mechanics: a set of lectures* (Benjamin Reading, Massachusetts, 1982).
[38] E. P. Gross, Nouvo Cimento **20**, 454 (1961).
[39] E. P. Gross, J. Math. Phys. **4**, 195 (1963).
[40] L. P. Pitaevskii, Sov. Phys. JETP **13**, 451 (1961).
[41] Y. Castin and J. Dalibard, Phys. Rev. A **55**, 4330 (1997).
[42] V. V. Goldman, I. F. Silvera, and A. J. Leggett, Phys. Rev. B **24**, 2870 (1981).
[43] D. A. Huse and E. D. Siggia, J. Low Temp. Phys. **46**, 137 (1982).
[44] Y. Kagan, E. L. Surkov, and G. Shlyapnikov, Phys. Rev. A **54**, R1753 (1996).
[45] Y. Kagan, E. L. Surkov, and G. Shlyapnikov, Phys. Rev. A **55**, R18 (1997).
[46] Y. Castin and R. Dum, Phys. Rev. Lett. **77**, 5315 (1996).
[47] Y. Kagan, E. L. Surkov, and G. Shlyapnikov, Phys. Rev. Lett. **79**, 2604 (1997).
[48] D. S. Jin *et al.*, Phys. Rev. Lett. **77**, 420 (1996).
[49] M.-O. Mewes *et al.*, Phys. Rev. Lett. **77**, 988 (1996).
[50] D. S. Jin *et al.*, Phys. Rev. Lett. **78**, 764 (1997).
[51] D. Stamper-Kurn, H.-J. Miesner, S. I. M. Andrews, and W. Ketterle, Phys. Rev. Lett. **81**, 500 (1998), cond-mat/9801262.
[52] A. Smerzi and S. Fantoni, Phys. Rev. Lett. **78**, 3589 (1997).
[53] N. Bogolyubov, J. Phys. USSR **11**, 23 (1947).
[54] P. R. de Gennes, *Superconductivity of Metals and Alloys* (Benjamin, New York, 1966).
[55] S. Stringari, Phys. Rev. Lett. **77**, 2360 (1996).
[56] P. Öhberg *et al.*, Phys. Rev. A **56**, R3346 (1997).
[57] M. Fliesser, A. Cordas, R. Graham, and P. Szepfalusy, Phys. Rev. A **56**, 4879 (1997), cond-mat/9707122.
[58] Y. Castin and R. Dum, Phys. Rev. Lett. **77**, 5315 (1996).
[59] L. Onsager, Nouvo Cimento **6**, 249 (1949).
[60] Y. Kagan, I. A. Vartan'yants, and G. V. Shlyapnikov, Sov. Phys. JETP **54**, 590 (1981).
[61] L. P. H. de Goey *et al.*, Phys. Rev. B **34**, 6183 (1986).
[62] L. P. H. de Goey, H. T. C. Stoof, B. J. Verhaar, and W. Glöckle, Phys. Rev. B **38**, 646 (1988).
[63] H. T. C. Stoof, L. P. H. de Goey, B. J. Verhaar, and W. Glöckle, Phys. Rev. B **38**, 11221 (1988).
[64] A. J. Moerdijk, H. M. J. M. Boesten, and B. J. Verhaar, Phys. Rev. A **53**, 916 (1996).
[65] D. V. Fedorov and A. S. Jensen, Phys. Rev. Lett. **71**, 4103 (1993).
[66] L. D. Landau and E. M. Lifshitz, *Quantum Mechanics, Non-relativistic Theory* (Pergamon Press, Oxford, 1977).
[67] Z. Zhen and J. Macek, Phys. Rev. A **38**, 1193 (1988).
[68] A. J. Moerdijk and B. J. Verhaar, Phys. Rev. A **53**, R19 (1996).
[69] K. T. Tang, J. P. Toennies, , and C. L. Yiu, Phys. Rev. Lett. **74**, 1548 (1995).
[70] W. Schöllkopf and J. P. Toennies, Science **266**, 1345 (1994).
[71] J. Stärck and W. Meyer, Chem. Phys. Lett. **225**, 229 (1994).
[72] G. V. Shlyapnikov, J. T. M. Walraven, U. M. Rahmanov, and M. W. Reynolds, Phys. Rev. Lett. **73**, 3247 (1994).
[73] P. O. Fedichev, U. M. Rahmanov, M. W. Reynolds, and G. V. Shlyapnikov, Phys. Rev. A **53**, 1447 (1996).
[74] R. Côté, E. J. Heller, and A. Dalgarno, Phys. Rev. A **53**, 234 (1996).
[75] V. Bagnato and J. Weiner, preprint.
[76] Private communications with P.S. Julienne and W.D. Phillips.
[77] P. Julienne, A. Smith, , and K. Burnett, *Advances in Atomic, Molecular and Optical Physics*, edited by B. Bederson and H. Walther (Academic Press, San Diego, 1996), Vol. 37, p. 369.
[78] D. Heinzen, *Atomic Physics*, edited by C. Wieman, D. Wineland, and S. Smith (AIP, New York, 1995), Vol. 14, p. 369.
[79] B. V. Svistunov and G. V. Shlyapnikov, Sov. Phys. JETP **70**, 460 (1990).
[80] B. V. Svistunov and G. V. Shlyapnikov, Sov. Phys. JETP **71**, 71 (1990).
[81] E. B. I. Abraham, N. W. M. Ritchie, W. I. McAlexander, and R. Hulet, J. Chem. Phys. **103**, 7773 (1990).
[82] W. T. Zemke and W. C. Stwalley, J. Phys. Chem. **97**, 2053 (1993).
[83] M. J. Holland, D. S. Jin, M. L. Chiofalo, and J. Cooper, Phys. Rev. Lett. **78**, 3801 (1997).
[84] W. B. Colson and A. Fetter, J. Low Temp. Phys. **33**, 231 (1978).
[85] E. Goldstein and P. Meystre, Phys. Rev. A **55**, 2935 (1997).
[86] T.-L. Ho and V. B. Shenoy, Phys. Rev. Lett. **77**, 3276 (1996).
[87] B. D. Esry, C. H. Green, J. P. Burke, and J. L. Bohn, Phys. Rev. Lett. **78**, 3594 (1997).
[88] C. K. Law, H. Pu, N. P. Bigelow, and J. H. Eberly, Phys. Rev. Lett. **79**, 3105 (1997).
[89] H. Pu and N. P. Bigelow, Phys. Rev. Lett. **80**, 1130 (1998).
[90] H. Pu and N. P. Bigelow, Phys. Rev. Lett. **80**, 1134 (1998).

[91] E. Fermi, J. Pasta, and S. Ulam, *Collected papers of Enrico Fermi* (Accademia nazionale dei Lincei and University of Chicago, Roma, 1965), Vol. 2, p. 978.
[92] F. M. Izrailev and B. Chirikov, Sov. Phys.-Doklady **11**, 30 (1966).
[93] R. Z. Sagdeev, D. A. Usikov, and G. M. Zaslavsky, *Non-linear Physics: From the Pendulum to Turbulence and Chaos*, *Contemporary Concepts in Physics* (Harwood Acad. Pub., Chur-New York, 1988).
[94] D. S. Hall *et al.*, Phys. Rev. Lett. **81**, 1539 (1998).
[95] D. S. Hall, M. R. Matthews, C. E. Wieman, and E. A. Cornell, Phys. Rev. Lett. **81**, 1543 (1998).
[96] F. Dalfovo, S. Giorgini, L. Pitaevskii, and S. Stringari, Rev. Mod. Phys. **71**, 463 (1999).
[97] P. O. Fedichev, G. V. Shlyapnikov, and J. T. M. Walraven, Phys. Rev. Lett **80**, 2269 (1998).
[98] T. D. Lee and C. N. Yang, Phys. Rev. **112**, 1419 (1958).
[99] V. N. Popov, Sov. Phys. JETP **20**, 1185 (1965).
[100] S. T. Beliaev, Sov. Phys. JETP **34**, 323 (1958).
[101] N. Hugenholtz and D. Pines, Phys. Rev. **116**, 489 (1959).
[102] V. N. Popov, *Functional Integrals in Quantum Field Theory and Statistical Physics* (D. Reidel Publishing Company, Dordrecht, 1983).
[103] P. Hohenberg and P. Martin, Ann. Phys. **34**, 291 (1965).
[104] P. Szepfalusy and I. Kondor, Ann. Phys. **82**, 1 (1974).
[105] H. Shi and A. Griffin, Phys. Rep. (1997).
[106] W. V. Liu, Phys. Rev. Lett. **79**, 4056 (1997), cond-mat/9708080.
[107] L. P. Pitaevskii and S. Stringari, Phys. Lett. A **235**, 398 (1997), cond-mat/9708104.
[108] S. Giorgini, Phys. Rev. A **57**, 2949 (1997), cond-mat/9709259.
[109] M. Andrews *et al.*, Phys. Rev. Lett. **79**, 553 (1997).
[110] A. A. Abrikosov, L. P. Gorkov, and I. E. Dzyaloshinski, *Methods of Quantum Field Theory in Statistical Physics* (Dover Publications Inc., New York, 1975).
[111] M. Fliesser, A. Cordas, R. Graham, and P. Szepfalusy, Phys. Rev. A **56**, R2533 (1997), cond-mat/9706002.
[112] L. Landau and E. Lifshitz, *Statistical Physics, Part 1* (Pergamon Press, Oxford-Frankfurt, 1980).
[113] A. Griffin, Phys. Rev. A **53**, 9341 (1996).
[114] B. Chirikov, preprint chao-dyn/9705003.
[115] E. A. Shapoval, Sov. Phys. JETP **20**, 675 (1964).
[116] L. P. Gor'kov and G. M. Eliashberg, Sov. Phys. JETP **21**, 940 (1965).
[117] G. Lŭders and K.-D. Usadel, in *The method of the Correlation function in Superconductivity Theory*, Vol. 56 of *Springer Tracts Modern Physics*, edited by G. Hŏhler (Springer-Verlag, New York, 1971).
[118] D. Hutchinson, E. Zaremba, and A. Griffin, Phys. Rev.Lett. **78**, 1842 (1997).
[119] R. Dodd, K. Burnett, M. Edwards, and C. Clark, Phys. Rev. A **57**, R32 (1998), preprint cond-mat/9712286.
[120] H. Shi and W.-M. Zheng, preprint cond-mat/9804108.
[121] V. Shenoy and T.-L. Ho, preprint cond-mat/9710274.
[122] E. Zaremba, Phys. Rev. A **57**, 518 (1998).
[123] G. Kavoulakis and C. Pethick, preprint cond-mat/9711224.
[124] S. Stringari, preprint cond-mat/980106.
[125] E. P. Wigner, Math. Ann. **53**, 36 (1951).
[126] E. P. Wigner, Math. Ann. **62**, 548 (1955).
[127] F. J. Dyson, J. Math. Phys. **3**, 140 (1955).
[128] G. Kavoulakis, G. Pethick, and H. Smith, Phys. Rev. A **57**, 2938 (1998).
[129] E. Zaremba, A. Griffin, and T. Nikuni, Phys. Rev. A **57**, 4695 (1998).
[130] A. Minguzzi and M. P. Tosi, J. Phys: Condens. Matter **9**, 10 211 (1998).
[131] D. Hutchinson, R. Dodd, and K. Burnett, e-print cond-mat/9805050.
[132] M. J. Bijlsma and H. Stoof, e-print cond-mat/9902065.
[133] A. Legget, in *Topics in superfluidity and superconductivity*, *Low Temperature Physics*, edited by M. Hoch and R. Lemmer (Springer Verlag, New York, 1992).
[134] S. Stringari, e-print cond-mat/9812362.
[135] J. R. Anglin and W. H. Zurek, cond-mat/9804035.
[136] R. Dum, I. Chirac, M. Lewenstein, and P. Zoller, Phys. Rev. Lett. **80**, 2972 (1998).
[137] M. Olshanii and M. Naraschewski, cond-mat/9804035.
[138] B. Jackson, J. F. McCann, and C. S. Adams, Phys. Rev. Lett. **80**, 3903 (1998).
[139] Y. Castin and R. Dum, to be published.
[140] T. Busch and J. Anglin, e-print cond-mat/9809408.
[141] A. E. Muryshev, H. B. van Linden van Heuvell, and G. V. Shlyapnikov, e-print cond-mat/9811408.

[142] D. Rokhsar, Phys. Rev. Lett. **79**, 1261 (1997).
[143] A. L. Fetter, cond-mat/9808070.
[144] A. Svidzinsky, A.L. Fetter, e-print cond-mat/9811348.
[145] H. Pu, C. K. Law, J. H. Eberly, and N. Bigelow, Phys. Rev. A **59**, 1533 (1999).
[146] R. J. Donnelly, *Quantized vortices in helium II* (Cambridge University Press, Cambridge, 1991).
[147] E. B. Sonin, Phys. Rev. B **55**, 485 (1997).
[148] D. J. Thouless, P. Ao, and Q. Niu, Phys. Rev. Lett. **76**, 3758 (1996).
[149] L. P. Pitaevskii, Sov. Phys.-JETP **8**, 888 (1959).
[150] A. L. Fetter, Phys. Rev. **136**, A1488 (1964).
[151] S. V. Iordanskii, Sov. Phys.-JETP **22**, 160 (1966).
[152] R. J. Dodd, K. Burnett, M. Edwards, and C. Clark, Phys. Rev. A **56**, 587 (1997).
[153] T. Isoshima and K. Machida, J. Phys. Soc. Jpn. **66**, 3602 (1997).

Summary

In this Thesis we develop a theory of dynamical and kinetic properties of trapped Bose condensates.

In Chapter 2 we review theoretical grounds of the physics of Bose-condensed gases. We discuss such concepts as Bose-Einstein phase transition, macroscopic description of an interacting Bose-condensed gas, elementary excitations and their description in terms of Bogolyubov-de Gennes equations, and vortex states in superfluids.

Then, in Chapter 3 we inspect the interparticle interaction in ultra-cold gases. First, we turn to the discussion of three-body recombination of ultra-cold atoms to a weakly bound s level. In this case characterized by large and positive scattering length a for pair interaction, in the zero temperature limit we obtain a universal relation, independent of the detailed shape of the interaction potential, for the (event) rate constant of three-body recombination: $\alpha_{\text{rec}} = 3.9\hbar a^4/m$, where m is the atom mass.

Then, we develop the idea of manipulating the value and the sign of the scattering length. Since the scattering length directly affects the mean field interaction between the atoms, this offers a possibility to investigate macroscopic quantum phenomena associated with BEC by observing the evolution of a Bose condensed gas in response to light. The physical picture of the influence of the light field on the elastic interaction between atoms is the following: A pair of atoms absorbs a photon and undergoes a virtual transition to an electronically excited quasimolecular state. Then it reemits the photon and returns to the initial electronic state at the same kinetic energy. As the interaction between atoms in the excited state is much stronger than in the ground state, already at moderate light intensities the scattering amplitude can be significantly changed.

In Chapter 4 we discuss the dynamics of two trapped interacting Bose-Einstein condensates in the absence of thermal cloud. The main goal of our work is to study the dynamics of Bose condensates and analyze how the system can acquire statistical properties and reach a new equilibrium state. We identify two regimes for the evolution: a regime of slow periodic oscillations and a stochastic regime of strong non-linear mixing leading to the damping of the relative motion of the condensates. We compare our predictions with an experiment recently performed at JILA, and argue that the occurrence of the stochastic regime provides a route to achieving a new thermal equilibrium in the system.

In Chapter 5 we develop a finite temperature perturbation theory (beyond the mean field) for a Bose-condensed gas and calculate temperature-dependent damping rates and energy shifts for Bogolyubov excitations of any energy. The theory is generalized for the case of excitations in a spatially inhomogeneous (trapped) Bose-condensed gas, where we emphasize the principal importance of inhomogeneity of the condensate density profile and develop the method of calculating the self-energy functions. The use of the theory is demonstrated by calculating the damping rates and energy shifts of low-energy excitations, i.e. the excitations with energies much smaller than the mean field interaction between particles. The damping is provided by the interaction of these excitations with the thermal excitations. We emphasize the key role of stochastization in the behavior of the thermal excitations for damping in non-spherical traps. The damping rates of the lowest excitations, following from our theory, are in fair agreement with the data of recent JILA and MIT experiments. For the quasiclassical excitations the boundary region of the condensate plays a crucial role, and the result for the damping

rates and energy shifts is drastically different from that in spatially homogeneous gases. We also analyze the frequency shifts and damping of sound waves in cylindrical Bose condensates and discuss the role of damping in the recent MIT experiment on the sound propagation.

Finally, in Chapter 6, we turn to dynamics of macroscopically excited Bose condensate states. In particular, we discuss dissipative dynamics of a vortex state in a trapped Bose-condensed gas at finite temperature and draw a scenario of decay of this state in a static trap. The interaction of the vortex with the thermal cloud transfers energy from the vortex to the cloud and induces the motion of the vortex core to the border of the condensate. Once the vortex reaches the border, it decays through the creation of phonons. We calculate the characteristic life-time of the vortex state and address the question of how the dissipative dynamics of vortices can be studied experimentally.

Samenvatting

In dit proefschrift wordt een theorie over de dynamische en kinetische eigenschapen van een opgesloten Bose-condensaat ontwikkeld.

In hoofdstuk 2 geven we een overzicht over de theoretische basis van de natuurkunde van Bose-gecondenseerde gassen. We bespreken concepten als de Bose- Einstein- faseovergang (BEC), de makroscopische beschrijving van een Bose-gecondenseerd gas, elementaire excitaties en hun beschrijving in termen van Bogolyubov-de-Gennes-vergelijkingen en vortex-toestanden in superfluida.

Vervolgens, in hoofdstuk 3 wordt de wisselwerking tussen deeltjes in ultrakoude gassen beschouwd. Eerst richten we de discussie op de drie-deeltjes-recombinatie van ultrakoude atomen naar een zwak gebonden s-niveau. In dit geval, dat wordt gekarakteriseerd door een grote en positieve verstrooiingslengte a voor paarwisselwerking, krijgen we, in de limiet dat de temperatuur naar nul gaat, een universele relatie voor de drie-deeltjes- (gebeurtenis-) recombinatieconstante, die niet afhankelijk is van de precieze vorm van de interactiepotentiaal: $\alpha_{\text{rec}} = 3.9\hbar a^4/m$, met m de atoommassa.

Vervolgens wordt het idee ontwikkeld om de waarde en het teken van de verstrooiingslengte te manipuleren. Omdat de verstrooiingslengte direct de gemiddeld-veld-interactie tussen de atomen beinvloedt, biedt dit de mogelijkheid om macroscopische quantum-fenomenen te onderzoeken die geassocieerd zijn aan BEC, door van een Bose-gecondenseerd gas de reactie op licht te observeren. Het natuurkundige beeld van de invloed van het lichtveld op de elastische interactie tussen atomen is het volgende: Een atomenpaar absorbeert een foton en ondergaat een virtuele overgang naar een electronisch aangeslagen quasimolekulaire toestand. Vervolgens zendt het het foton weer uit en keert terug in de oorspronkelijke electronische toestand met de zelfde kinetische energie. Omdat de interactie tussen atomen in aangeslagen toestand veel sterker is dan tussen grondtoestandsatomen, kan de verstrooiingsamplitude al bij een matige lichtintensiteit significant veranderd worden.

In hoofdstuk 4 bespreken we de dynamica van twee opgesloten wisselwerkende Bose-Einstein-condensaten in de afwezigheid van een thermische wolk. Het hoofddoel van ons werk is de dynamica te bestuderen van Bose-condensaten en te analyseren hoe het systeem statistische eigenschappen kan verkrijgen en een nieuwe evenwichtstoestand bereikt. We onderscheiden twee ontwikkelingsregimes: een regime van langzame periodische oscillaties en een stochastisch regime van sterke niet-lineaire menging dat tot het dempen van de relatieve beweging van de condensaten leidt. We vergelijken onze voorspellingen met een experiment dat recentelijk in JILA is uitgevoerd en argumenteren dat het vóórkomen van het stochastische regime een route biedt om in het systeem tot een nieuw thermisch evenwicht te komen.

In hoofdstuk 5 ontwikkelen we een eindige- temperatuur-storingstheorie (voorbij de gemiddeld-veldbenadering) voor een Bose-gecondenseerd gas, en berekenen temperatuur-afhankelijke dempingssnelheden en energieverschuivingen voor Bogolyubov-excitaties van willekeurige energie. De theorie wordt veralgemeniseerd voor het geval van excitaties in een ruimtelijk inhomogeen (gevangen) Bose-gecondenseerd gas, waar we benadrukken hoe belangrijk inhomogeniteiten in het dichtheidsprofiel van het condensaat zijn, en ontwikkelen de methode om zelfenergiefunkties uit te rekenen. Het nut van de theorie wordt gedemonstreerd door de dempingssnelheid en de energieverschuiving van laag-energetische excitaties uit te rekenen. Dit zijn excitaties met energieën die veel lager zijn dan de gemiddeld-veld-interactie van deze excitaties. De demping wordt veroorzaakt door de interactie van deze excitaties met thermische excitaties. We benadrukken de sleutelrol van de stochastisering in

het gedrag van de thermische excitaties voor demping in niet-bolvormige vallen. De dempingssnelheden van de laagste excitaties volgens onze theorie, zijn in redelijke overeenstemming met recente data van JILA en MIT experimenten. In het geval van quasiklassieke excitaties, speelt het randgebied van het condensaat een cruciale rol, en het resultaat voor de dempingssnelheden verschilt drastisch van dat in ruimtelijk homogene gassen. We analyseren ook de frequentieverschuivingen en de demping van geluidsgolven in cylindrische Bosecondensaten en bespreken de rol van demping in het recente MIT experiment aan geluidsvoorplanting in een Bose-condensaat.

Tenslotte, in hoofstuk 6, wordt de dynamica van macroscopisch aangeslagen Bosecondensaten behandeld. In het bijzonder bespreken we dissipatieve dynamica van een vortextoestand in een opgesloten Bose-gecondenseerd gas bij eindige temperatuur en schetsen een vervalsscenario van deze toestand in een statische val. De interactie van de vortex met de thermische wolk hevelt energie over van de vortex naar de wolk en induceert de beweging van de vortexkern naar de rand van het condensaat. Wanneer de vortex de rand heeft bereikt, vervalt het door de opwekking van fononen. We berekenen de karakteristieke levensduur van de vortextoestand en behandelen de vraag hoe de dissipatieve dynamica van vortices het beste experimenteel kan worden bestudeerd.